Journal of Oncology

DNA Repair in Cancer

Lead Guest Editor: Zhihua Kang
Guest Editors: Qingyuan Yang and Yintao Li

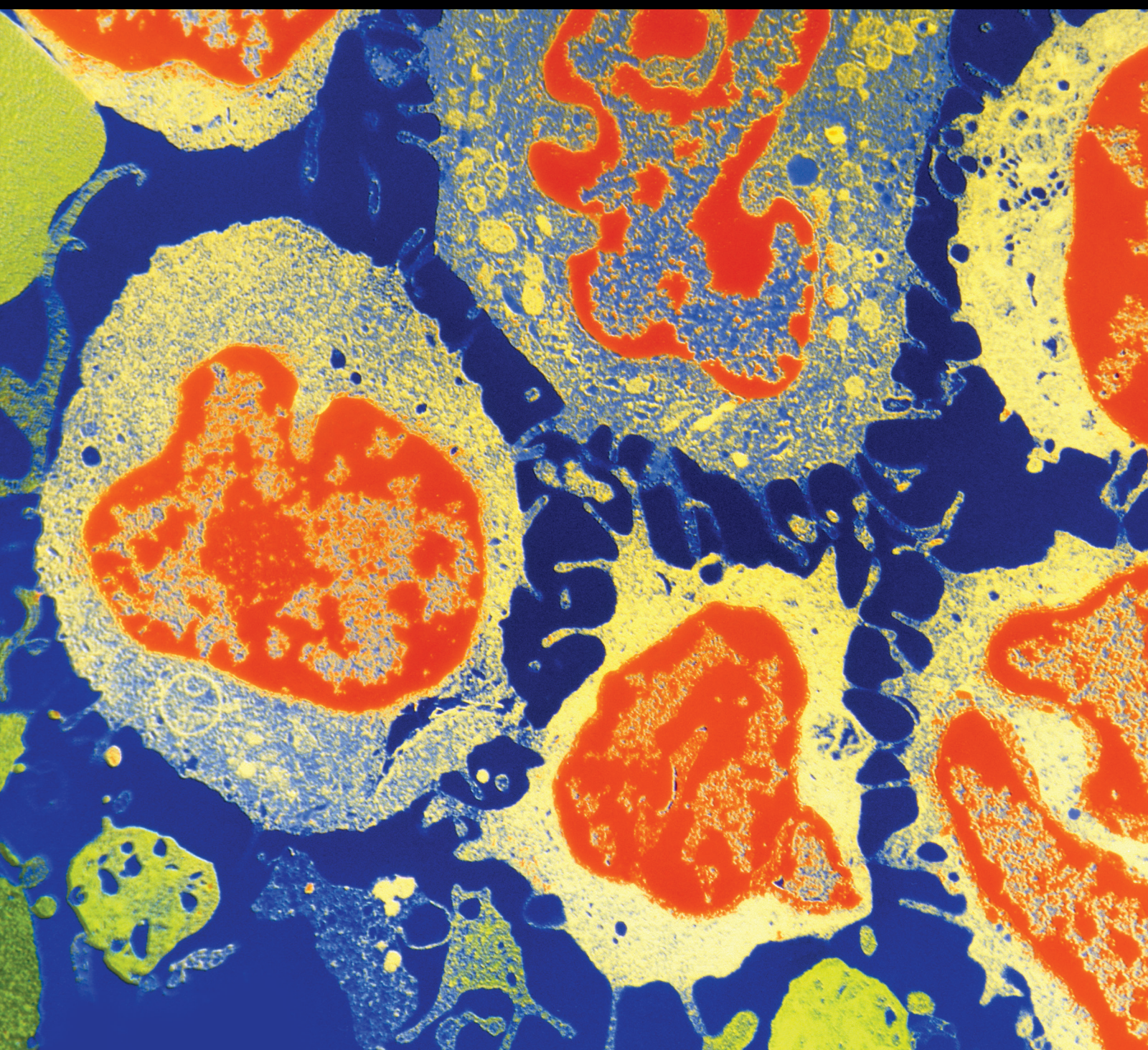

DNA Repair in Cancer

Journal of Oncology

DNA Repair in Cancer

Lead Guest Editor: Zhihua Kang
Guest Editors: Qingyuan Yang and Yintao Li

Editorial Board

Contents

Hindawi
Journal of Oncology
Volume 2019, Article ID 8676947, 2 pages
https://doi.org/10.1155/2019/8676947

Editorial

DNA Repair in Cancer

Zhihua Kang,[1,2] **Qingyuan Yang**,[3] **and Yintao Li**[4]

[1]*Department of Laboratory Medicine, Huashan Hospital, Fudan University, Shanghai, China*
[2]*Department of Radiation Oncology, Rutgers Cancer Institute of New Jersey, Rutgers University, New Brunswick, NJ, USA*
[3]*Department of Radiation Oncology, Massachusetts General Hospital, Harvard University, Boston, MA, USA*
[4]*Molecular and Cellular Oncology, MD Anderson, The University of Texas, Houston, TX, USA*

Correspondence should be addressed to Zhihua Kang; kangzhihua@yahoo.com

Received 15 July 2019; Accepted 15 July 2019; Published 24 July 2019

DNA repair system has evolved to maintain the genomic integrity to defend against both endogenous and exogenous sources of DNA damage, such as endogenous factors include reactive oxygen species, replication errors or mistakes in meiosis and exogenous factors include ultraviolet (UV) radiation, ionizing radiation (IR), and some other chemicals or chemotherapeutic agents. Multiple repair pathways (direct repair, base excision repair, nucleotide excision repair, mismatch repair, nonhomologous end joining, and homologous recombination pathways) can be aroused from the diverse forms of DNA lesions including mismatch paired bases, small deletions or insertions, and DNA single or double-strand breaks. These repair pathways also exert crosstalk with others to complete the whole DNA repair process.

The deficient DNA repair causing prolonged existence of DNA damages can lead to genes mutations, chromosome rearrangements, genomic instability, and finally carcinogenesis. Indeed, defects in DNA repair pathways contribute to many heritable cancer predisposition syndromes; however, cancer-related DNA repair deficiency may also occur in sporadic cancer case. Defective DNA repair is common in carcinogenesis and plays a critical role in cancer progression. For example, genetic mutations in DNA mismatch repair genes are involved in reducing mismatch repair and increasing the risk to colon and uterine tumors; BRCA1, BRCA2, and PALB2 genes mutations result in defective homologous recombination repair and are associated with the carcinogenesis of breast and ovarian cancer. In these years, many cancer-related germline mutations in DNA repair have been reported; thus to detect these genetic variations gives us a chance to evaluate the cancer risk of the individual with these mutations.

Furthermore, these defects in DNA repair pathways may have therapeutic implications for clinical practice. Most recently, a series of therapeutic strategy have been exploited, such as platinum chemotherapies and PARP inhibitors in homologous recombination defected breast and ovarian cancers and inhibitors of immune checkpoints CTLA-4, PD1/PD-L1 in the case of mismatch repair deficiency cancers. These observations give the direction for further research to investigate the defects in DNA repair pathways that may serve as very useful biomarkers for the choice of suitable oncotherapy.

This special issue includes 4 high-quality peer-reviewed articles and 1 review that brings us new ideas and findings in DNA repair in different types of cancers focusing on the genetic changes in DNA repair genes, the influences from these changes to carcinogenesis, and also the therapeutic implications. We have reasons to believe that these articles will enlighten and motivate not only the new inspirations but also the scientific advances in the study of DNA repair in cancer.

Conflicts of Interest

The authors declare that they have no conflicts of interest.

Acknowledgments

The authors would like to thank the all the editorial board members of Journal of Oncology, for their kind assistance, support, and preparation of this special issue. In addition,

they would like to express their gratitude to the authors and reviewers for their contributions to this special issue.

Zhihua Kang
Qingyuan Yang
Yintao Li

Hindawi
Journal of Oncology
Volume 2019, Article ID 4325105, 14 pages
https://doi.org/10.1155/2019/4325105

Review Article

DNA Repair Deficiency in Breast Cancer: Opportunities for Immunotherapy

Elaine Gilmore,[1] Nuala McCabe,[1,2] Richard D. Kennedy,[1,2] and Eileen E. Parkes[1]

[1]*Queen's University Belfast, Centre for Cancer Research and Cell Biology, 97 Lisburn Road, Belfast BT9 7AE, UK*
[2]*Almac Diagnostics, 20 Seagoe Road, Craigavon BT63 5QD, UK*

Correspondence should be addressed to Eileen E. Parkes; e.parkes@qub.ac.uk

Received 22 February 2019; Revised 4 May 2019; Accepted 29 May 2019; Published 19 June 2019

Guest Editor: Zhihua Kang

Historically the development of anticancer treatments has been focused on their effect on tumor cells alone. However, newer treatments have shifted attention to targets on immune cells, resulting in dramatic responses. The effect of DNA repair deficiency on the microenvironment remains an area of key interest. Moreover, established therapies such as DNA damaging treatments such as chemotherapy and PARP inhibitors further modify the tumor microenvironment. Here we describe DNA repair pathways in breast cancer and activation of innate immune pathways in DNA repair deficiency, in particular, the STING (STimulator of INterferon Genes) pathway. Breast tumors with DNA repair deficiency are associated with upregulation of immune checkpoints including PD-L1 (Programmed Death Ligand-1) and may represent a target population for single agent or combination immunotherapy treatment.

1. Introduction

Each individual cell endures hundreds of thousands of insults to its DNA each day [1]. Genomic instability is a pervasive feature associated with tumor cells and is the result of an accumulation of DNA damage within a cell [2]. Damage to DNA is triggered by many factors such as the generation of reactive oxidative species during metabolism (endogenous damage) and exposure to harmful environmental stimuli such as cigarette smoke or chemotherapy (exogenous damage) [3]. Efficient DNA damage responses such as cell cycle arrest and repair are therefore essential in order to maintain genomic integrity and stability [2].

DNA repair deficiency, in particular defects affecting the homologous recombination and Fanconi Anemia/BRCA repair pathway, is estimated to occur in 25% of breast cancers [4]. Notably, an estimated 60–69% of triple negative breast cancers (with absence of oestrogen receptor (ER) progesterone receptor (PR) as well as nonamplified HER2) are reported to have a defect in DNA repair, with features in common with BRCA1/2 mutated tumors described as "BRCAness" [5, 6].

Although loss of DNA repair pathways can result in tumor development, they can be exploited using targeted therapies. Moreover, the interaction of DNA damage with immune system activation and evasion provides novel therapeutic opportunities.

The roles of the host immune system and tumor microenvironment are now recognised as being crucial to the response to anticancer therapy [7]. The presence of infiltrating lymphocytes has been associated with improved outcomes in breast, ovarian, lung, colorectal and oropharyngeal cancers, and melanoma [8–11]. Notably triple negative breast cancer (TNBC) has been correlated with higher levels of lymphocytic infiltration compared to other subtypes of breast cancer [12]. Expression of the immune checkpoint Programmed cell Death Ligand-1 (PD-L1) is also increased in TNBC compared to non-TNBC [13].

The IMpassion130 study of the PD-L1 targeting antibody atezolizumab in combination with nab-paclitaxel demonstrated a significant improvement in overall survival in PD-L1 positive TNBC (22.0 vs 15.5 months) indicating the potential clinical impact of exploiting immunotherapies in this subgroup of breast cancer [14]. However, responses to

immunotherapy are not restricted to TNBC, with responses observed in the neoadjuvant setting in both TNBC and hormone-receptor positive breast cancer [15], and in PD-L1 positive trastuzumab-resistant HER2 positive breast cancer [16].

A deeper understanding of the interconnectivity between DNA repair deficiency and immune response will enable rational trial design of single agent and combination immune checkpoint targeting therapies. Here we discuss how tumor cell intrinsic immune responses to loss of DNA repair result in modification of the tumor microenvironment and are associated with lymphocytic infiltration. In addition, chronic stimulation of immune pathways as a result of DNA repair deficiency favours an immunosuppressive microenvironment, with immune checkpoint upregulation, and may predict response to immune checkpoint blockade.

2. DNA Damage Repair Pathways

A series of interconnecting pathways exist within cells which function to repair DNA damage [17]. Although the DNA damage response is composed of different repair mechanisms which target distinct types of damage, they all encompass similar coordinated processes to detect DNA damage, recruit repair factors at the site, and then physically repair the damaged DNA [17].

In cancer cells, DNA repair mechanisms can be dysfunctional which leaves cells dependent on remaining pathways and therefore particularly vulnerable to therapies which target these specific pathways (Table 1) [18].

2.1. Base Excision Repair. Subtle changes to DNA such as single-strand breaks (SSBs) are repaired via the base excision repair (BER) mechanism [19]. This method of repair involves the removal of damaged bases form the double helix and the excision of the damaged section from the DNA structure [19]. Single nucleotide polymorphisms (SNPs) in members of the base excision repair pathway, XRCC1 and APE1, have been reported as contributing to increased risk of breast cancer, although population studies have not yielded consistent results [20, 21].

2.2. Nucleotide Excision Repair. Nucleotide excision repair (NER) is the mechanism responsible for the repair of single-strand lesions which cause a structural distortion within the DNA double helix [22]. Nucleotides surrounding the damaged site are excised and replaced by DNA replication machinery [17]. Defects in NER have been identified in early stage breast cancer and also reported to contribute to increased breast cancer risk women with exposure to cigarette smoke [23, 24].

2.3. Mismatch Repair. During replication, base mismatches can occur which distort the helical DNA structure [25]. These distortions are recognised by DNA damage response machinery which initiates the excision of the mismatched DNA, and the damaged site is then replaced with newly synthesised DNA [25]. Defects in mismatch repair (MMR) machinery are rarely seen in breast cancer, affecting 0.8–1.7% of women with breast cancer [26, 27] whereas MMR defects are seen in 15% of sporadic colorectal cancers [28]. There is now a known association between mismatch repair mutation and microsatellite instability with response to immune checkpoint therapies such as anti-PD-1; therefore identifying these women may be of clinical importance [29].

2.4. Nonhomologous End Joining. The repair mechanism nonhomologous end joining (NHEJ) is a simpler pathway which functions throughout the cell cycle to repair DSBs [30]. Repair is mediated by ligating the ends of the broken DNA strands together and therefore is prone to high rates of DNA deletion and mutation [17]. Two distinct NHEJ pathways are identified: classical and alternative NHEJ. Alternative NHEJ is a less-well-defined process which has been shown to have a higher probability of causing translocations and large deletions [31]. When faithful repair, via homologous recombination, is lost by mutation or epigenetic alterations to this pathway, repair of double-strand breaks is performed by NHEJ [32].

2.5. Homologous Recombination. Homologous recombination (HR) is one of the repair pathways responsible for the detection and repair of double-strand breaks (DSBs) [33, 34]. This mechanism of repair is often described as conservative as the original DNA sequence is restored at the damaged lesion [35]. The process of HR is largely restricted to the S and G2 phase of the cell cycle [36]. Nucleotides are excised both upstream and downstream of the damaged site and new DNA is synthesised using the homologous sister chromatid as a template [37]. HR defects occur in between 25 and 40% of breast cancers, from both germline and somatic mutations of key components of the HR pathway such as *BRCA1/BRCA2* [4, 6].

2.6. Fanconi Anemia/BRCA Pathway Loss. The Fanconi Anemia (FA)/BRCA pathway is a complex mechanism that involves the function of 19 genes and reestablishes DNA replication following DNA damage through the coordination of NER, translesional synthesis, and HR [38]. The FA/BRCA pathway is lost in approximately 25% of breast cancers due to mutation or silencing of one of constituent genes [4].

BRCA1 was the first identified breast cancer susceptibility gene [39, 40] and is currently the newest member of the FA family. Biallelic mutations in *BRCA1* (typically embryonically lethal) were identified in a patient with early onset ovarian cancer with hypersensitivity to platinum based treatment and therefore deemed a new subtype of Fanconi Anemia (FANCS) [41]. *BRCA2* (*FANCD1*) was identified as a FA family member in 2002, following sequencing of *BRCA1* and *BRCA2* in cells from patients with FANCB and FANCD1 [42]. Mutations in other FA family members have been demonstrated to predispose to breast cancer, including *PALB2 (FANCN), BRIP1 (FANCJ), RAD51C (FANCO), SLX4 (FANCP),* and *FANCM* [43–50]. In summary, of the identified genes predisposing to hereditary breast cancer, the majority are FA family members.

Table 1: DNA repair pathways mutated in breast cancer and potential therapeutic interventions.

DNA Repair Pathway	*Defective mutation in Breast Cancer*	*Therapeutic Intervention*
Homologous recombination	BRCA1, BRCA2, ATM, ATR, CHK1, CHK2, BARD1, RAD51D, NBS1, PALB2, FANCD2, CtIP, PALB2 [17, 51–54]	Platinum based chemotherapies [55], PARP inhibitors (immune checkpoint blockade)
Non-homologous end-joining	DNA-PK, KU70/80 [56]	DNAPK inhibitors, ionizing radiation
Mismatch repair	MLH1, MSH2, MSH6, PMS2 [57, 58]	Immune checkpoint blockade
Base excision repair, Nucleotide excision repair, Translesional synthesis	APE1, XRCC1, ERCC2 [59, 60]	APE1 inhibitors [61]

2.7. Somatic Mutations of DNA Repair Genes in Breast Cancer. While *BRCA1* and *BRCA2* are highly penetrant germline cancer predisposition genes, associated with familial breast cancers, somatic alterations also affect these genes [78–81]. Somatic mutations of the FA pathway also occur frequently in cancer and have been reported in 11.2% of breast cancers [82]. Promoter hypermethylation of *BRCA1* has been reported in 13% of sporadic breast tumors [83], with promoter hypermethylation of *FANCC (PALB2), FANCO (RAD51C),* and *FANCF* also reported [84–86]. Collectively, somatic and germline mutations and alternations of BRCA and related HR genes result in a phenotype termed "BRCAness" [87]. However, there may be significant clinical variation in how germline vs somatic mutations and alterations behave in response to therapy, exemplified by improved response to carboplatin vs docetaxel observed in patients with germline *BRCA1* mutations but not in those with BRCA1 methylation or low mRNA expression [55]. However, while novel methods may allow variants of unknown significance and novel mutations of unknown pathogenic impact to be more clearly classified [88], taking this phenotypic approach to classification of *BRCA*-mutant-like HR-deficient cancers allows for clinical trial design targeting this subgroup of breast cancer.

2.8. Transcriptomic Identification of DNA Repair Deficiency. Tumors with loss of the FA/BRCA DNA repair pathway are sensitive to DNA damaging agents that cross-link DNA and stall DNA replication such as alkylating agents and anthracyclines. We previously identified a gene expression signature assay capable of prospectively identifying this distinct molecular subgroup of breast cancer patients with loss of the FA/BRCA pathway who benefited from chemotherapy [89]. Importantly, characterisation of the genes activated by loss of the FA/BRCA pathway revealed interferon-type immune gene signalling [90].

Consistent with this observation, both *BRCA1* and *BRCA2* mutant breast cancers are known to be associated with lymphocytic infiltration [91, 92]. Cell line modelling demonstrates that loss of *BRCA1/2* results in upregulation of interferon related genes [93, 94]. Importantly the CXCL10/CXCR3 axis is activated in *BRCA*-mutant breast cancer and has been implicated in breast cancer progression and metastasis in both *in vivo* and clinical studies [95, 96].

3. Immune Response in Breast Cancer

A number of clinical trials have reported a favourable predictive and prognostic value of tumor infiltrating lymphocytes (TILs) in different pathological subtypes of breast cancer [9, 97, 98]. Lymphocytic infiltration is particularly recognised in tumors associated with genomic instability, such as those with a *BRCA1* mutation [4, 91]. Increasing presence of TILs has been correlated with improved recurrence free survival following chemotherapeutic treatment of triple negative and HER2+ breast cancers [99]. In TNBC, a phase III clinical trial reported that each consecutive 10% increase in intratumoral and stromal TILs resulted in 15% reduced risk of recurrence and 17% reduced risk of cancer related death, irrespective of the type of chemotherapy administered [100]. However, in the same study increased TILs were predictive of poorer outcome in ER positive HER2 negative breast cancer. Notably, high FoxP3+ T-regulatory cells (T_{regs}) have been associated with poorer outcomes in ER positive disease, yet improved outcomes in ER negative breast cancer [101, 102]. Examining lymphocytic infiltration as a whole may overlook the subtle effects of the different populations of lymphocytes present in the tumor and stroma.

Whereas BRCA1/2 mutant breast tumors have been recognised to be associated with increased lymphocytic infiltrate [87], early data suggests that loss of other DNA repair response proteins (for example, ATM) results in a markedly altered immune response and tumor microenvironment, with low levels of tumor infiltrating lymphocytes [103]. The evolution of the term "BRCAness" to describe a BRCA-mutant phenotype in tumors without BRCA1/2 mutations has enabled classification of this important subgroup of breast cancer but may overlook subtle differences in immune responses that may vary depending on specific "BRCAness" associated alterations. For example, although it is known that loss of heterozygosity may have a greater influence on tumor

behavior than biallelic alterations resulting from two somatic events [88], the exact impact biallelic vs monoallelic alterations of HR-related genes may have on immune activation and response to immune blockade is unknown.

Despite the T-cell immune infiltration commonly present in *BRCA*-mutant and DNA damage response deficient breast cancers, tumor growth and invasion continue. Therefore DNA repair deficient tumors develop mechanisms of bypassing the antitumorigenic immune response, thriving in an inflamed microenvironment. The chronic inflammation mediated by DNA repair deficiency within the tumor microenvironment promotes cellular proliferation and invasion and, in addition, dysregulated pathways of immune equilibrium, thereby promoting immunosuppression [104–106].

3.1. STING Activation in DNA Damage Response Deficiency. Defects in DNA repair genes including *BRCA1* and *ATM* have been shown to result in constitutive activation of the STimulator of INterferon Genes (STING) pathway in response to accumulation of cytosolic DNA [90, 107, 108]. Failed DNA repair results in the formation of micronuclei, within which cyclic GMP-AMP synthase (cGAS) colocalises with damaged DNA [109, 110]. Ruptured micronuclei result in activation of cGAS with subsequent synthesis of 2'3'-cGAMP which potently activates the STING pathway [111, 112]. Downstream activation of TANK-binding kinase 1 (TBK1) and interferon regulatory factor 3 (IRF3) then occurs, as well as canonical and noncanonical NFκB pathways, resulting in upregulation of interferon stimulated genes [113, 114]. Interestingly, as well as activation of the STING pathway in DNA repair deficient cells, DNA damaging chemotherapies (including irinotecan, doxorubicin, and etoposide) and radiotherapy have similarly been demonstrated to activate the cGAS-STING immune response pathway [115–117].

STING agonists are now in early phase clinical trials in combination with immune checkpoint therapies based on their ability to induce immune responses in solid tumors [118, 119]. Activation of the cytosolic RNA-sensing RIG-I pathway has also been identified in breast cancer treated with doxorubicin [120], and similarly to STING agonists, RIG-I agonists are also in clinical development, with immunostimulatory effects on the tumor microenvironment and tumor clearance in murine models [121].

STING agonists cause upregulation of immune checkpoints including PD-L1 in the microenvironment [122], and upregulation of PD-L1 in response to DNA damage has been shown to be dependent on STING [90, 123]. PD-L1 expressing tumors (with PD-L1 identified on infiltrating immune cells ± epithelial cells) are more likely to respond to targeted immune therapies.

However, STING activation following radiotherapy has been shown to drive infiltration of immunosuppressive myeloid derived suppressor cells (MDSCs) [124]. In breast cancer, infiltration of MDSCs has been reported to promote progression and metastasis and may mediate resistance to immunotherapies [125]. Whether infiltration of these immunosuppressive cells is mediated by STING activation in breast cancer remains unclear. STING pathway activation may therefore have dichotomous effects on the tumor microenvironment. While STING activation in the acute phase is typically recognised to have an antitumorigenic immunogenic effect, chronic cGAS-STING activation may in fact result in an immunosuppressive microenvironment, activating the senescence associated secretory phenotype [126–128] and upregulation of immune checkpoints [90]. Moreover, chronic activation of cGAS-STING in chromosomally unstable tumors has been shown to result in STING-dependent metastasis [129]. The potential role of the STING pathway in the tumor immune microenvironment is illustrated in Figure 1.

3.2. Immune Checkpoints in Breast Cancer. Immune checkpoints are a number of inhibitory pathways within the immune system responsible for maintaining self-tolerance and modulation of the immune response [130]. Studies have reported that tumors are able to select particular immune checkpoint pathways to evade the immune system, particularly T-cells which target tumor antigens. This results in immune checkpoint proteins being frequently dysregulated in cancer [131].

When an antigen is recognised by the T-cell receptor, an immune response is initiated and then regulated by immune checkpoints via inhibitory and costimulatory signals [132]. Costimulatory receptor agonists or antagonists of inhibitory signals augment antigen-specific T-cell responses [133].

Although other forms of immunotherapy are also used in the clinical setting, the use of immune checkpoint targeted therapies has undoubtedly been remarkably successful, unleashing the potential of the antitumor immune response and revolutionising the management of human cancers [134]. Targeting the PD-1/L1 axis has been most fruitful in clinical trials, with many ongoing combination studies now using PD-1/L1 as a backbone of therapy (Table 2).

3.3. PD-1 and Ligands PD-L1/PD-L2. PD-1 is a transmembrane inhibitory coreceptor. Expression of PD-1 on T-cells and PD-L1 ligand interaction has been shown to have immunosuppressive functions in the tumor microenvironment [135]. PD-L2 expression is much more restricted than PD-L1 and so is mainly found on the surface of Antigen Presenting Cells (APCs) associated with its role in regulating the priming of T-cells [136].

PD-L1 expression is reported to be upregulated across a range of cancer types including breast, gastric, and lung cancers, although the significance of PD-L1 on prognosis and outcome remains uncertain in breast cancer [137, 138]. In the tumor microenvironment, PD-1/PD-L1 interaction results in T-cell death and inhibition of cytotoxic T-cell function [139]. Additionally, immunosuppressive Interleukin-10 (IL-10) production is stimulated [140]. Furthermore, PD-L1 expression enhances the conversion of helper T-cells (T_h1) into immunosuppressive T_{regs} [141, 142]. Inhibiting the PD-1/PD-L1 pathway using PD-1 or PD-L1 targeting antibodies restores lymphocyte function and therefore cytotoxicity [143].

Table 2: Current and completed clinical trials of immune checkpoint inhibition in breast cancer.

Immunotherapy	*Subtype*	*Target*	*Combination*	*Study*	*Phase*
Pembrolizumab	TNBC ER+/HER2-	PD-1	Single agent	NCT02555657 KEYNOTE-119 [62]	3
Pembrolizumab	BRCA mutated	PD-1	Single Agent	NCT03025035	2
Pembrolizumab	TNBC ER+/HER2-	PD-1	Single agent	NCT02447003 KEYNOTE-086 [63]	2
Pembrolizumab	TNBC ER+/HER2-	PD-1	Single agent	NCT01848834 KEYNOTE-012 [64]	1B
Pembrolizumab	TNBC ER+/HER2-	PD-1	Single agent	NCT02054806 KEYNOTE-028 [65]	1
Pembrolizumab	ER/PR-	PD-1	Single Agent	NCT03197389	1
Pembrolizumab	TNBC and HR+HER2-	PD-1	Decitabine + Soc NACT	NCT02957968	2
Pembrolizumab	TNBC	PD-1	EDP1503	NCT03775850	2
Pembrolizumab	TNBC	PD-1	Imprime PGG	NCT02981303	2
Pembrolizumab	HR+HER2-	PD-1	Eribulin	NCT03222856 KELLY [66]	2
Pembrolizumab	TNBC	PD-1	Chemotherapy	NCT01042379 I-SPY 2 [64, 67]	2
Pembrolizumab	TNBC	PD-1	Galinpepimut-S	NCT03761914	2
Pembrolizumab	TNBC	PD-1	Nab-paclitaxel + Epirubicin + Cyclophosphamide	NCT03289819	2
Pembrolizumab	TNBC	PD-1	Chemotherapy	NCT02622074 KEYNOTE-173 [68]	1B
Pembrolizumab	ER+HER2- / TNBC	PD-1	Radiation Radiation	NCT03366844	1
Pembrolizumab	Metastatic BC	PD-1	High Intensity Ultrasound	NCT03237572	1
Pembrolizumab	All	PD-1	Stereotactic Ablative Radiosurgery	NCT02303366 BOSTON II	1
Pembrolizumab	TNBC	PD-1	PVX-410 vaccine	NCT03362060	1
PDR001	TNBC	PD-1	Canakinumab CJM112 Trametinib EGF816	NCT02900664	1B
PDR001	TNBC	PD-1	LCL161 Everolimus Panobinostat QBM076	NCT02890069	1
PDR001	TNBC	PD-1	NZV930 NZV930 + NIR178	NCT03549000	1
Durvalumab	TNBC	PD-L1	Single agent Taxane-anthracycline chemotherapy	NCT02685059 GeparNuevo [69]	2
Durvalumab +/- Tremelimumab	All	PD-L1 +/- CTLA-4	Poly ICLC	NCT02643303	2
Durvalumab	BRCA mutated HER2-	PD-L1	Olaparib +Bevacizumab	NCT02734004 MEDIOLA [70]	2
Durvalumab	TNBC	PD-L1	Paclitaxel and Carboplatin	NCT03616886 SYNERGY	2
Durvalumab	BRCA mutated HER2-	PD-L1	Olaparib	NCT02734004 MEDIOLA [70]	1

Table 2: Continued.

Immunotherapy	*Subtype*	*Target*	*Combination*	*Study*	*Phase*
Durvalumab	TNBC	PD-L1	Paclitaxel, Carboplatin and Oleclumab	NCT03616886 SYNERGY	1
Durvalumab	TNBC	PD-L1	Cediranib Olaparib Cediranib + Olaparib	NCT02484404	1
Atezolizumab	TNBC	PD-L1	Single agent	NCT01375842 [71]	1
Atezolizumab	TNBC	PD-L1	Nab-paclitaxel	NCT02425891 IMpassion130 [14]	3
Atezolizumab	HER2+	PD-L1	Trastuzumab Emtansine	NCT02924883 KATE2 [72]	2
Atezolizumab	TNBC	PD-L1	Cabozantinib	NCT03170960	1B
Atezolizumab	TNBC	PD-L1	RO7198457	NCT03289962	1
Nivolumab	TNBC	PD-L1	Romidepsin + Cisplatin	NCT02393794	2
Nivolumab	TNBC	PD-L1	Capecitabine	NCT03487666 OXEL [73]	2
Nivolumab	Metastatic	PD-L1	Nab-paclitaxel	NCT02309177	1
Nivolumab	All	PD-L1	COM701	NCT03667716	1
Avelumab	TNBC	PD-L1	Additional	NCT02926196 A-Brave [74]	3
Avelumab	TNBC	PD-L1	Utomilumab	NCT02554812 JAVELIN [75]	2
Avelumab	All	PD-L1	Utomilumab +/- Radiation Utomilumab + PF-04518600 PF-04518600 +/- Radiation Utomilumab + PF-04518600 + Radiation Cisplatin + Radiation	NCT03217747	2
FAZ053	TNBC	PD-L1	Single Agent PDR001	NCT02936102	1
LY3300054	HR+HER2-	PD-L1	Single Agent Ramucirumab Abemaciclib Merestinib LY3321367	NCT02791334	1
Tremelimumab	TNBC	CTLA-4	Monotherapy	NCT02527434 [76]	2
MSB0011359C	ER+ and/or PR+, HER2-	PD-L1 and TGF-β	Radiation	NCT03524170 RACHEL 1	1
LAG525	TNBC	LAG3	Single agent PDR001 / Carboplatin or combination	NCT03499899	2
Toripalimab	TNBC	PD-1	Single Agent	NCT02838823	1
TT1-621	All	CD47	Single Agent +PD1/PDL1 inhibitor +Pegylated interferon- α2a +T-Vec +Radiation	NCT02890368	1
Ipilimumab + Nivolumab	HER2-	CTLA-4 PD-1	Bicalutamide	NCT03650894	2

Table 2: Continued.

Immunotherapy	*Subtype*	*Target*	*Combination*	*Study*	*Phase*
Ipilimumab + Nivolumab	HER2-	CTLA-4 PD-1	--	NCT03789110 NIMBUS	2
Epacadostat + Pembrolizumab	All	IDO-1 PD-1	INCAGN01876 (anti-GITR)	NCT03277352	1/2
Ipilimumab + Nivolumab	All	PD-1 PD-L1	Entinostat	NCT02453620	1
Nivolumab + Pembrolizumab + Atezolizumab	HER2+	PD-L1 PD-1 PD-L1	FT500 (Natural Killer cell)	NCT03841110	1
Ipilimumab + Nivolumab	All	CTLA-4 + PD-L1	Cryoablation	NCT02833233 [77]	N/A

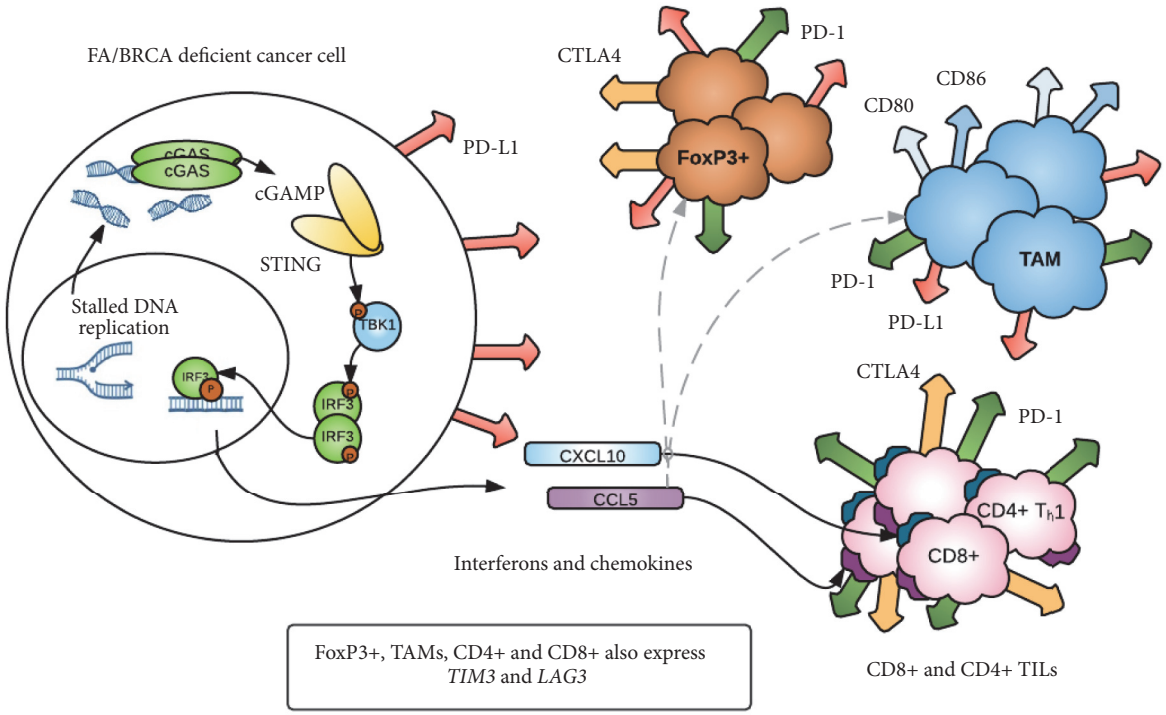

Figure 1: STING pathway activation in DNA repair deficient breast cancer. Stalled replication forks or damaged DNA as a result of mutations in Fanconi Anemia/BRCA repair pathway genes results in cytosolic DNA, detected by cGAS. 2'3'-cGAMP is produced, which then activates STING. STING dimerises or oligomerises, and TBK1 and IRF3 are phosphorylated. IRF3 then translocates to the nucleus resulting in the expression of immune genes including CXCL10 and CCL5. Note: other downstream activators of the STING pathway, notably TRAF6 and NFκB, are not shown in this instance. CXCL10 and CCL5 are implicated in chemoattraction of CD8+ and CD4+ T-cells. However the tumor microenvironment may also contain immunosuppressive FoxP3+ CD4+ cells which express CTLA4, PD-1, PD-L1, LAG3, and TIM3; tumor-associated macrophages (TAMs) which express PD-1, PD-L1, CD80 and CD86, LAG3, and TIM3. Tumor infiltrating lymphocytes (TILs) may express CTLA4, PD-1, TIM3, and LAG3. Therefore, DNA repair deficiency results in activation of the cGAS-STING pathway which has both antitumorigenic and protumorigenic effects within the tumor microenvironment.

PD-L1 has been reported to be expressed epithelial cells in 20% of triple negative breast cancers [13] and has been proposed as a biomarker of response to immunotherapy. However the failure to respond in PD-L1 positive breast tumors (in up to 75% depending on the treatment setting) and the observed response in some PD-L1 low or negative tumors indicate that other markers of response need to be identified [134, 144]. The most promising of these in solid tumors has been the presence of microsatellite instability, leading to approval of immune checkpoint therapy in all advanced solid tumors with mismatch repair defects [145]. However, as discussed above, the incidence of these defects

in breast cancer is low. Similarly tumor mutational burden (TMB) is a promising biomarker in other solid tumors, but most breast cancers do not typically demonstrate increased TMB [146].

Increased PD-L1 expression is identified in breast tumors deficient in DNA repair, and infiltrating immune-cell PD-1 and PD-L1 expression is higher in breast cancers with *BRCA1* or *BRCA2* mutations [90, 147]. Treatment with the DNA damaging agent doxorubicin results in increased expression of PD-L1 on breast cancer cells [148]. Interestingly, STING agonists given in combination with anti-PD-1 treatment result in improved responses in preclinical models [122].

Therefore, a close relationship is observed between DNA repair deficiency and upregulation of PD-L1 expression. Breast cancers with DNA repair deficiency, or BRCAness, may benefit from single agent immunotherapy targeting this pathway. However, independent of BRCAness, treatment of breast cancers with DNA damaging agents in combination with anti-PD-1/PD-L1 targeted therapy may result in enhanced tumor responses.

4. Immunotherapy in Breast Cancer

In metastatic TNBC, the combination of PD-L1 targeting atezolizumab with nab-paclitaxel resulted in a median 9.5-month improvement in overall survival (HR 0.62, 95% CI 0.45–0.86) in patients with PD-L1 positive immune infiltration [14]. In early stage breast cancer, neoadjuvant treatment of TNBC with anti-PD-1 in combination with chemotherapy resulted in an increase in pathological complete response (pCR) rates of 40% above expected [15]. These promising results indicate the potential of immunotherapy in breast cancer, although single agent anti-PD-1 treatment in the metastatic setting has not demonstrated a similar magnitude, with response rates of less than 20% in unselected advanced triple negative breast cancer, supporting combination approaches in future clinical trials [149].

Over 50 immune checkpoint therapy single agent and combination trials are ongoing in breast cancer, summarised in Table 2. The rate of translating these promising preclinical findings into the clinic is highly commendable and offers many patients a much-needed treatment option. However, the lack of an effective biomarker to select patients for immune checkpoint therapy exposes many patients who may derive no benefit from treatment to the risk of potentially serious immune mediated side effects, such as colitis, pneumonitis, liver toxicity, and durable endocrine effects including hypophysitis [150].

4.1. PARP Inhibitor and Immunotherapy Combinations in Breast Cancer. Poly(ADP-ribose) polymerase (PARP) inhibitors (inhibiting PARP1, involved in base excision repair) initially demonstrated efficacy in potentiating the effects of DNA damagers such as temozolomide [151]. Subsequently treatment with PARP inhibitors was found to result in synthetic lethality in BRCA1/2 mutant tumors [152, 153] and the PARP inhibitors olaparib and talazoparib are now FDA-approved as monotherapy treatments in BRCA1/2 mutant advanced breast cancer [154, 155].

As discussed above, the immune microenvironment of DNA repair deficient tumors is typically immunosuppressive with an exhausted T-cell infiltrate expressing high levels of checkpoints. However, as described by Yap and colleagues, the targeted cell death caused by PARP inhibitors has the potential to "reset" the tumor microenvironment and polarise the immune response towards a T_{h1} antitumorigenic profile, resulting in a shift from immune escape to elimination of the tumor [156]. Therefore PARP inhibitors represent a promising combination therapy with immune checkpoint targeting therapies.

PARP inhibitors have now been demonstrated in a number of preclinical studies to activate the innate immune cGAS-STING pathway [157–160]. These studies have further elucidated the mechanism of action of PARP inhibitors beyond synthetic lethality. Strikingly, treatment *in vivo* with the PARP inhibitor talazoparib in immunocompromised compared to immunocompetent models results in diminished responses [157]. Moreover, STING-dependent infiltration of CD8+ T-cells was demonstrated to be required for response to the PARP inhibitor olaparib [160]. These preclinical studies build a strong case for PARP inhibitor–immune checkpoint combination studies and the crucial role of the STING pathway in mediating immune responses. Interestingly these studies demonstrate a PARP inhibitor driven immune response in both HR-deficient and -proficient models [157, 160], supporting the rationale for PARP-immune checkpoint combinations beyond BRCA-mutant or HR-deficient disease.

In breast cancer, the combination of olaparib and durvalumab resulted in an overall response rate of 63% (95% CI 44–80%) at 28 weeks in 30 patients with germline BRCA1/2 mutations [161]. These promising results have led to the expansion of this study beyond germline BRCA-mutant disease to encompass homologous recombination deficient cancers [70]. In advanced TNBC the combination of niraparib and pembrolizumab demonstrated clinical benefit in 20 out of 46 patients, notably including 4 patients with no identified HR defect or detectable PD-L1 expression [162]. While it is likely that the dual combination of PARP inhibition and immune checkpoint blockade results in most marked responses in DNA repair deficient cancers, the addition of a third immune-stimulating or targeted agent may enhance responses in repair competent tumors. For example, the addition of antiangiogenic therapy may further stimulate an antitumorigenic immune response by inhibiting immunosuppressive effects of VEGF-A, which promotes infiltration of MDSCs and T_{regs} and prevents dendritic cell maturation [163]. A number of triplet combination studies, including PARPi, antiangiogenic and immune checkpoint blockade, are ongoing (Table 2).

5. Conclusions

It is clear that the immune system plays a significant role in tumor development, progression, and also response to therapy. Immune checkpoints are implicated in the process of immunosuppression and therefore represent ideal targets for therapeutic manipulation to encourage an antitumor

immune response. As outlined here and elsewhere, there is a strong argument for the immune response to genomic instability as an independent biomarker in identifying candidates for immune targeting treatments [164].

DNA repair deficient breast cancer, identified using genomic or transcriptomic biomarkers of DNA repair, is associated with upregulation of immune checkpoints and an immune-cell infiltrated microenvironment. While activation of immune pathways such as STING in the acute phase promotes an antitumorigenic response, in the chronic phase DNA damage repair deficient tumors instead exploit this STING-mediated immune response, tailoring this to promote a proinvasive microenvironment favouring tumor growth. Moreover, this immune microenvironment can be further hijacked by chronic stimulation of pathways such as the senescence associated secretory phenotype, again favouring immunosuppression and immune escape [165].

As the immune microenvironment of chronically inflamed DNA repair deficient cancer consists of both antitumorigenic and immunosuppressive cell populations, therapies which therefore enhance the antitumor immune infiltration and activation, in combination with immune checkpoint therapies, represent a promising treatment strategy.

Conflicts of Interest

Richard D. Kennedy and Nuala McCabe are employees of Almac Diagnostics.

Authors' Contributions

Eileen E. Parkes, Richard D. Kennedy, and Nuala McCabe were responsible for conceptualization; Elaine Gilmore, Nuala McCabe, Richard D. Kennedy, and Eileen E. Parkes wrote and prepared the original draft; Eileen E. Parkes, Richard D. Kennedy, Nuala McCabe, and Elaine Gilmore wrote, reviewed, and edited the manuscript; Eileen E. Parkes and Richard D. Kennedy were responsible for visualization; Eileen E. Parkes, Richard D. Kennedy, and Nuala McCabe supervised the work.

Acknowledgments

Eileen E. Parkes is supported by the Academy of Medical Sciences, the Conquer Cancer Foundation of the American Society of Clinical Oncology, and the Prostate Cancer Foundation.

References

[1] S. P. Jackson and J. Bartek, "The DNA-damage response in human biology and disease," *Nature*, vol. 461, no. 7267, pp. 1071–1078, 2009.

[2] S. Negrini, V. G. Gorgoulis, and T. D. Halazonetis, "Genomic instability—an evolving hallmark of cancer," *Nature Reviews Molecular Cell Biology*, vol. 11, no. 3, pp. 220–228, 2010.

[3] A. Tubbs and A. Nussenzweig, "Endogenous DNA damage as a source of genomic instability in cancer," *Cell*, vol. 168, no. 4, pp. 644–656, 2017.

[4] N. Turner, A. Tutt, and A. Ashworth, "Hallmarks of "BRCAness" in sporadic cancers," *Nature Reviews Cancer*, vol. 4, no. 10, pp. 814–819, 2004.

[5] E. H. Lips, L. Mulder, J. Hannemann et al., "Indicators of homologous recombination deficiency in breast cancer and association with response to neoadjuvant chemotherapy," *Annals of Oncology*, vol. 22, no. 4, pp. 870–876, 2011.

[6] S. Akashi-Tanaka, C. Watanabe, T. Takamaru et al., "BRCAness predicts resistance to taxane-containing regimens in triple negative breast cancer during neoadjuvant chemotherapy," *Clinical Breast Cancer*, vol. 15, no. 1, pp. 80–85, 2015.

[7] D. Hanahan and R. A. Weinberg, "Hallmarks of cancer: the next generation," *Cell*, vol. 144, no. 5, pp. 646–674, 2011.

[8] R. M. Bremnes, L. Busund, T. L. Kilvær et al., "The role of tumor-infiltrating lymphocytes in development, progression, and prognosis of non–small cell lung cancer," *Journal of Thoracic Oncology*, vol. 11, no. 6, pp. 789–800, 2016.

[9] S. J. Luen, R. Salgado, S. Fox et al., "Tumor-infiltrating lymphocytes in advanced HER2-positive breast cancer treated with pertuzumab or placebo in addition to trastuzumab and docetaxel: a retrospective analysis of the CLEOPATRA study," *The Lancet Oncology*, vol. 18, no. 1, pp. 52–62, 2017.

[10] J. R. Webb, K. Milne, P. Watson, R. J. deLeeuw, and B. H. Nelson, "Tumor-infiltrating lymphocytes expressing the tissue resident memory marker CD103 are associated with increased survival in high-grade serous ovarian cancer," *Clinical Cancer Research*, vol. 20, no. 2, pp. 434–444, 2014.

[11] M. J. Ward, S. M. Thirdborough, T. Mellows et al., "Tumour-infiltrating lymphocytes predict for outcome in HPV-positive oropharyngeal cancer," *British Journal of Cancer*, vol. 110, no. 2, pp. 489–500, 2014.

[12] S. Loi, S. Michiels, R. Salgado et al., "Tumor infiltrating lymphocytes are prognostic in triple negative breast cancer and predictive for trastuzumab benefit in early breast cancer: results from the FinHER trial," *Annals of Oncology*, vol. 25, no. 8, pp. 1544–1550, 2014.

[13] E. A. Mittendorf, A. V. Philips, F. Meric-Bernstam et al., "PD-L1 expression in triple-negative breast cancer," *Cancer Immunology Research*, vol. 2, no. 4, pp. 361–370, 2014.

[14] P. Schmid, S. Adams, H. S. Rugo et al., "Atezolizumab and nab-paclitaxel in advanced triple-negative breast cancer," *The New England Journal of Medicine*, vol. 379, no. 22, pp. 2108–2121, 2018.

[15] R. Nanda, M. C. Liu, C. Yau et al., "Pembrolizumab plus standard neoadjuvant therapy for high-risk breast cancer (BC): Results from I-SPY 2," *Journal of Clinical Oncology*, vol. 35, article no 506, Supplement 15, 2017.

[16] S. Loi, A. Giobbie-Hurder, A. Gombos et al., "Pembrolizumab plus trastuzumab in trastuzumab-resistant, advanced, HER2-positive breast cancer (PANACEA): a single-arm, multicentre, phase 1b–2 trial," *The Lancet Oncology*, vol. 20, no. 3, pp. 371–382, 2019.

[17] C. J. Lord and A. Ashworth, "The DNA damage response and cancer therapy," *Nature*, vol. 481, no. 7381, pp. 287–294, 2012.

[18] M. J. O'Connor, "Targeting the DNA damage response in cancer," *Molecular Cell*, vol. 60, no. 4, pp. 547–560, 2015.

[19] M. L. Hegde, T. K. Hazra, and S. Mitra, "Early steps in the DNA base excision/single-strand interruption repair pathway in mammalian cells," *Cell Research*, vol. 18, no. 1, pp. 27–47, 2008.

[20] M. Cuchra, B. Mucha, L. Markiewicz et al., "The role of base excision repair in pathogenesis of breast cancer in the Polish population," *Molecular Carcinogenesis*, vol. 55, no. 12, pp. 1899–1914, 2016.

[21] C. Patrono, "Polymorphisms in base excision repair genes: Breast cancer risk and individual radiosensitivity," *World Journal of Clinical Oncology*, vol. 5, no. 5, pp. 874–882, 2014.

[22] E. C. Friedberg, "How nucleotide excision repair protects against cancer," *Nature Reviews Cancer*, vol. 1, no. 1, pp. 22–33, 2001.

[23] J. J. Latimer, J. M. Johnson, C. M. Kelly et al., "Nucleotide excision repair deficiency is intrinsic in sporadic stage i breast cancer," *Proceedings of the National Acadamy of Sciences of the United States of America*, vol. 107, no. 50, pp. 21725–21730, 2010.

[24] L. E. Mechanic, R. C. Millikan, J. Player et al., "Polymorphisms in nucleotide excision repair genes, smoking and breast cancer in African Americans and whites: a population-based case–control study," *Carcinogenesis*, vol. 27, no. 7, pp. 1377–1385, 2006.

[25] G. M. Li, "Mechanisms and functions of DNA mismatch repair," *Cell Research*, vol. 18, no. 1, pp. 85–98, 2008.

[26] H. Davies, S. Morganella, C. A. Purdie et al., "Whole-genome sequencing reveals breast cancers with mismatch repair deficiency," *Cancer Research*, vol. 77, no. 18, pp. 4755–4762, 2017.

[27] M. E. Roberts, S. A. Jackson, L. R. Susswein et al., "MSH6 and PMS2 germ-line pathogenic variants implicated in Lynch syndrome are associated with breast cancer," *Genetics in Medicine*, vol. 20, no. 10, pp. 1167–1174, 2018.

[28] J. M. D. Wheeler, W. F. Bodmer, and N. J. McC Mortensen, "DNA mismatch repair genes and colorectal cancer," *Gut*, vol. 47, no. 1, pp. 148–153, 2000.

[29] D. T. Le, J. N. Uram, H. Wang et al., "PD-1 blockade in tumors with mismatch-repair deficiency," *The New England Journal of Medicine*, vol. 372, no. 26, pp. 2509–2520, 2015.

[30] A. J. Davis and D. J. Chen, "DNA double strand break repair via non-homologous end-joining," *Transl Cancer Res*, vol. 2, no. 3, pp. 130–143, 2013.

[31] M. Gostissa, F. W. Alt, and R. Chiarle, "Mechanisms that promote and suppress chromosomal translocations in lymphocytes," *Annual Review of Immunology*, vol. 29, no. 1, pp. 319–350, 2011.

[32] M. R. Lieber, "The mechanism of double-strand DNA break repair by the nonhomologous DNA end-joining pathway," *Annual Review of Biochemistry*, vol. 79, pp. 181–211, 2010.

[33] R. G. Sargent, M. A. Brenneman, and J. H. Wilson, "Repair of site-specific double-strand breaks in a mammalian chromosome by homologous and illegitimate recombination.," *Molecular and Cellular Biology*, vol. 17, no. 1, pp. 267–277, 1997.

[34] C. Arnaudeau, C. Lundin, and T. Helleday, "DNA double-strand breaks associated with replication forks are predominantly repaired by homologous recombination involving an exchange mechanism in mammalian cells," *Journal of Molecular Biology*, vol. 307, no. 5, pp. 1235–1245, 2001.

[35] W. D. Wright, S. S. Shah, and W.-D. Heyer, "Homologous recombination and the repair of DNA double-strand breaks," *The Journal of Biological Chemistry*, vol. 293, no. 27, pp. 10524–10535, 2018.

[36] X. Zhao, C. Wei, J. Li et al., "Cell cycle-dependent control of homologous recombination," *Acta Biochimica et Biophysica Sinica*, vol. 49, no. 8, pp. 655–668, 2017.

[37] M. E. Moynahan, T. Y. Cui, and M. Jasin, "Homology-directed DNA repair, mitomycin-C resistance, and chromosome stability is restored with correction of a Brca1 mutation," *Cancer Research*, vol. 61, no. 12, pp. 4842–4850, 2001.

[38] R. D. Kennedy and A. D. D'Andrea, "The fanconi anemia/BRCA pathway: new faces in the crowd," *Genes & Development*, vol. 19, no. 24, pp. 2925–2940, 2005.

[39] J. M. Hall, M. K. Lee, B. Newman et al., "Linkage of early-onset familial breast cancer to chromosome 17q21," *Science*, vol. 250, no. 4988, pp. 1684–1689, 1990.

[40] Y. Miki, J. Swensen, D. Shattuck-Eidens et al., "A strong candidate for the breast and ovarian cancer susceptibility gene *BRCA1*," *Science*, vol. 266, no. 5182, pp. 66–71, 1994.

[41] S. L. Sawyer, L. Tian, M. Kähkönen et al., "Biallelic mutations in BRCA1 cause a new Fanconi anemia subtype," *Cancer Discovery*, vol. 5, no. 2, pp. 135–142, 2015.

[42] N. G. Howlett, T. Taniguchi, S. Olson et al., "Biallelic inactivation of BRCA2 in Fanconi anemia," *Science*, vol. 297, no. 5581, pp. 606–609, 2002.

[43] M. Tischkowitz and B. Xia, "PALB2/FANCN: Recombining cancer and fanconi anemia," *Cancer Research*, vol. 70, no. 19, pp. 7353–7359, 2010.

[44] A. C. Antoniou, S. Casadei, T. Heikkinen et al., "Breast-cancer risk in families with mutations in PALB2," *The New England Journal of Medicine*, vol. 371, no. 6, pp. 497–506, 2014.

[45] C. Cybulski, W. Kluźniak, T. Huzarski et al., "Clinical outcomes in women with breast cancer and a PALB2 mutation: a prospective cohort analysis," *The Lancet Oncology*, vol. 16, no. 6, pp. 638–644, 2015.

[46] M. Levitus, Q. Waisfisz, B. C. Godthelp et al., "The DNA helicase BRIP1 is defective in Fanconi anemia complementation group J," *Nature Genetics*, vol. 37, no. 9, pp. 934-935, 2005.

[47] O. Levran, C. Attwooll, R. T. Henry et al., "The BRCA1-interacting helicase BRIP1 is deficient in Fanconi anemia," *Nature Genetics*, vol. 37, no. 9, pp. 931–933, 2005.

[48] Y. Kim, G. S. Spitz, U. Veturi, F. P. Lach, A. D. Auerbach, and A. Smogorzewska, "Regulation of multiple DNA repair pathways by the Fanconi anemia protein SLX4," *Blood*, vol. 121, no. 1, pp. 54–63, 2013.

[49] S. Shah, Y. Kim, I. Ostrovnaya et al., "Assessment of SLX4 mutations in hereditary breast cancers," *PLoS ONE*, vol. 8, no. 6, Article ID e66961, 2013.

[50] J. I. Kiiski, L. M. Pelttari, S. Khan et al., "Exome sequencing identifies FANCM as a susceptibility gene for triple-negative breast cancer," *Proceedings of the National Acadamy of Sciences of the United States of America*, vol. 111, no. 42, pp. 15172–15177, 2014.

[51] J. S. Brown, B. O'Carrigan, S. P. Jackson, and T. A. Yap, "Targeting DNA repair in cancer: beyond PARP inhibitors," *Cancer Discovery*, vol. 7, no. 1, pp. 20–37, 2017.

[52] T. Aparicio and J. Gautier, "BRCA1-CtIP interaction in the repair of DNA double-strand breaks," *Molecular & Cellular Oncology*, vol. 3, no. 4, Article ID e1169343, 2016.

[53] K. J. Patel, "Fanconi anemia and breast cancer susceptibility," *Nature Genetics*, vol. 39, no. 2, pp. 142-143, 2007.

[54] R. Roy, J. Chun, and S. N. Powell, "BRCA1 and BRCA2: Different roles in a common pathway of genome protection," *Nature Reviews Cancer*, vol. 12, no. 1, pp. 68–78, 2012.

[55] A. Tutt, H. Tovey, M. C. Cheang et al., "Carboplatin in BRCA1/2-mutated and triple-negative breast cancer BRCAness subgroups: the TNT Trial," *Nature Medicine*, vol. 24, no. 5, pp. 628–637, 2018.

[56] B. J. Sishc and A. J. Davis, "The role of the core non-homologous end joining factors in carcinogenesis and cancer," *Cancers (Basel)*, vol. 9, no. 7, 2017.

[57] H. Murata, N. H. Khattar, L. Gu, and G. Li, "Roles of mismatch repair proteins hMSH2 and hMLH1 in the development of sporadic breast cancer," *Cancer Letters*, vol. 223, no. 1, pp. 143–150, 2005.

[58] N. Benachenhou, S. Guiral, I. Gorska-Flipot, D. Labuda, and D. Sinnett, "Frequent loss of heterozygosity at the DNA mismatch-repair loci hMLH1 and hMSH3 in sporadic breast cancer," *British Journal of Cancer*, vol. 79, no. 7-8, pp. 1012–1017, 1999.

[59] P. Chacko, B. Rajan, T. Joseph, B. S. Mathew, and M. Radhakrishna Pillai, "Polymorphisms in DNA repair gene XRCC1 and increased genetic susceptibility to breast cancer," *Breast Cancer Research and Treatment*, vol. 89, no. 1, pp. 15–21, 2005.

[60] M. Majidinia and B. Yousefi, "DNA repair and damage pathways in breast cancer development and therapy," *DNA Repair*, vol. 54, pp. 22–29, 2017.

[61] F. Shah, D. Logsdon, R. A. Messmann, J. C. Fehrenbacher, M. L. Fishel, and M. R. Kelley, "Exploiting the Ref-1-APE1 node in cancer signaling and other diseases: from bench to clinic," *npj Precision Oncology*, vol. 1, no. 1, article no 19, 2017.

[62] H. S. Rugo, J.-P. Delord, S.-A. Im et al., "Safety and antitumor activity of pembrolizumab in patients with estrogen receptor–positive/human epidermal growth factor receptor 2–negative advanced breast cancer," *Clinical Cancer Research*, vol. 24, no. 12, pp. 2804–2811, 2018.

[63] S. Adams, P. Schmid, H. S. Rugo et al., "Pembrolizumab monotherapy for previously treated metastatic triple-negative breast cancer: cohort A of the phase II KEYNOTE-086 study," *Annals of Oncology*, vol. 30, no. 3, pp. 397–404, 2019.

[64] R. Nanda, L. Q. M. Chow, E. C. Dees et al., "Pembrolizumab in patients with advanced triple-negative breast cancer: Phase Ib keynote-012 study," *Journal of Clinical Oncology*, vol. 34, no. 21, pp. 2460–2467, 2016.

[65] C. Solinas, A. Gombos, S. Latifyan, M. Piccart-Gebhart, M. Kok, and L. Buisseret, "Targeting immune checkpoints in breast cancer: an update of early results," *ESMO Open*, vol. 2, no. 5, Article ID e000255, 2017.

[66] J. M. García, A. Llombart, J. L. Alonso et al., "Abstract CT152: A phase II study of pembrolizumab and eribulin in patients with HR-positive/HER2-negative metastatic breast cancer previously treated with anthracyclines and taxanes (KELLY study)," *Cancer Research*, vol. 78, supplement 13, Article ID CT152, 2018.

[67] L. J. Esserman, D. A. Berry, A. DeMichele et al., "Pathologic complete Response Predicts Recurrence-Free Survival More Effectively by Cancer Subset: Results From the I-SPY 1 TRIAL—CALGB 150007/150012, ACRIN 6657," *Journal of Clinical Oncology*, vol. 30, no. 26, pp. 3242–3249, 2012.

[68] P. Schmid, Y. H. Park, E. Muñoz-Couselo et al., "Pembrolizumab (pembro) + chemotherapy (chemo) as neoadjuvant treatment for triple negative breast cancer (TNBC): preliminary results from KEYNOTE-173," *Journal of Clinical Oncology*, vol. 35, article no 556, supplement 15, 2017.

[69] S. Loibl, M. Untch, N. Burchardi et al., "Randomized phase II neoadjuvant study (GeparNuevo) to investigate the addition of durvalumab to a taxane-anthracycline containing chemotherapy in triple negative breast cancer (TNBC)," *Journal of Clinical Oncology*, vol. 36, article no 104, supplement 15, 2018.

[70] S. Domchek, S. Postel-Vinay, S. Im et al., "Abstract OT3-05-03: MEDIOLA: an open-label, phase I/II basket study of olaparib (PARP inhibitor) and durvalumab (anti-PD-L1 antibody)–Additional breast cancer cohorts," *Cancer Research*, vol. 79, supplement 4, Article ID OT3-05-03, 2019.

[71] L. A. Emens, C. Cruz, J. P. Eder et al., "Long-term clinical outcomes and biomarker analyses of atezolizumab therapy for patients with metastatic triple-negative breast cancer," *JAMA Oncology*, vol. 5, no. 1, article no 74, 2019.

[72] S. Verma, D. Miles, L. Gianni et al., "Trastuzumab emtansine for HER2-positive advanced breast cancer," *The New England Journal of Medicine*, vol. 367, no. 19, pp. 1783–1791, 2012.

[73] K. Khoury, C. Isaacs, M. Gatti-Mays et al., "Abstract OT3-04-01: Nivolumab or capecitabine or combination therapy as adjuvant therapy for triple negative breast cancer (TNBC) with residual disease following neoadjuvant chemotherapy: The OXEL study," *Cancer Research*, vol. 79, supplement 4, Article ID OT3-04-01, 2019.

[74] C. Omarini, G. Guaitoli, S. Pipitone et al., "Neoadjuvant treatments in triple-negative breast cancer patients: where we are now and where we are going," *Cancer Management and Research*, vol. 10, pp. 91–103, 2018.

[75] L. Y. Dirix, I. Takacs, G. Jerusalem et al., "Avelumab, an anti-PD-L1 antibody, in patients with locally advanced or metastatic breast cancer: A phase 1b JAVELIN solid tumor study," *Breast Cancer Research and Treatment*, vol. 167, no. 3, pp. 671–686, 2018.

[76] K. Oualla, H. M. El-Zawahry, B. Arun et al., "Novel therapeutic strategies in the treatment of triple-negative breast cancer," *Therapeutic Advances in Medical Oncology*, vol. 9, no. 7, pp. 493–511, 2017.

[77] J. Abdo, D. L. Cornell, S. K. Mittal, and D. K. Agrawal, "Immunotherapy plus cryotherapy: potential augmented abscopal effect for advanced cancers," *Frontiers in Oncology*, vol. 8, article no 85, 2018.

[78] D. Robinson, E. M. Van Allen, and Y.-M. Wu, "Integrative clinical genomics of advanced prostate cancer," *Cell*, vol. 161, no. 5, pp. 1215–1228, 2015.

[79] Y. A. Wang, J. Jian, C. Hung et al., "Germline breast cancer susceptibility gene mutations and breast cancer outcomes," *BMC Cancer*, vol. 18, no. 1, article no 315, 2018.

[80] Network TCGAR, "Integrated genomic analyses of ovarian carcinoma," *Nature*, vol. 474, no. 7353, pp. 609–615, 2011.

[81] R. P. Kaur, G. Shafi, R. P. Benipal, and A. Munshi, "Frequency of pathogenic germline mutations in cancer susceptibility genes in breast cancer patients," *Medical Oncology*, vol. 35, no. 6, article no 81, 2018.

[82] Y. Shen, Y.-H. Lee, J. Panneerselvam, J. Zhang, L. W. M. Loo, and P. Fei, "Mutated fanconi anemia pathway in non-fanconi anemia cancers," *Oncotarget*, vol. 6, no. 24, pp. 20396–20403, 2015.

[83] M. Esteller, J. M. Silva, G. Dominguez et al., "Promoter hypermethylation and BRCA1 inactivation in sporadic breast and ovarian tumors," *Journal of the National Cancer Institute*, vol. 92, no. 7, pp. 564–569, 2000.

[84] A. Potapova, A. M. Hoffman, A. K. Godwin, T. Al-Saleem, and P. Cairns, "Promoter hypermethylation of the PALB2 susceptibility gene in inherited and sporadic breast and ovarian cancer," *Cancer Research*, vol. 68, no. 4, pp. 998–1002, 2008.

[85] T. Hansmann, G. Pliushch, M. Leubner et al., "Constitutive promoter methylation of BRCA1 and RAD51C in patients with familial ovarian cancer and early-onset sporadic breast cancer," *Human Molecular Genetics*, vol. 21, no. 21, pp. 4669–4679, 2012.

[86] M. Wei, J. Xu, J. Dignam et al., "Estrogen receptor α, BRCA1, and FANCF promoter methylation occur in distinct subsets of sporadic breast cancers," *Breast Cancer Research and Treatment*, vol. 111, no. 1, pp. 113–120, 2008.

[87] C. J. Lord and A. Ashworth, "BRCAness revisited," *Nature Reviews Cancer*, vol. 16, no. 2, pp. 110–120, 2016.

[88] N. Riaz, P. Blecua, R. S. Lim et al., "Pan-cancer analysis of bi-allelic alterations in homologous recombination DNA repair genes," *Nature Communications*, vol. 8, no. 1, article no 857, 2017.

[89] J. M. Mulligan, L. A. Hill, S. Deharo et al., "Identification and validation of an anthracycline/cyclophosphamide-based chemotherapy response assay in breast cancer," *Journal of the National Cancer Institute*, vol. 106, no. 1, Article ID djt335, 2014.

[90] E. E. Parkes, S. M. Walker, L. E. Taggart et al., "Activation of STING-dependent innate immune signaling By S-phase-specific DNA damage in breast cancer," *Journal of the National Cancer Institute*, vol. 109, no. 1, Article ID djw199, 2016.

[91] S. R. Lakhani, J. Jacquemier, J. P. Sloane et al., "Multifactorial analysis of differences between sporadic breast cancers and cancers involving BRCA1 and BRCA2 mutations," *Journal of the National Cancer Institute*, vol. 90, no. 15, pp. 1138–1145, 1998.

[92] A. L. Bane, J. C. Beck, I. Bleiweiss et al., "BRCA2 mutation-associated breast cancers exhibit a distinguishing phenotype based on morphology and molecular profiles from tissue microarrays," *The American Journal of Surgical Pathology*, vol. 31, no. 1, pp. 121–128, 2007.

[93] C. DelloRusso, P. L. Welcsh, W. Wang, R. L. Garcia, M. King, and E. M. Swisher, "Functional characterization of a novel BRCA1-null ovarian cancer cell line in response to ionizing radiation," *Molecular Cancer Research*, vol. 5, no. 1, pp. 35–45, 2007.

[94] H. Xu, J. Xian, E. Vire et al., "Up-regulation of the interferon-related genes in BRCA2 knockout epithelial cells," *The Journal of Pathology*, vol. 234, no. 3, pp. 386–397, 2014.

[95] X. Ma, K. Norsworthy, N. Kundu et al., "CXCR3 expression is associated with poor survival in breast cancer and promotes metastasis in a murine model," *Molecular Cancer Therapeutics*, vol. 8, no. 3, pp. 490–498, 2009.

[96] A. A. Ejaeidi, B. S. Craft, L. V. Puneky, R. E. Lewis, and J. M. Cruse, "Hormone receptor-independent CXCL10 production is associated with the regulation of cellular factors linked to breast cancer progression and metastasis," *Experimental and Molecular Pathology*, vol. 99, no. 1, pp. 163–172, 2015.

[97] Y. J. Ku, H. H. Kim, J. H. Cha et al., "Predicting the level of tumor-infiltrating lymphocytes in patients with triple-negative breast cancer: Usefulness of breast MRI computer-aided detection and diagnosis," *Journal of Magnetic Resonance Imaging*, vol. 47, no. 3, pp. 760–766, 2018.

[98] C. Herrero-Vicent, A. Guerrera, J. Gavilá et al., "Predictive and prognostic impact of tumor-infiltrating lymphocytes in triple-negative breast cancer treated with neoadjuvant chemotherapy," *ecancermedicalscience*, vol. 11, article no 759, 2017.

[99] P. Savas, R. Salgado, C. Denkert et al., "Clinical relevance of host immunity in breast cancer: from TILs to the clinic," *Nature Reviews Clinical Oncology*, vol. 13, no. 4, pp. 228–241, 2016.

[100] S. Loi, N. Sirtaine, F. Piette et al., "Prognostic and predictive value of tumor-infiltrating lymphocytes in a phase III randomized adjuvant breast cancer trial in node-positive breast cancer comparing the addition of docetaxel to doxorubicin with doxorubicin-based chemotherapy: BIG 02-98," *Journal of Clinical Oncology*, vol. 31, no. 7, pp. 860–867, 2013.

[101] A. Balsari, A. Merlo, P. Casalini et al., "FOXP3 expression and overall survival in breast cancer," *Journal of Clinical Oncology*, vol. 27, no. 11, pp. 1746–1752, 2009.

[102] N. R. West, S. E. Kost, S. D. Martin et al., "Tumor-infiltrating FOXP3(+) lymphocytes are associated with cytotoxic immune responses and good clinical outcome in oestrogen receptor-negative breast cancer," *British Journal of Cancer*, vol. 108, no. 1, pp. 155–162, 2013.

[103] B. Weigelt, R. Bi, R. Kumar et al., "The landscape of somatic genetic alterations in breast cancers from ATM germline mutation carriers," *JNCI: Journal of the National Cancer Institute*, vol. 110, no. 9, pp. 1030–1034, 2018.

[104] G. Landskron, M. De la Fuente, P. Thuwajit, C. Thuwajit, and M. A. Hermoso, "Chronic inflammation and cytokines in the tumor microenvironment," *Journal of Immunology Research*, vol. 2014, Article ID 149185, 19 pages, 2014.

[105] P. Allavena, A. Sica, G. Solinas, C. Porta, and A. Mantovani, "The inflammatory micro-environment in tumor progression: The role of tumor-associated macrophages," *Critical Review in Oncology/Hematology*, vol. 66, no. 1, pp. 1–9, 2008.

[106] I. S. Pateras, S. Havaki, X. Nikitopoulou et al., "The DNA damage response and immune signaling alliance: Is it good or bad? Nature decides when and where," *Pharmacology & Therapeutics*, vol. 154, pp. 36–56, 2015.

[107] H. Ishikawa and G. N. Barber, "STING is an endoplasmic reticulum adaptor that facilitates innate immune signalling," *Nature*, vol. 455, no. 7213, pp. 674–678, 2008.

[108] A. Härtlova, S. F. Erttmann, F. A. M. Raffi et al., "DNA damage primes the type i interferon system via the cytosolic DNA sensor STING to promote anti-microbial innate immunity," *Immunity*, vol. 42, no. 2, pp. 332–343, 2015.

[109] S. M. Harding, J. L. Benci, J. Irianto, D. E. Discher, A. J. Minn, and R. A. Greenberg, "Mitotic progression following DNA damage enables pattern recognition within micronuclei," *Nature*, vol. 548, no. 7668, pp. 466–470, 2017.

[110] K. J. MacKenzie, P. Carroll, C.-A. Martin et al., "CGAS surveillance of micronuclei links genome instability to innate immunity," *Nature*, vol. 548, no. 7668, pp. 461–465, 2017.

[111] L. Sun, J. Wu, F. Du, X. Chen, and Z. J. Chen, "Cyclic GMP-AMP synthase is a cytosolic DNA sensor that activates the type I interferon pathway," *Science*, vol. 339, no. 6121, pp. 786–791, 2013.

[112] J. Wu, L. Sun, X. Chen et al., "Cyclic GMP-AMP is an endogenous second messenger in innate immune signaling by cytosolic DNA," *Science*, vol. 339, no. 6121, pp. 826–830, 2013.

[113] T. Li and Z. J. Chen, "The cGAS–cGAMP–STING pathway connects DNA damage to inflammation, senescence, and cancer," *The Journal of Experimental Medicine*, vol. 215, no. 5, pp. 1287–1299, 2018.

[114] L. Corrales, V. Matson, B. Flood, S. Spranger, and T. F. Gajewski, "Innate immune signaling and regulation in cancer immunotherapy," *Cell Research*, vol. 27, no. 1, pp. 96–108, 2017.

[115] J. Ahn, T. Xia, H. Konno, K. Konno, P. Ruiz, and G. N. Barber, "Inflammation-driven carcinogenesis is mediated through STING," *Nature Communications*, vol. 5, article no 5166, 2014.

[116] L. Deng, H. Liang, M. Xu et al., "STING-dependent cytosolic DNA sensing promotes radiation-induced type I interferon-dependent antitumor immunity in immunogenic tumors," *Immunity*, vol. 41, no. 5, pp. 543–852, 2014.

[117] R. D. Wilkinson, D. I. Johnston, E. E. Parkes, N. McCabe, and R. D. Kennedy, "Abstract 3787: exploring the effect of chemotherapies on STING-dependent cytokine release," *Cancer Research*, vol. 78, Supplement 13, Article ID 3787, 2018.

[118] K. J. Harrington, J. Brody, M. Ingham et al., "LBA15Preliminary results of the first-in-human (FIH) study of MK-1454, an agonist of stimulator of interferon genes (STING), as monotherapy or in combination with pembrolizumab (pembro) in patients with advanced solid tumors or lymphomas," *Annals of Oncology*, vol. 29, supplement 8, Article ID mdy424.015, 2018.

[119] S. Iurescia, D. Fioretti, and M. Rinaldi, "Targeting Cytosolic Nucleic Acid-Sensing Pathways for Cancer Immunotherapies," *Frontiers in Immunology*, vol. 9, article no 711, 2018.

[120] D. R. Ranoa, A. D. Parekh, S. P. Pitroda et al., "Cancer therapies activate RIG-I-like receptor pathway through endogenous non-coding RNAs," *Oncotarget*, vol. 7, no. 18, pp. 26496–26515, 2016.

[121] K. Kübler, N. Gehrke, S. Riemann et al., "Targeted activation of RNA helicase retinoic acid–inducible gene-i induces proimmunogenic apoptosis of human ovarian cancer cells," *Cancer Research*, vol. 70, no. 13, pp. 5293–5304, 2010.

[122] J. Fu, D. B. Kanne, M. Leong et al., "STING agonist formulated cancer vaccines can cure established tumors resistant to PD-1 blockade," *Sci Transl Med*, vol. 7, no. 283, Article ID 283ra52, 2015.

[123] L. Corrales, L. H. Glickman, S. M. McWhirter et al., "Direct activation of STING in the tumor microenvironment leads to potent and systemic tumor regression and immunity," *Cell Reports*, vol. 11, no. 7, pp. 1018–1030, 2015.

[124] H. Liang, L. Deng, Y. Hou et al., "Host STING-dependent MDSC mobilization drives extrinsic radiation resistance," *Nature Communications*, vol. 8, no. 1, article no 1736, 2017.

[125] H. Zhu, Y. Gu, Y. Xue, M. Yuan, X. Cao, and Q. Liu, "$CXCR2^+$ MDSCs promote breast cancer progression by inducing EMT and activated T cell exhaustion," *Oncotarget*, vol. 8, no. 70, pp. 114554–114567, 2017.

[126] S. Glück, B. Guey, M. F. Gulen et al., "Innate immune sensing of cytosolic chromatin fragments through cGAS promotes senescence," *Nature Cell Biology*, vol. 19, no. 9, pp. 1061–1070, 2017.

[127] Z. Dou, K. Ghosh, M. G. Vizioli et al., "Cytoplasmic chromatin triggers inflammation in senescence and cancer," *Nature*, vol. 550, no. 7676, pp. 402–406, 2017.

[128] H. Yang, H. Wang, J. Ren, Q. Chen, and Z. J. Chen, "cGAS is essential for cellular senescence," *Proceedings of the National Acadamy of Sciences of the United States of America*, vol. 114, no. 23, pp. E4612–E4620, 2017.

[129] S. F. Bakhoum, B. Ngo, A. M. Laughney et al., "Chromosomal instability drives metastasis through a cytosolic DNA response," *Nature*, vol. 553, article no 467, 2018.

[130] D. M. Pardoll, "The blockade of immune checkpoints in cancer immunotherapy," *Nature Reviews Cancer*, vol. 12, no. 4, pp. 252–264, 2012.

[131] M. Nishino, N. H. Ramaiya, H. Hatabu, and F. S. Hodi, "Monitoring immune-checkpoint blockade: Response evaluation and biomarker development," *Nature Reviews Clinical Oncology*, vol. 14, no. 11, pp. 655–668, 2017.

[132] T. F. Gajewski, H. Schreiber, and Y. X. Fu, "Innate and adaptive immune cells in the tumor microenvironment," *Nature Immunology*, vol. 14, pp. 1014–1022, 2013.

[133] K. M. Mahoney, P. D. Rennert, and G. J. Freeman, "Combination cancer immunotherapy and new immunomodulatory targets," *Nature Reviews Drug Discovery*, vol. 14, no. 8, pp. 561–584, 2015.

[134] J. Lee, R. Kefford, and M. Carlino, "PD-1 and PD-L1 inhibitors in melanoma treatment: past success, present application and future challenges," *Immunotherapy*, vol. 8, no. 6, pp. 733–746, 2016.

[135] L. T. Nguyen and P. S. Ohashi, "Clinical blockade of PD1 and LAG3 — potential mechanisms of action," *Nature Reviews Immunology*, vol. 15, no. 1, pp. 45–56, 2015.

[136] S. Liang, Y. Latchman, J. Buhlmann et al., "Regulation of PD-1, PD-L1, and PD-L2 expression during normal and autoimmune responses," *European Journal of Immunology*, vol. 33, no. 10, pp. 2706–2716, 2003.

[137] X. Wang, F. Teng, L. Kong, and J. Yu, "PD-L1 expression in human cancers and its association with clinical outcomes," *OncoTargets and Therapy*, pp. 5023–5039, 2016.

[138] M. Z. Baptista, L. O. Sarian, S. F. M. Derchain, G. A. Pinto, and J. Vassallo, "Prognostic significance of PD-L1 and PD-L2 in breast cancer," *Human Pathology*, vol. 47, no. 1, pp. 78–84, 2016.

[139] J. He, Y. Hu, M. Hu, and B. Li, "Development of PD-1/PD-L1 pathway in tumor immune microenvironment and treatment for non-small cell lung cancer," *Scientific Reports*, vol. 5, no. 1, Article ID 13110, 2015.

[140] D. G. Brooks, S. Ha, H. Elsaesser, A. H. Sharpe, G. J. Freeman, and M. B. Oldstone, "IL-10 and PD-L1 operate through distinct pathways to suppress T-cell activity during persistent viral infection," *Proceedings of the National Acadamy of Sciences of the United States of America*, vol. 105, no. 51, pp. 20428–20433, 2008.

[141] H. Guan, Y. Wan, J. Lan et al., "PD-L1 is a critical mediator of regulatory B cells and T cells in invasive breast cancer," *Scientific Reports*, vol. 6, no. 1, Article ID 35651, 2016.

[142] S. Amarnath, C. W. Mangus, J. C. M. Wang et al., "The PDL1-PD1 axis converts human TH1 cells into regulatory T cells," *Science Translational Medicine*, vol. 3, no. 111, Article ID 111ra120, 2011.

[143] H. O. Alsaab, S. Sau, R. Alzhrani et al., "PD-1 and PD-L1 checkpoint signaling inhibition for cancer immunotherapy: mechanism, combinations, and clinical outcome," *Frontiers in Pharmacology*, vol. 8, article no. 561, 2017.

[144] F. Bertucci and A. Gonçalves, "Immunotherapy in breast cancer: the emerging role of PD-1 and PD-L1," *Current Oncology Reports*, vol. 19, no. 10, article no 64, 2017.

[145] M. M. Boyiadzis, J. M. Kirkwood, J. L. Marshall, C. C. Pritchard, N. S. Azad, and J. L. Gulley, "Significance and implications of FDA approval of pembrolizumab for biomarker-defined disease," *Journal for ImmunoTherapy of Cancer*, vol. 6, no. 1, article no 35, 2018.

[146] T. A. Chan, M. Yarchoan, E. Jaffee et al., "Development of tumor mutation burden as an immunotherapy biomarker: utility for the oncology clinic," *Annals of Oncology*, vol. 30, no. 1, pp. 44–56, 2019.

[147] M. W. Audeh, F. Dadmanesh, and J. Yearley, "Abstract P4-04-01: PDL-1 expression in primary breast cancers with germline mutations in BRCA 1 and 2," *Cancer Research*, vol. 76, supplement 4, Article ID P-P4-04-01, 2016, http://cancerres.aacrjournals.org/content/76/4_Supplement/P4-04-01.abstract.

[148] D. Samanta, Y. Park, X. Ni et al., " Chemotherapy induces enrichment of CD47 + /CD73 + /PDL1 + immune evasive triple-negative breast cancer cells ," *Proceedings of the National Acadamy of Sciences of the United States of America*, vol. 115, no. 6, pp. E1239–E1248, 2018.

[149] S. Adams, M. E. Gatti-Mays, K. Kalinsky et al., "Current landscape of immunotherapy in breast cancer," *JAMA Oncology*, 2019.

[150] Y. Wang, S. Zhou, F. Yang et al., "Treatment-related adverse events of PD-1 and PD-L1 inhibitors in clinical trialsa systematic review and meta-analysis," *JAMA Oncology*, 2019.

[151] R. Plummer, C. Jones, M. Middleton et al., "Phase i study of the poly(ADP-Ribose) polymerase inhibitor, AG014699, in combination with temozolomide in patients with advanced solid tumors," *Clinical Cancer Research*, vol. 14, no. 23, pp. 7917–7923, 2008.

[152] H. Farmer, H. McCabe, C. J. Lord et al., "Targeting the DNA repair defect in BRCA mutant cells as a therapeutic strategy," *Nature*, vol. 434, no. 7035, pp. 917–921, 2005.

[153] H. E. Bryant, N. Schultz, H. D. Thomas et al., "Specific killing of BRCA2-deficient tumours with inhibitors of poly(ADP-ribose) polymerase," *Nature*, vol. 434, no. 7035, pp. 913–917, 2005.

[154] M. Robson, S. Im, E. Senkus et al., "Olaparib for metastatic breast cancer in patients with a germline BRCA mutation," *The New England Journal of Medicine*, vol. 377, no. 6, pp. 523–533, 2017.

[155] J. K. Litton, H. S. Rugo, J. Ettl et al., "Talazoparib in patients with advanced breast cancer and a germline BRCA mutation," *The New England Journal of Medicine*, vol. 379, no. 8, pp. 753–763, 2018.

[156] R. A. Stewart, P. G. Pilié, and T. A. Yap, "Development of PARP and immune-checkpoint inhibitor combinations," *Cancer Research*, vol. 78, no. 24, pp. 6717–6725, 2018.

[157] J. Shen, W. Zhao, Z. Ju et al., "PARPi triggers the STING-dependent immune response and enhances the therapeutic efficacy of immune checkpoint blockade independent of BRCAness," *Cancer Research*, vol. 79, no. 2, pp. 311–319, 2019.

[158] T. Sen, B. L. Rodriguez, L. Chen et al., "Targeting DNA damage response promotes anti-tumor immunity through STING-mediated T-cell activation in small cell lung cancer," *Cancer Discovery*, vol. 9, no. 5, Article ID CD-18-1020, pp. 646–661, 2019.

[159] R. M. Chabanon, G. Muirhead, D. B. Krastev et al., "PARP inhibition enhances tumor cell–intrinsic immunity in ERCC1-deficient non–small cell lung cancer," *The Journal of Clinical Investigation*, vol. 129, no. 3, pp. 1211–1228, 2019.

[160] C. Pantelidou, O. Sonzogni, M. De Oliveria Taveira et al., "PARP inhibitor efficacy depends on CD8+ T cell recruitment via intratumoral STING pathway activation in BRCA-deficient models of triple-negative breast cancer," *Cancer Discovery*, vol. 9, no. 6, Article ID CD-18-1218, pp. 722–737, 2019.

[161] S. Domchek, S. Postel-Vinay, Y. Bang et al., "Abstract PD6-11: an open-label, multitumor, phase II basket study of olaparib and durvalumab (MEDIOLA): results in germline *BRCA*-mutated (g *BRCA* m) HER2-negative metastatic breast cancer (MBC)," *Cancer Research*, vol. 78, supplement 4, Article ID PD6-11, 2018.

[162] S. Vinayak, S. Tolaney, L. Schwartzberg et al., "bstract PD5-02: durability of clinical benefit with niraparib + pembrolizumab in patients with advanced triple-negative breast cancer beyond *BRCA*: (TOPACIO/Keynote-162)," *Cancer Research*, vol. 79, supplement 4, Article ID PD5-02, 2019.

[163] D. Fukumura, J. Kloepper, Z. Amoozgar, D. G. Duda, and R. K. Jain, "Enhancing cancer immunotherapy using antiangiogenics: opportunities and challenges," *Nature Reviews Clinical Oncology*, vol. 15, no. 5, pp. 325–340, 2018.

[164] K. W. Mouw, M. S. Goldberg, P. A. Konstantinopoulos, and A. D. D'Andrea, "DNA damage and repair biomarkers of immunotherapy response," *Cancer Discovery*, vol. 7, no. 7, pp. 675–693, 2017.

[165] V. G. Gorgoulis and T. D. Halazonetis, "Oncogene-induced senescence: the bright and dark side of the response," *Current Opinion in Cell Biology*, vol. 22, no. 6, pp. 816–827, 2010.

Hindawi
Journal of Oncology
Volume 2019, Article ID 7091815, 9 pages
https://doi.org/10.1155/2019/7091815

Research Article

TDG Gene Polymorphisms and Their Possible Association with Colorectal Cancer: A Case Control Study

Narasimha Reddy Parine,[1] **Ibrahim O. Alanazi**,[2] **Jilani Purusottapatnam Shaik**,[1] **Sooad Aldhaian**,[1] **Abdulrahman M. Aljebreen**,[3,4] **Othman Alharbi**,[3,4] **Majid A. Almadi**,[3,4] **Nahla A. Azzam**,[3,4] **and Mohammad Alanazi**[1]

[1]*Genome Research Chair, Department of Biochemistry, College of Science, King Saud University, Riyadh 11451, Saudi Arabia*
[2]*National Center for Biotechnology, King Abdulaziz City for Science and Technology (KACST), P.O. Box 6086, Riyadh 11461, Saudi Arabia*
[3]*College of Medicine, King Saud University, Riyadh, Saudi Arabia*
[4]*Division of Gastroenterology, King Khalid University Hospital, King Saud University, Riyadh, Saudi Arabia*

Correspondence should be addressed to Narasimha Reddy Parine; reddyparine@gmail.com

Received 27 January 2019; Revised 5 April 2019; Accepted 7 May 2019; Published 23 May 2019

Guest Editor: Qingyuan Yang

Genetic alterations that might lead to colorectal cancer involve essential genes including those involved in DNA repair, inclusive of base excision repair (BER). *Thymine DNA glycosylase* (*TDG*) is one of the most well characterized BER genes that catalyzes the removal of thymine moieties from G/T mismatches and is also involved in many cellular functions, such as the regulation of gene expression, transcriptional coactivation, and the control of epigenetic DNA modification. Mutation of the *TDG* gene is implicated in carcinogenesis. In the present study, we aimed to investigate the association between *TDG* gene polymorphisms and their involvement in colon cancer susceptibility. One hundred blood samples were obtained from colorectal cancer patients and healthy controls for the genotyping of seven SNPs in the *TDG* gene. DNA was extracted from the blood, and the polymorphic sites (SNPs) rs4135113, rs4135050, rs4135066, rs3751209, rs1866074, and rs1882018 were investigated using TaqMan genotyping. One of the six *TDG* SNPs was associated with an increased risk of colon cancer. The AA genotype of the *TDG* SNP rs4135113 increased the risk of colon cancer development by more than 3.6-fold, whereas the minor allele A increased the risk by 1.6-fold. It also showed a 5-fold higher risk in patients over the age of 57. SNP rs1866074 showed a significant protective association in CRC patients. The GA genotype of *TDG* rs3751209 was associated with a decreased risk in males. There is a significant relationship between *TDG* gene function and colorectal cancer progression.

1. Introduction

The development of cancer is a multistep process involving aberrations in many cellular processes, including differentiation, cell cycle regulation, cell death, proliferation, and genomic conservation due to functional alterations in a variety of genes. *Thymine DNA glycosylase* (*TDG*) is a member of the mismatch uracil glycosylase subfamily. All of these uracil DNA glycosylase (UDG) enzymes have a monofunctional approach of action [1]. UDGs recruit a common base-flipping, DNA intercalation method for substrate identification and catalyze the removal of the N-glycosidic bond of the flipped base, thus creating an abasic site [2]. TDG has a crucial role in DNA repair, particularly BER, in which it specifically identifies G: U and G: T mismatches resulting from the impulsive deamination of 5-methylcytosine. In addition to its DNA repair function, TDG is also involved in other critical cellular processes, such as the regulation of gene expression, transcriptional coactivation, and the regulation of epigenetic DNA modification [3]. TDG has been shown to interact with some transcription factors and especially with nuclear receptors. TDG initiates the BER pathway, which utilizes the base-flipping method to delete the target bases from the DNA forming an AP site. This happens when TDG binds to the promoters of the BER proteins APE, DNA ligase, and Pol β [4].

The role of TDG in cancer progression is a hotly debated issue [5]. Its interaction with tumor suppressor P53 (TP53) proteins initially suggested that TDG merely acts as a tumor suppressor. Overexpression of TDG recruits TP53 proteins to the cyclin dependent kinase inhibitor 1A (p21Waf1) gene promoter and increases its transcriptional activity [6]. Moreover, TP53 binding to the TDG promoter will transcriptionally regulate its expression and control the nuclear translocation of TDG [7]. The relationship between TDG and cancer has been studied by a number of research groups who have suggested that genetic variants in *TDG* and other DNA repair genes confer susceptibility to colorectal cancer [8]. Xu and colleagues showed that *TDG* positively regulates the Wnt signaling pathway and is a key driver necessary for the progression of CRC [9]. They also reported that hypermethylation of *TDG* in multiple myeloma cell lines reduced its gene expression. As a result, DNA repair activity became less efficient [10] in pancreatic adenocarcinoma [11]. Finally, a lack of the DNA mismatch repair protein PMS2 (*PMS2)* and reduced *TDG* expression in rectal cancer has been found to produce a supermutator phenotype at CpG sites [12].

Recent studies reported that the SNP rs2888805 (Val367Met) in *TDG* might be implicated in nonmelanoma skin cancer [13]. The *TDG* SNPs rs167715 and rs4135087 might also be associated with the progression of ovarian cancer in most of the BRCA1/2 mutation carriers [14]. The coding region SNP rs369649741 (Arg66Gly) has been reported to be associated with a high risk in familial colorectal cancer patients [8]. Significant associations have been demonstrated between the risk of cancers, including esophageal squamous cell carcinoma and gastric cancer, and the rs4135054 SNP in *TDG* [15]. This study was conducted to determine the association of the DNA repair gene *TDG* SNPs and colon cancer risk in the Saudi population.

2. Materials and Methods

2.1. Study Population and Patient Selection. The study population was composed of 100 colorectal cancer patients and 192 control subjects from a Saudi population. Patients were recruited from King Saud Medical City. CRC was confirmed via histopathological examination. The age of the CRC cases varied from 21 to 90 years, with a mean age of 61.10 ± 12.17 years. The main exclusion conditions were autoimmune disorders, hereditary nonpolyposis colorectal cancer (HNPCC), or a previous history of any other disorders. CRC patients who had undergone prior chemoradiotherapy were also excluded. A total of 192 controls were recruited. The age of the controls varied from 21 to 87 years with a mean of 57.2 ± 8.34 years. The primary details of the volunteers were collected by a prestructured questionnaire. Each participant was informed in detail about the present study and signed standard consent. The Ethics Committee of King Saud Medical City approved the present study.

2.2. Single Nucleotide Polymorphisms (SNPs) Selection, DNA Extraction, and Genotyping. Genomic DNA was extracted from blood samples using a blood DNA kit (QIAGEN DNeasy Blood & Tissue Kit). According to previous reports, six SNPs located in the *TDG* gene were analyzed: rs4135113 (C__31582396_10), rs4135050 (C___1970689_10), rs4135066 (C___1970695_10), rs3751209 (C__11162283_20), rs1866074 (C___3152280_10), and rs1882018 (C__11490839_10). The preliminary data on the SNPs are shown in Table 1. These SNPs were also selected based on literature reviews of SNP associations with various diseases in diverse ethnic groups. The genotyping analysis was conducted using QuantStudio™ 7 Flex Real-Time PCR System (Applied Biosystems) with an endpoint reading of the genotypes [16].

3. Results

A total of 100 colorectal cancer patients and 192 normal controls from a Saudi Arabia population were included in the present study. The clinical and the demographic features of the study subjects are described in Supplementary Table 1 (Suppl. Table 1). Both CRC and normal samples were classified based on demographic parameters such as age and gender. Colorectal cancer samples were further classified based on tumor location, namely, colon or rectum. The average age of the CRC samples was 57.10 ± 12.17 years and of the controls was 58.2 ± 8.34 years.

All six SNPs in the normal control and CRC patient group obeyed Hardy-Weinberg equilibrium (HWE) (Table 1). Table 1 depicts the details of the SNPs used in the present study including the minor allele frequency and the HWE p-value. Out of the six SNPs, two SNPs, rs4135113 and rs1866074, showed a significant association with colorectal cancer. The genotypic distribution of rs4135113 was 75% GG, 18% GA, and 7% AA in colorectal cancer patients and 82% GG, 16% GA, and 2% AA in normal samples. SNP rs4135113 (Gly199Ser) showed a significant risk association with colorectal cancer in Saudi patients for its genotype AA (OR: 3.640, CI: 1.034–12.819, p = 0.03286) (Table 2). The frequency of the minor allele A in patient samples also showed a significant difference compared with that in the healthy controls (OR: 1.675, CI: 1.013–2.769, p = 0.04264) (Table 2).

The genotypic distribution of rs1866074 was 22% AA, 39% AG, and 39% GG in colorectal cancer patients and 12% AA, 43% AG, and 45% GG in the normal samples. The GG allele frequency was low in colorectal cancer patients compared with that in the controls. SNP rs1866074 showed a protective association of the GG allele (OR: 0.501, CI: 0.251–1, p = 0.047) and the additive (AG+GG) allele (OR: 0.51, CI: 0.269–0.964, p = 0.036) (Table 2). The remaining SNPs, rs4135050, rs4135066, rs3751209, and rs1882018, did not show any association with colorectal cancer in the overall analysis (Table 2).

3.1. Stratification Analysis. After an overall analysis, we compared the TDG genotype frequencies based on gender. The genotype distributions of male (n = 58) and female (n = 42) patients were compared with those of matched healthy individuals (Tables 3 and 4). Only rs3751209 showed a protective association in female colon cancer patients with

Table 1: Primary information for *TDG* polymorphisms.

Genotyped SNP	rs4135113	rs4135050	rs4135066	rs3751209	rs1882018	rs1866074
Chromosome	12	12	12	12	12	12
Chromosome Position	103982915	103968698	103972562	103979822	103969403	103980664
Base change	G>A (Gly199Ser)	T>A	C>T	G>A	C>T	A>G
MAF in our controls	0.10	0.21	0.77	0.31	0.23	0.66
p-value for HWE	0.11	0.11	0.09	0.4	0.09	0.52

MAF: minor allele frequency.
HWE: Hardy–Weinberg equilibrium.

Table 2: Genotype frequencies of *TDG* gene polymorphism in colorectal cases and controls.

SNP	Variant	Patients Cases	Controls	OR	CI	χ^2 Value	p-value
rs4135050	TT	58 (0.58)	124 (0.65)	Ref			
	TA	34 (0.34)	55 (0.29)	1.322	0.779–2.244	1.07	0.30107
	AA	8 (0.08)	12 (0.06)	1.425	0.553–3.676	0.54	0.46173
	TA+AA	42 (0.42)	67 (0.35)	1.340	0.816–2.201	1.34	0.24664
	T	150 (0.75)	303 (0.79)	Ref			
	A	50 (0.25	79 (0.21)	1.278	0.853–1.916	1.42	0.23347
rs1882018	CC	58 (0.58)	118 (0.62)	Ref			
	CT	32 (0.32)	59 (0.31)	1.103	0.648–1.880	0.13	0.71725
	TT	10 (0.10)	14 (0.07)	1.453	0.609–3.470	0.71	0.39800
	CT+TT	42 (0.42)	73 (0.38)	1.171	0.715–1.916	0.39	0.53104
	C	148 (0.74)	295 (0.77)	Ref			
	T	52 (0.26)	87 (0.23)	1.191	0.802–1.771	0.75	0.38613
rs4135066	CC	4 (0.04)	14 (0.08)	Ref			
	CT	38 (0.38)	58 (0.30)	2.293	0.702–7.493	1.96	0.16114
	TT	58 (0.58)	119 (0.62)	1.706	0.538–5.413	0.84	0.35998
	CT+TT	96 (0.96)	177 (0.92)	1.898	0.608–5.927	1.25	0.26277
	C	46 (0.23)	86 (0.23)	Ref			
	T	154 (0.77)	296 (0.77)	0.973	0.647–1.462	0.02	0.89402
rs3751209	GG	51 (0.51)	87 (0.46)	Ref			
	GA	38 (0.38)	88 (0.46)	0.737	0.441–1.232	1.36	0.24320
	AA	11 (0.11)	16 (0.08)	1.173	0.505–2.722	0.14	0.71041
	GA+AA	49 (0.49)	104 (0.54)	0.804	0.495–1.305	0.78	0.37654
	G	140 (0.70)	262 (0.69)	Ref			
	A	60 (0.30)	120 (0.31)	0.936	0.645–1.357	0.12	0.72602
rs1866074	AA	22 (0.22)	24 (0.12)	Ref			
	AG	39 (0.39)	82 (0.43)	0.519	0.260–1.037	3.50	0.06152
	GG	39 (0.39)	85 (0.45)	*0.501*	0.251–1.000	3.91	*0.04799*
	AG+GG	78 (0.78)	167 (0.88)	*0.510*	0.269–0.964	4.39	*0.03615*
	A	83 (0.42)	130 (0.34)	Ref			
	G	117 (0.58)	252 (0.66)	0.727	0.511–1.034	3.16	0.07567
rs4135113	GG	75 (0.75)	156 (0.82)	Ref			
	GA	18 (0.18)	31 (0.16)	1.208	0.635–2.297	0.33	0.56458
	AA	7 (0.07)	4 (0.02)	3.640	1.034–12.819	4.55	*0.03286*
	GA+AA	25 (0.25)	35 (0.18)	1.486	0.830–2.660	1.79	0.18130
	G	168 (0.84)	343 (0.90)	Ref			
	A	32 (0.16)	39 (0.10)	1.675	1.013–2.769	4.11	*0.04264*

Table 3: Genotype frequencies of *TDG* gene polymorphisms in male colorectal cases and controls.

SNP	Variant	Patients Cases	Controls	OR	CI	χ^2 Value	p-value
rs4135050	TT	32 (0.55)	60 (0.63)	Ref			
	TA	21 (0.36)	27 (0.28)	1.458	0.714–2.977	1.08	0.29910
	AA	5 (0.09)	8 (0.08)	1.172	0.354–3.879	0.07	0.79493
	TA+AA	26 (0.45)	35 (0.37)	1.393	0.717–2.707	0.96	0.32771
	T	85 (0.73)	147 (0.77)	Ref			
	A	31 (0.27)	43 (0.23)	1.247	0.731–2.126	0.66	0.41728
rs1882018	CC	35 (0.60)	60 (0.63)	Ref			
	CT	18 (0.31)	27 (0.29)	1.143	0.552–2.366	0.13	0.71901
	TT	5 (0.09)	8 (0.08)	1.071	0.325–3.531	0.01	0.90971
	CT+TT	23 (0.40)	35 (0.37)	1.127	0.576–2.204	0.12	0.72787
	C	88 (0.76)	147 (0.77)	Ref			
	T	28 (0.24)	43 (0.23)	1.088	0.631–1.875	0.09	0.76200
rs4135066	CC	3 (0.05)	7 (0.07)	Ref			
	CT	21 (0.36)	30 (0.32)	1.633	0.378–7.054	0.44	0.50827
	TT	34 (0.59)	58 (0.61)	1.368	0.332–5.643	0.19	0.66390
	CT+TT	55 (0.95)	88 (0.93)	1.458	0.362–5.877	0.28	0.59390
	C	27 (0.23)	44 (0.23)	Ref			
	T	89 (0.77)	146 (0.77)	0.993	0.575–1.716	0.001	0.98108
rs3751209	GG	36(0.62)	44 (0.46)	Ref			
	GA	15 (0.26)	45 (0.47)	*0.407*	0.196–0.847	5.92	0.01495
	AA	7 (0.12)	6 (0.07)	1.426	0.440–4.622	0.35	0.55296
	GA+AA	22 (0.38)	51 (0.54)	0.527	0.271–1.027	3.58	0.05840
	G	87 (0.75)	133 (0.70)	Ref			
	A	29 (0.25)	57 (0.30)	0.778	0.461–1.311	0.89	0.34517
rs1866074	AA	12 (0.20)	12 (0.13)	Ref			
	AG	23 (0.40)	40 (0.42)	0.575	0.222–1.487	1.32	0.25137
	GG	23 (0.40)	43 (0.45)	0.535	0.208–1.379	1.70	0.19227
	AG+GG	46 (0.80)	83 (0.87)	0.554	0.230–1.333	1.77	0.18362
	A	47 (0.41)	64 (0.34)	Ref			
	G	69 (0.59)	126 (0.66)	0.746	0.463–1.202	1.45	0.22776
rs4135113	GG	45 (0.78)	75 (0.79)	Ref			
	GA	9 (0.16)	18 (0.19)	0.833	0.345–2.012	0.16	0.68491
	AA	4 (0.07)	2 (0.02)	3.333	0.587–18.937	2.05	0.15266
	GA+AA	13 (0.22)	20 (0.21)	1.083	0.492–2.387	0.04	0.84257
	G	99 (0.85)	168 (0.88)	Ref			
	A	17 (0.15)	22 (0.12)	1.311	0.664–2.588	0.61	0.43370

the GA genotype (OR, 0.407; CI: 0.196–0.847, p = 0.01495). The heterozygous GA genotype frequency was low in colorectal cancer patients compared with that in the controls (Table 3). No other SNPs showed any significant association with colorectal cancer based on gender (Tables 3 and 4). The frequency of the A allele in patient samples also showed a significant difference compared with that of the healthy individuals (OR: 2.238, CI: 1.059–4.729, p = 0.03159).

The *TDG* genotype distribution was further correlated with the age at colon cancer diagnosis and tumor location. To assess the association of the analyzed SNPs with age at colon cancer diagnosis, we divided the patients into two groups based on the median age of the samples: ≤57 (n = 53) or >57 (n = 47) years of age. The distributions of genotype and allele frequencies for each SNP are shown in Tables 5 and 6. SNP rs4135113, which showed a significant association with CRC in the overall analysis, showed a significant risk association in CRC patients in the group of individuals above 57 years of age. The AA genotype frequency was higher in patients than in healthy individuals. This genotype showed a 5-fold increased risk of colon cancer in the Saudi Arabian population (OR: 5.588; CI: 1.032–30.254; p = 0.02745). In addition to this, the rs4135113 minor allele A also showed a 2-fold increased risk for colorectal cancer in the Saudi population (OR: 2.184, CI: 1.077–4.431; p = 0.02778) (Table 6). A linkage disequilibrium analysis revealed that there was a difference in strength among the SNP associations in cases and controls (Figure 1).

Table 4: Genotype frequencies of *TDG* gene polymorphisms in female colorectal cases and controls.

SNP	Variant	Patients Cases	Controls	OR	CI	χ^2 Value	p-value
rs4135050	TT	26 (0.62)	64 (0.67)	Ref			
	TA	13 (0.31)	28 (0.29)	1.143	0.513–2.544	0.11	0.74356
	AA	3 (0.07)	4 (0.04)	1.846	0.386–8.828	0.60	0.43682
	TA+AA	16 (0.38)	32 (0.33)	1.231	0.579–2.615	0.29	0.58890
	T	65 (0.77)	156 (0.81)	Ref			
	A	19 (0.23)	36 (0.19)	1.267	0.677–2.370	0.55	0.45905
rs1882018	CC	23 (0.55)	58 (0.60)	Ref			
	CT	14 (0.33)	32 (0.34)	1.103	0.500–2.436	0.06	0.80789
	TT	5 (0.12)	6 (0.06)	2.101	0.584–7.568	1.33	0.24858
	CT+TT	19 (0.45)	38 (0.40)	1.261	0.606–2.623	0.39	0.53475
	C	60 (0.71)	148 (0.77)	Ref			
	T	24 (0.29)	44 (0.23)	1.345	0.753–2.405	1.01	0.31578
rs4135066	CC	1 (0.02)	8 (0.08)	Ref			
	CT	17 (0.40)	28 (0.29)	4.857	0.558–42.3	2.40	0.12134
	TT	24 (0.57)	60 (0.63)	3.200	0.379–26.983	1.26	0.26149
	CT+TT	41 (0.98)	88 (0.92)	3.727	0.451–30.794	1.70	0.19254
	C	19 (0.23)	44 (0.23)	Ref			
	T	65 (0.77)	148 (0.77)	1.017	0.552–1.876	0.0012	0.95677
rs3751209	GG	15 (0.36)	43 (0.45)	Ref			
	GA	23 (0.54)	43 (0.45)	1.533	0.706–3.331	1.17	0.27879
	AA	4 (0.10)	10 (0.10)	1.147	0.313–4.207	0.04	0.83645
	GA+AA	27 (0.64)	53 (0.55)	1.460	0.691–3.087	0.99	0.32021
	G	53 (0.63)	129 (0.67)	Ref			
	A	31 (0.37)	63 (0.33)	1.198	0.701–2.047	0.44	0.50919
rs1866074	AA	10 (0.24)	12 (0.14)	Ref			
	AG	16 (0.38)	42 (0.44)	0.457	0.165–1.265	2.32	0.12761
	GG	16 (0.38)	42 (0.44)	0.457	0.165–1.265	2.32	0.12761
	AG+GG	32 (0.76)	84 (0.88)	0.457	0.180–1.162	2.79	0.09493
	A	36 (0.43)	66 (0.34)	Ref			
	G	48 (0.57)	126 (0.66)	0.698	0.413–1.180	1.80	0.17917
rs4135113	GG	30 (0.71)	81 (0.84)	Ref			
	GA	9 (0.21)	13 (0.14)	1.869	0.725–4.821	1.71	0.19133
	AA	3 (0.07)	2 (0.02)	4.050	0.645–25.439	2.56	0.10991
	GA+AA	12 (0.29)	15 (0.16)	2.160	0.908–5.140	3.11	0.07773
	G	69 (0.82)	175 (0.91)	Ref			
	A	15 (0.18)	17 (0.09)	2.238	1.059–4.729	4.62	0.03159

4. Discussion

To the best of our knowledge, very few studies have been reported which correlate variation in the *TDG* gene with cancer [16–18]. With the aim of studying the role played by the polymorphisms in the *TDG* gene in CRC risk, we investigated six SNPs (rs4135113, rs4135050, rs4135066, rs3751209, rs1866074, and rs1882018) distributed in different regions of the *TDG* gene. The SNPs were selected based on their location in the *TDG* gene: rs4135113 is located in exon 5; rs4135050, rs4135066, and rs1882018 are in intron 1; and rs3751209 and rs1866074 are in intron 2 and intron 3, respectively. We chose these SNPs to study the effect of mutations in exons and introns. Mutations in an exon might affect the synthesized protein, whereas intron mutations might affect the RNA processing machinery and RNA splicing and stability, which could impact the level of expression and/or protein output [17]. Five of the SNPs were located in intronic region and four of them are in regulatory regions. SNPs rs4135066, rs4135050, and rs1882018 are located in aligned intronic regions flanking alternative conserved exon region (ACE). SNPs rs4135050 and rs1882018 are in exonic splicing silencer (ESS) region, and rs1866074 is in exonic splicing enhancer region.

All six SNPs in the normal control and CRC patient group obeyed the Hardy-Weinberg equilibrium (HWE). Out of the six SNPs, two showed a significant association with CRC. SNP rs4135113 showed a significant risk association of its genotype AA (OR: 3.640, CI: 1.0341–2.819, p = 0.03286)

Table 5: Genotype frequencies of *TDG* gene polymorphisms in colorectal cases and controls in the below-57-year-old group.

SNP	Variant	Patients Cases	Controls	OR	CI	χ^2 Value	p-value
rs4135050	TT	31 (0.58)	67 (0.68)	Ref			
	TA	19 (0.36)	25 (0.25)	1.643	0.789–3.418	1.78	0.18271
	AA	3 (0.06)	7 (0.07)	0.926	0.224–3.824	0.01	0.91567
	TA+AA	22 (0.42)	32 (0.32)	1.486	0.745–2.962	1.27	0.25944
	T	81 (0.76)	159 (0.80)	Ref			
	A	25 (0.24)	39 (0.20)	1.258	0.712–2.223	0.63	0.42813
rs1882018	CC	30 (0.57)	61 (0.62)	Ref			
	CT	17 (0.32)	31 (0.31)	1.115	0.534–2.327	0.08	0.77161
	TT	6 (0.11)	7 (0.07)	1.743	0.538–5.642	0.87	0.34986
	CT+TT	23 (0.43)	38 (0.38)	1.231	0.625–2.423	0.36	0.54797
	C	77 (0.73)	153 (0.77)	Ref			
	T	29 (0.27)	45 (0.23)	1.281	0.745–2.200	0.80	0.36989
rs4135066	CC	2 (0.04)	9 (0.09)	Ref			
	CT	21 (0.40)	31 (0031)	3.048	0.598–15.547	1.93	0.16466
	TT	30 (0.56)	59 (0.60)	2.288	0.465–11.265	1.08	0.29768
	CT+TT	51 (0.96)	90 (0.91)	2.550	0.530–12.260	1.45	0.22791
	C	25 (0.24)	49 (0.25)	Ref			
	T	81 (0.76)	149 (0.75)	1.066	0.613–1.851	0.05	0.82191
rs3751209	GG	26 (0.49)	46 (0.46)	Ref			
	GA	20 (0.38)	44 (0.44)	0.804	0.394–1.643	0.36	0.54978
	AA	7 (0.13)	9 (0.10)	1.376	0.459–4.128	0.33	0.56807
	GA+AA	27 (0.51)	53 (0.54)	0.901	0.462–1.758	0.09	0.76037
	G	72 (0.68)	136 (0.69)	Ref			
	A	34 (0.32)	62 (0.31)	1.036	0.624–1.719	0.02	0.89161
rs1866074	AA	13 (0.25)	13 (0.13)	Ref			
	AG	22 (0.42)	42 (0.42)	0.524	0.208–1.322	1.90	0.16815
	GG	18 (0.33)	44 (0.43)	0.409	0.159–1.052	3.53	0.06029
	AG+GG	40 (0.75)	86 (0.87)	0.465	0.198–1.094	3.16	0.07536
	A	48 (0.45)	68 (0.34)	Ref			
	G	58 (0.55)	130 (0.66)	0.632	0.390–1.023	3.50	0.06132
rs4135113	GG	41 (0.77)	80 (0.81)	Ref			
	GA	10 (0.19)	17 (0.17)	1.148	0.482–2.732	0.10	0.75528
	AA	2 (0.04)	2 (0.02)	1.951	0.265–14.35	0.45	0.50442
	GA+AA	12 (0.23)	19 (0.19)	1.232	0.546–2.784	0.25	0.61496
	G	92 (0.87)	177 (0.89)	Ref			
	A	14 (0.13)	21 (0.11)	1.283	0.623–2.639	0.46	0.49826

and of the minor allele A (OR: 1.675, CI: 1.013–2.769, p = 0.04264) with colorectal cancer in Saudi patients. The SNP rs1866074 showed a protective association of the GG allele (OR: 0.501, CI: 0.251–1, p = 0.047) and the additive (AG+GG) allele (OR: 0.51, CI: 0.269–0.964, p = 0.036). Our genotyping results showed that there was no association of the other four SNPs (rs4135050, rs4135066, rs3751209, and rs1882018) with CRC patients in the Saudi population in the overall analysis.

The SNP located in the coding region of the *TDG* gene, rs4135113, a G/A transition (missense mutation, Gly199Ser), was studied to detect if there was any association with CRC. There is recent evidence supporting an association between this polymorphism and the development of cancer. Sjolund et al. [15] reported that the Gly199Ser polymorphism occurs in approximately 10% of the global population and the expression of TDG with the G199S variant in human breast epithelial cells might lead to an increased number of DNA double-strand breaks. Thus, it initiates and activates DNA damage that induces cellular transformation and chromosomal aberrations [18]. Our results showed that the A/A genotype variation increases the risk of CRC by approximately fourfold in Saudi patients and is statistically significant (OR= 3.64, p-value = 0.03) (Table 2). Further investigation was conducted to explore the correlation of this polymorphic site with the clinicopathological factors and we observed that rs4135113 showed a fivefold increased risk in old aged patients. A study carried out by Wen-Bin and colleagues (2009) on a Chinese population showed a significant association of

Table 6: Genotype frequencies of *TDG* gene polymorphisms in colorectal cases and controls in the above-57-year-old group.

SNP	Variant	Patients Cases	Controls	OR	CI	χ^2 Value	p-value
rs4135050	TT	27 (0.57)	57 (0.62)	Ref			
	TA	15 (0.32)	30 (0.33)	1.056	0.488–2.281	0.02	0.89062
	AA	5 (0.11)	5 (0.05)	2.111	0.563–7.914	1.27	0.25994
	TA+AA	20 (0.43)	35 (0.38)	1.206	0.590–2.466	0.26	0.60699
	T	69 (0.73)	144 (0.78)	Ref			
	A	25 (0.27)	40 (0.22)	1.304	0.733–2.321	0.82	0.36543
rs1882018	CC	28 (0.60)	57 (0.62)	Ref			
	CT	15 (0.32)	28 (0.30)	1.091	0.503–2.363	0.05	0.82605
	TT	4 (0.08)	7 (0.08)	1.163	0.314–4.307	0.05	0.82075
	CT+TT	19 (0.40)	35 (0.38)	1.105	0.539–2.267	0.07	0.78518
	C	71 (0.76)	142 (0.77)	Ref			
	T	23 (0.24)	42 (0.23)	1.095	0.612–1.962	0.09	0.75960
rs4135066	CC	2 (0.04)	5 (0.05)	Ref			
	CT	17 (0.36)	27 (0.29)	1.574	0.274–9.045	0.26	0.60894
	TT	28 (0.60)	60 (0.65)	1.167	0.213–6.387	0.03	0.85883
	CT+TT	45 (0.94)	87 (0.95)	1.293	0.241–6.930	0.09	0.76356
	C	21 (0.22)	37 (0.20)	Ref			
	T	73 (0.78)	147 (0.80)	0.875	0.478–1.602	0.19	0.66485
rs3751209	GG	25 (0.53)	41 (0.45)	Ref			
	GA	18 (0.38)	44(0.47)	0.671	0.320–1.407	1.12	0.28959
	AA	4 (0.09)	7 (0.08)	0.937	0.249–3.527	0.01	0.92351
	GA+AA	22 (0.47)	51 (0.55)	0.707	0.349–1.432	0.93	0.33531
	G	68 (0.72)	126 (0.68)	Ref			
	A	26 (0.28)	58 (0.32)	0.831	0.480–1.438	0.44	0.50706
rs1866074	AA	9 (0.19)	11 (0.12)	Ref			
	AG	17 (0.36)	4 (0.43)	0.519	0.182–1.481	1.52	0.21694
	GG	21 (0.45)	41 (0.45)	0.626	0.224–1.747	0.81	0.36892
	AG+GG	38 (0.81)	81 (0.88)	0.573	0.219–1.500	1.31	0.25305
	A	35 (0.37)	62 (0.34)	Ref			
	G	59 (0.63)	122 (0.66)	0.857	0.510–1.438	0.34	0.55817
rs4135113	GG	34 (0.72)	76 (0.83)	Ref			
	GA	8 (0.17)	14 (0.15)	1.277	0.490–3.33	0.25	0.61607
	AA	5 (0.11)	2 (0.02)	*5.588*	1.032–30.254	4.86	0.02745
	GA+AA	13 (0.28)	16 (0.17)	1.816	0.787–4.191	1.99	0.15870
	G	76 (0.81)	166 (0.90)	Ref			
	A	18 (0.19)	18 (0.10)	*2.184*	1.077–4.431	4.84	0.02778

rs4135113 with an increased micronucleus in the Chinese population. A few other studies have reported that this SNP has no association with an increased risk of lung cancer, rectal cancer, or gastric adenocarcinoma in a Polish population and a Chinese population [19–21].

We also investigated the effect of rs4135050 on the risk of CRC when the T was substituted by A. The genotype AA in our study showed an elevated CRC risk, although the difference was not statistically significant (Table 2). In an urban Puerto Rican population, the one-carbon nutrient status was not associated with the DNA uracil concentration in this SNP [22].

The SNP rs4135066 has the C substituted by a T. In this investigation, the homozygous TT showed an increased risk of CRC; however, this was not statistically significant (Table 2). A recent study by Barry et al. in an American population showed that the SNP rs4135066 was not statistically associated with prostate cancer [23]. In the rs3751209 polymorphism, the A/G variation in our study showed a reduction in the CRC risk, but the difference did not reach statistical significance (Table 2). A recent study by Osorio et al. showed that this SNP was not associated with breast cancer risk in BRCA1/2 mutation carriers [14]. Another SNP studied was rs1866074, which is located in the intronic region and results from a transition mutation where A is substituted by G. A recent case control study showed that the increase in the frequency of micronuclei in bladder cancer among the AG and GG carriers improved patient

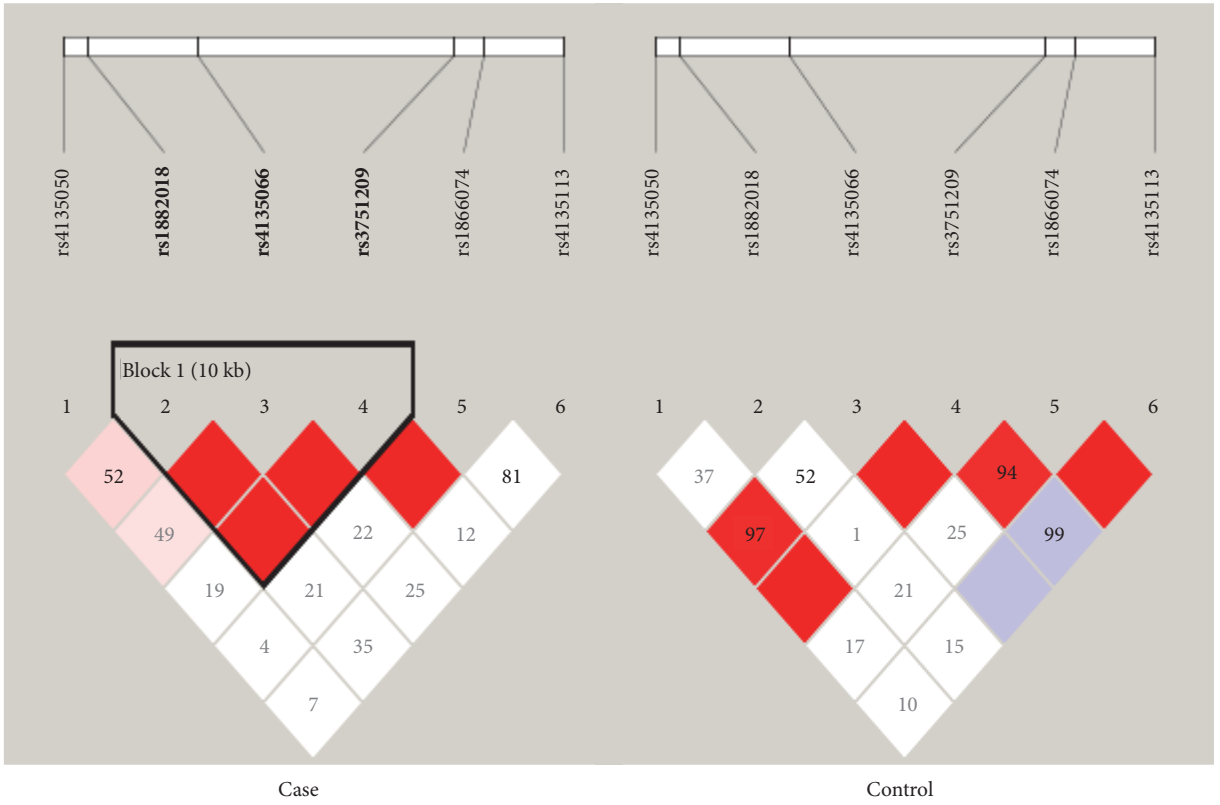

Figure 1: Pairwise LD among the six SNPs in colon cancer and controls. The bright red color indicates a high D′.

prognosis [24]. In this investigation, we observed that the GG genotype and the AG+GG additive genotype decreased the risk of CRC (Table 2). Finally, rs1882018 was studied during this investigation, which is also located in the intronic region and is produced as a result of a transition mutation where A is substituted by G. Our results showed that the GG genotype increased the risk of BC, but the finding did not reach statistical significance (Table 2). A previous study carried out by Wei et al. showed that this SNP had a protective effect against the development of bladder cancer [25].

5. Conclusions

In conclusion, the present study showed a significant association between the *TDG* gene and colorectal cancer progression in a Saudi population. One of the six *TDG* SNPs showed an increased risk of colon cancer. *TDG* rs4135113 increased the risk of colon cancer development by more than 3.6- and 1.6-fold in CRC patients in general, and 5-fold in patients aged more than 57 years. SNP rs1866074 showed a significant protective association in CRC patients. The GA genotype of *TDG* rs3751209 showed a decreased risk of CRC in males. Thus, there is a significant relationship between *TDG* gene function and colorectal cancer progression. However, further studies are required to determine the exact effect of amino acid (Gly199Ser) replacement using in vitro methods.

Data Availability

The data used to support the findings of this study are available from the corresponding author upon request.

Conflicts of Interest

All authors declare no conflicts of interest.

Acknowledgments

This project is financially supported by King Saud University through the vice deanship of scientific research.

Supplementary Materials

Suppl. Table 1: General clinical parameters of the study participants. *(Supplementary Materials)*

References

[1] N. Schormann, R. Ricciardi, and D. Chattopadhyay, "Uracil-DNA glycosylases—structural and functional perspectives on an essential family of DNA repair enzymes," *Protein Science*, vol. 23, no. 12, pp. 1667–1685, 2014.

[2] L. Aravind and E. V. Koonin, "The alpha/beta fold uracil DNA glycosylases: a common origin with diverse fates," *Genome Biology*, vol. 1, no. 4, Article ID RESEARCH0007, 2000.

[3] D. Cortázar, C. Kunz, Y. Saito, R. Steinacher, and P. Schär, "The enigmatic thymine DNA glycosylase," *DNA Repair*, vol. 6, no. 4, pp. 489–504, 2007.

[4] R. Métivier, R. Gallais, and C. Tiffoche, "Cyclical DNA methylation of a transcriptionally active promoter," *Nature*, vol. 452, pp. 45–50, 2008.

[5] S. R. Dalton and A. Bellacosa, "DNA demethylation by TDG," *Epigenomics*, vol. 4, no. 4, pp. 459–467, 2012.

[6] E.-J. Kim and S.-J. Um, "Thymine-DNA glycosylase interacts with and functions as a coactivator of p53 family proteins," *Biochemical and Biophysical Research Communications*, vol. 377, no. 3, pp. 838–842, 2008.

[7] N. M. Da Costa, A. Hautefeuille, M.-P. Cros et al., "Transcriptional regulation of thymine DNA glycosylase (TDG) by the tumor suppressor protein p53," *Cell Cycle*, vol. 11, no. 24, pp. 4570–4578, 2012.

[8] P. Broderick, T. Bagratuni, J. Vijayakrishnan, S. Lubbe, I. Chandler, and R. S. Houlston, "Evaluation of NTHL1, NEIL1, NEIL2, MPG, TDG, UNG, and SMUG1 genes in familial colorectal cancer predisposition," *BMC Cancer*, vol. 6, article 243, no. 1, 2006.

[9] X. Xu, T. Yu, J. Shi et al., "Thymine DNA glycosylase is a positive regulator of Wnt signaling in colorectal cancer," *The Journal of Biological Chemistry*, vol. 289, no. 13, pp. 8881–8890, 2014.

[10] B. Peng, E. M. Hurt, D. R. Hodge, S. B. Thomas, and W. L. Farrar, "DNA hypermethylation and partial gene silencing of human thymine-DNA glycosylase in multiple myeloma cell lines," *Epigenetics*, vol. 1, no. 3, pp. 138–145, 2006.

[11] T. Yatsuoka, T. Furukawa, T. Abe et al., "Genomic analysis of the thymine-DNA glycosylase (TDG) gene on 12q22–q24. 1 in human pancreatic ductal adenocarcinoma," *International Journal of Pancreatology*, vol. 25, no. 2, pp. 97–102, 1999.

[12] P. Vasovcak, A. Krepelova, M. Menigatti et al., "Unique mutational profile associated with a loss of TDG expression in the rectal cancer of a patient with a constitutional PMS2 deficiency," *DNA Repair*, vol. 11, no. 7, pp. 616–623, 2012.

[13] I. Ruczinski, T. J. Jorgensen, Y. Y. Shugart et al., "A population-based study of dna repair gene variants in relation to non-melanoma skin cancer as a marker of a cancer-prone phenotype," *Carcinogenesis*, vol. 33, no. 9, pp. 1692–1698, 2012.

[14] M. P. Fogarty, M. E. Cannon, S. Vadlamudi, and K. J. Gaulton, "Identification of a regulatory variant that binds FOXA1 and FOXA2 at the CDC123/CAMK1D type 2 diabetes GWAS locus," *PLoS Genetics*, vol. 10, no. 9, Article ID e1004633, 2014.

[15] W.-Q. Li, N. Hu, P. L. Hyland et al., "Genetic variants in DNA repair pathway genes and risk of esophageal squamous cell carcinoma and gastric adenocarcinoma in a Chinese population," *Carcinogenesis*, vol. 34, no. 7, pp. 1536–1542, 2013.

[16] M. Alanazi, A. A. K. Pathan, J. P. Shaik et al., "The hOGG1 Ser326Cys gene polymorphism and breast cancer risk in saudi population," *Pathology & Oncology Research*, vol. 23, no. 3, pp. 525–535, 2017.

[17] D. Penny, M. P. Hoeppner, A. M. Poole, and D. C. Jeffares, "An overview of the introns-first theory," *Journal of Molecular Evolution*, vol. 69, no. 5, pp. 527–540, 2009.

[18] A. Sjolund, A. A. Nemec, N. Paquet et al., "A Germline polymorphism of thymine DNA glycosylase induces genomic instability and cellular transformation," *PLoS Genetics*, vol. 10, no. 11, Article ID e1004753, 2014.

[19] M. Krześniak, D. Butkiewicz, A. Samojedny, M. Chorazy, and M. Rusin, "Polymorphisms in TDG and MGMT genes - epidemiological and functional study in lung cancer patients from Poland," *Annals of Human Genetics*, vol. 68, no. 4, pp. 300–312, 2004.

[20] K. Curtin, C. M. Ulrich, W. S. Samowitz et al., "Candidate pathway polymorphisms in one-carbon metabolism and risk of rectal tumor mutations," *International Journal of Molecular Epidemiology and Genetics*, vol. 2, no. 1, pp. 1–8, 2011.

[21] R. M. Kohli and Y. Zhang, "TET enzymes, TDG and the dynamics of DNA demethylation," *Nature*, vol. 502, no. 7472, pp. 472–479, 2013.

[22] A. Chanson, L. D. Parnell, E. D. Ciappio et al., "Polymorphisms in uracil-processing genes, but not one-carbon nutrients, are associated with altered dna uracil concentrations in an urban puerto rican population," *The American Journal of Clinical Nutrition*, vol. 89, no. 6, pp. 1927–1936, 2009.

[23] K. H. Barry, S. Koutros, S. I. Berndt et al., "Genetic variation in base excision repair pathway genes, pesticide exposure, and prostate cancer risk," *Environmental Health Perspectives*, vol. 119, no. 12, pp. 1726–1732, 2011.

[24] B. Pardini, C. Viberti, A. Naccarati et al., "Increased micronucleus frequency in peripheral blood lymphocytes predicts the risk of bladder cancer," *British Journal of Cancer*, vol. 116, no. 2, pp. 202–210, 2017.

[25] H. Wei, A. Kamat, M. Chen et al., "Association of polymorphisms in oxidative stress genes with clinical outcomes for bladder cancer treated with bacillus calmette-guérin," *PLoS ONE*, vol. 7, no. 6, Article ID e38533, 2012.

Hindawi
Journal of Oncology
Volume 2019, Article ID 7820275, 14 pages
https://doi.org/10.1155/2019/7820275

Research Article

MicroRNA Expression Changes in Women with Breast Cancer Stratified by DNA Repair Capacity Levels

Jarline Encarnación-Medina,[1] **Carmen Ortiz**,[1] **Ralphdy Vergne**,[2] **Luis Padilla**,[2] **and Jaime Matta**[1]

[1]*Basic Sciences Department, Division of Pharmacology & Toxicology and Cancer Biology, Ponce Research Institute, Ponce 00716-2348, PR, USA*
[2]*Biology Department, University of Puerto Rico at Ponce, Ponce 00716-9996, PR, USA*

Correspondence should be addressed to Jarline Encarnación-Medina; jencarnacion@psm.edu

Received 25 January 2019; Revised 15 March 2019; Accepted 17 April 2019; Published 5 May 2019

Guest Editor: Qingyuan Yang

Breast cancer (BC) is the most commonly diagnosed cancer in women worldwide and is the leading cause of death among Hispanic women. Previous studies have shown that women with a low DNA repair capacity (DRC), measured through the nucleotide excision repair (NER) pathway, have an increased BC risk. Moreover, we previously reported an association between DRC levels and the expression of the microRNA (miRNA) let-7b in BC patients. MiRNAs can induce genomic instability by affecting the cell's DNA damage response while influencing the cancer pathobiology. The aim of this pilot study is to identify plasma miRNAs related to variations in DRC levels in BC cases. *Hypothesis*. Our hypothesis consists in testing whether DRC levels can be correlated with miRNA expression levels. *Methods*. Plasma samples were selected from 56 (27 cases and 29 controls) women recruited as part of our BC cohort. DRC values were measured in lymphocytes using the host-cell reactivation assay. The samples were divided into two categories: low (≤3.8%) and high (>3.8%) DRC levels. MiRNAs were extracted to perform an expression profile analysis. *Results*. Forty miRNAs were identified to be BC-related ($p<0.05$, MW), while 18 miRNAs were found to be differentially expressed among BC cases and controls with high and low DRC levels ($p<0.05$, KW). Among these candidates are miR-299-5p, miR-29b-3p, miR-302c-3p, miR-373-3p, miR-636, miR-331-5p, and miR-597-5p. Correlation analyses revealed that 4 miRNAs were negatively correlated within BC cases with low DRC ($p<0.05$, Spearman's correlation). Results from multivariate analyses revealed that the clinicopathological characteristics may not have a direct effect on specific miRNA expression. *Conclusion*. This pilot study provides evidence of four miRNAs that are negatively regulated in BC cases with low DRC levels. Additional studies are needed in order to have a complete framework regarding the overall DRC levels, miRNA expression profiles, and tumor characteristics.

1. Introduction

The American Cancer Society estimates that in 2019, 268,600 new breast cancer (BC) cases and 41,760 cancer-related deaths will occur in the US [1]. The Center of Disease Control (CDC) reported that BC is the second cause of death among women in the US and the leading cause of death among Hispanic women. In the US and Puerto Rico (PR), BC now accounts for approximately 30% of all new cancers in women [2, 3]. In PR, 2,205 new BC cases and 444 BC deaths were reported by the Puerto Rico Cancer Registry in 2015 [3].

Cancer is a complex disease with genetic, epigenetic, and environmental risk factors. Genomic instability is a known hallmark of cancer as described by Hanahan and Weinberg (2011) [4]. Dysregulation of various DNA repair pathways contributes to this genomic instability due to inability of the cell to repair certain types of DNA damage [5, 6]. Defective DNA repair measured in blood cells has been identified as a risk factor for different types of cancer [7–9], including BC [9]. At least 5 DNA repair pathways have been described which contain approximately 200 DNA repair genes [10–12]. Nucleotide excision repair (NER) is a very versatile repair pathway that involves around 30 proteins that act to replace damaged nucleotides [13]. NER is the predominant mechanism by which bulky DNA adducts are repaired. These can be formed by multiple sources of DNA damage including

UV light, exogenous chemicals, and chemotherapeutic agents like cisplatin [13]. Previous studies from our laboratory demonstrate the critical importance of the overall DRC levels for BC risk through the NER pathway using lymphocytes as surrogate markers [14, 15]. Recently, our laboratory showed that there is substantial variability in overall DRC levels among the four principal molecular BC subtypes and that women with triple-negative (TN) BC have the lowest DRC [16]. These findings confirm the importance of the NER pathway in sporadic BC and highlight the need for more research to understand how changes in DRC levels are associated with multiple endpoints in the complex process of BC carcinogenesis.

The epigenome has been proposed as an intermediary between genotype and phenotype [17]. Hence, the use of epigenetic analysis holds substantial promise for identifying mechanisms through which genetic and environmental factors contribute to disease risk [18]. Epigenetic changes have been associated with DRC levels once the BC malignancy is developed. For example, plasma levels of let-7b microRNA (miRNA) have been associated with high DRC levels in women with BC [19]. MiRNAs are endogenous, short (19–24 nucleotides) non-protein-coding RNAs that regulate gene expression at the posttranscriptional level via binding to 3′-untranslated regions of protein-coding transcripts [20]. Their aberrant expression in peripheral blood has been associated with different types of cancer [21]. MiRNAs are pleiotropic in terms of functions and have been shown to regulate the expression of a broad range of genes involved in cancer. However, very little is known of their role in the regulation of DRC levels in BC. Therefore, the main objectives of this pilot study were to (1) identify miRNAs that are related to BC, (2) identify miRNAs that are correlated with DRC levels in women with BC, and (3) test whether the clinicopathological characteristics from the women studied contribute to DRC levels.

2. Materials and Methods

Use of Human Subjects. The Ponce Health Sciences University Institutional Review Board approved this study (IRB #130207-JM). Each participant signed an Informed Consent form, providing permission to collect a blood sample and to review their pathology reports. All participants completed a 7-page epidemiological questionnaire requesting demographic data and BC risk factors which was administered by the study nurse.

Patient Recruitment. Participants in this study were selected from our BC cohort recruited from 2006 to 2013 (1,187 women with and without BC) as described in Matta et al. 2012 [22]. For each participant, blood samples were collected along with epidemiological data through a questionnaire. Plasma and lymphocytes were isolated from the blood samples. BC cases included in this study were recently diagnosed, treatment-naïve (had not received blood transfusions, chemotherapy, or radiotherapy) patients with primary breast tumors. Controls (women without BC) were required to have a normal breast examination performed by a primary care physician and a normal mammography, 6 months prior to study enrolment, and no prior history of any cancer type. Pathology reports from BC cases were obtained for diagnosis confirmation and collection of clinicopathological variables such as tumor size and grade, type of cancer, hormone receptor status, and other clinically relevant information. Using the hormone receptor status data for estrogen (ER) and progesterone (PR) receptors, along with HER2, the tumors of the BC cases were classified into four principal molecular subtypes: luminal A (ER+, PR+, HER2−), luminal B (ER+, PR+, HER2+), HER2+ (ER−, PR−, HER2+), and triple negative (TN) (ER−, PR−, HER2−). For this pilot study, 56 participants, 27 BC cases and 29 controls, were selected from our BC cohort including cases and controls with high and low DRC.

DNA Repair Capacity Measurements. Peripheral blood lymphocytes were separated, purified, and grown from each patient sample, as previously reported [9, 22]. The isolated lymphocytes were used as surrogate markers of the patients' overall DRC [23, 24], measured using the host-cell reactivation (HCR) assay. This assay allows for the measurement of in vivo DRC, as previously published [9, 25–28]. The lymphocytes' capacity to repair the foreign DNA was measured via HCR [25] within a specific time frame (40 h) that mirrored the true cellular process [24]. Results reflected the cells' inherent DRC, measured primarily in terms of their NER pathway activity [25]. Briefly, the lymphocytes were transfected with a plasmid, previously damaged with UVC light, containing the luciferase reporter gene. To calculate DRC, the luciferase activity after repair of the UVC-damaged plasmid DNA was compared with the undamaged plasmid DNA. The amount of residual luciferase remaining after the allotted repair time (activity in luminescence units) was a percentage that represented the amount of the individuals' DRC. DRC levels were established as previously described using the cut-off of ≥3.8% for high DRC and <3.8% for low DRC [19].

MicroRNA Expression Profile. MicroRNA expression profiling was performed utilizing the TaqMan Array Human MicroRNA A Cards v 2.0 (Applied Biosystems). miRNAs were extracted from the 56 plasma samples using the Ambion *mir*Vana miRNA Isolation Kit (Life Technologies; Grand Island, NY). RNA concentration and quality were determined using a NanoDrop 1000; 0.5–1 mg total RNA was reverse-transcribed with pools of miRNA-specific RT primers. A preamplification step using Megaplex PreAmp Primers, Human Pool A v2.1, was performed to increase sensitivity. Single-stranded cDNA was synthesized from 200 ng of total RNA in 8 Multiplex RT primer pool reactions containing stem-looped RT primers that were specific to mature miRNA. The resulting cDNA samples were diluted, combined with TaqMan Universal PCR Master Mix (Applied Biosystems), and then loaded onto the TaqMan Array. Quantitative PCR was carried out under the following thermocycler conditions: 30 min at 16°C, 30 min at 42°C, 5 min at 85°C and then held at 4°C. Experimental Ct fluorescence evaluation was performed by testing for experimental outliers, and only cycles between 20 and 40 Ct were considered. Sample normalization was

performed using U6 as endogenous miRNA. All the miRNA expression experiments were performed at the Molecular Genomics Core, H. Lee Moffitt Cancer Center (Tampa, Florida).

Statistical Analyses. To assess mean expression differences between BC cases and controls, a Mann–Whitney test was performed. Comparisons among miRNA expression levels among groups were performed using a Kruskal–Wallis test. The hierarchical microRNA clustering was performed using Morpheus heatmap generator [29] and tested for correlations using the Pearson's correlation test. Proportion analyses were performed using cross-tables, and differences were detected using a chi-square test. Significant correlations between miRNA expression and DRC levels were evaluated using the Spearman's correlation. Statistical significance was defined using a p-value of 0.05 or less based on a two-tailed test. Analyses were performed using Prism 8 (GraphPad Software; San Diego, CA) and Minitab® 18 (Minitab Inc.; State College, PA).

Multivariate Analysis. The principal component (PC) algorithm creates a series of artificial coordinates using the original matrix data, to localize the samples relative to each other. This analysis is best interpreted using a score plot graph. This graph consolidates the sample cluster formation where the closer the samples are located, the less the variability among them. The PC matrix for this study was constructed using the miRNA relative expression values, excluding the miRNAs with missing values from the analysis. The PC matrix was constructed with these miRNAs along with some of the epidemiological and clinicopathological information for each participant including case or control classification, DRC levels (high and low), tumor grade, and molecular subtype classification. Multivariate analyses and PC graphs were created in Minitab® 18 (Minitab Inc.; State College, PA).

3. Results

3.1. Epidemiological and Clinicopathological Variables. As an initial analysis, differences between cases and controls regarding known BC risk factors were assessed for body mass index (BMI), pregnancy, parity, breastfeeding practices, use of oral contraceptives, regularity of menstrual periods, history of endometriosis, hysterectomy, age of hysterectomy, oophorectomy, age of oophorectomy, family history of cancer, and BC history. Cross-table analyses showed no significant differences in the study cohort stratified by these variables ($p>0.05$, Pearson's chi-square test) (Table 1). However, statistically significant differences were found between BC cases and controls stratified by age ($p=0.0239$), age of menarche ($p=0.0001$), and use of hormone replacement therapy ($p=0.0420$). Differences in clinicopathological characteristics were evaluated among BC cases stratified in terms of low (<3.8%) and high (≥3.8%) DRC levels (Table 2). The clinicopathological characteristics analyzed were hormone receptor status (estrogen: ER, progesterone: PR, and HER2), Ki-67 expression, tumor grade and site, and type of BC. No significant differences were found regarding any of these clinicopathological characteristics between BC cases with low and high DRC levels (Table 2). Using the hormone receptor status information, BC cases were stratified into the four principal molecular subtypes: luminal A (ER+, PR+, HER2−), luminal B (ER+, PR+, HER2+), HER2+ (ER−, PR−, HER2+), and triple negative (ER−, PR−, HER2−). However, no significant differences were observed among groups ($p>0.05$, Pearson's chi-square test) (Table 2).

3.2. Identification of Breast Cancer-Related MicroRNAs. A case-control stratification was performed to identify the miRNAs that were significantly related to BC in Hispanic women. The qualitative aspect of the data is illustrated using hierarchical clustering where only the rows were taken into consideration to assure that the generated heatmap captured the miRNA expression from BC cases and controls separately (Figure S1). The heatmap proportion with higher miRNA expression abundance was composed of BC cases (Figure S1(a)) when compared with the control group (Figure S1(b)). A correlation analysis was performed to measure the distance between the expression profiles from BC cases and controls and to assess any linear relationship between expression patterns; however, no significant correlation was found (data not shown) ($p>0.05$, Pearson's chi-square test).

In general, the miRNA expression values obtained from this experiment cannot be defined in terms of a normal or Gaussian distribution ($\mu=0$, $\sigma=1$) without any further statistical modifications. Consequently, the mean differences in miRNA expression among cases and controls were analyzed through a nonparametric test. This allowed us to, at first, identify BC-related miRNAs. This initial statistical analysis resulted in 40 miRNA candidates differentially expressed between BC cases and controls (Table 3). From these 40 candidate miRNAs, only miR-18a-5p, miR-372-3p, and miR-652-3p were highly expressed in controls rather than in BC cases, while the remaining 37 miRNAs were overexpressed in BC cases (Table 3).

In order to identify miRNAs related to the overall DRC levels, BC cases and controls were stratified into low (<3.8%) and high (≥3.8%) DRC (Figure 1). Correlation analyses were performed focusing on low DRC BC cases only (Figure 2). Negative correlations were found between let-7b, miR-222-3p, miR-18a-5p, and miR-520-3p relative expression and DRC levels below the cut-off point of 3.8% ($p<0.05$, Spearman's correlation) (Figure 2).

3.3. DNA Repair Capacity-Related MiRNAs. Differential expression of the 40 BC-related candidates was tested for relevance to DRC levels in BC cases and controls stratified by DRC levels using a Kruskal–Wallis (KW) test. To assess mean differences in miRNA expression among groups stratified by DRC as a dichotomous variable, a post hoc test was performed (Table 3). The following miRNAs were differentially expressed among the four study groups: miR-518f-3p, miR-628-5p, miR-299-5p, miR-29b-3p, miR-302c-3p, miR-323-3p, miR-367-3p, miR-373-3p, miR-636, miR-331-5p, miR-363-3p, and miR-597-5p (Figure 3). MicroRNAs with a high relative expression, miR-518f-3p and miR-628-5p, were plotted using a logarithmic scale (Figures 3(a) and 3(b)).

Table 1: Description of the study group including DNA repair capacity levels and selected breast cancer risk factors in cases and controls.

Epidemiological characteristics	Controls n=29 (%)	BC cases n=27 (%)	p-value
DRC			
Low (<3.8%)	15 (26.8)	18 (32.1)	0.2561
High (≥3.8%)	14 (25.0)	9 (16.1)	
Age			
21-40	7 (12.5)	0 (0.0)	0.0239
41-60	11 (19.6)	14 (25.0)	
61+	11 (19.6)	13 (23.2)	
BMI			
<25 kg/m^2	14 (25.0)	9 (16.1)	0.2772
≥25 kg/m^2	14 (25.0)	18 (32.1)	
Missing	1 (1.8)	0 (0.0)	
Ever been pregnant			
Yes	26 (46.4)	24 (42.9)	0.9262
No	3 (5.4)	3 (5.4)	
Age at first birth			
≤19	6 (10.7)	4 (7.1)	0.6075
20-29	14 (25.0)	16 (28.6)	
≥30	6 (10.7)	2 (3.6)	
Missing	0 (0.0)	2 (3.6)	
Parity			
Nulliparous	3 (5.4)	3 (5.4)	0.2244
1-2 children	15 (26.8)	8 (14.3)	
≥3 children	11 (19.6)	16 (28.6)	
Ever breastfeed			
Yes	15 (26.8)	11 (19.6)	0.4102
No	14 (25.0)	16 (28.6)	
Length of breastfeeding			
Never	14 (25.0)	11 (19.6)	0.0585
1-5 months	13 (23.2)	11 (19.6)	
≥6 months	2 (3.6)	0 (0.0)	
Missing	0 (0.0)	5 (8.9)	
Oral contraceptive use			
Yes	13 (23.2)	8 (14.3)	0.2405
No	16 (28.6)	19 (33.9)	
Age started oral contraceptive			
<20	2 (3.6)	1 (1.8)	1
≥21	11 (19.6)	7 (12.5)	
Regular menstrual periods			
Yes	15 (26.8)	19 (33.9)	0.1534
No	14 (25.0)	8 (14.3)	
Age Menarche			
≤12	0 (0.0)	11 (19.6)	0.0001
≥13	26 (46.4)	14 (25.0)	
Missing	3 (5.4)	2 (3.6)	
History of endometriosis			
Yes	3 (5.4)	1 (1.8)	0.3349
No	26 (46.4)	26 (46.4)	
Hysterectomy			
Yes	9 (16.1)	6 (10.7)	0.4568
No	20 (35.7)	21 (37.5)	

Table 1: Continued.

Epidemiological characteristics	Controls n=29 (%)	BC cases n=27 (%)	p-value
Age of hysterectomy			
≤40	6 (10.7)	1 (1.8)	0.1264
41-49	1 (1.8)	3 (5.4)	
≥50	2 (3.6)	2 (3.6)	
Oophorectomy			
Yes	8 (14.3)	6 (10.7)	0.5589
No	20 (35.7)	21 (37.5)	
Missing	1 (1.8)	0 (0.0)	
Age of oophorectomy			
≤40	4 (7.1)	2 (3.6)	0.1264
41-49	2 (3.6)	2 (3.6)	
≥50	2 (3.6)	2 (3.6)	
Menopause (actually)			
Yes	4 (7.1)	3 (5.4)	0.7664
No	23 (41.1)	22 (39.3)	
Missing	2 (3.6)	2 (3.6)	
Hormone replacement therapy			
Yes	14 (25.0)	6 (10.7)	0.0420
No	15 (26.8)	21 (37.5)	
Smoking			
Yes	1 (1.8)	3 (5.4)	0.2659
No	28 (50.0)	24 (39.3)	
Alcohol consumption			
Yes	5 (8.9)	5 (8.9)	0.9008
No	24 (42.9)	22 (39.3)	
Family history of cancer (not BC)			
Yes	13 (23.2)	13 (23.3)	0.8034
No	16 (28.6)	14 (25.0)	
BC history in any family member			
Yes	16 (28.6)	12 (21.4)	0.4224
No	13 (23.2)	15 (26.8)	

Pearson's chi-square test was performed to assess significance among groups.
DRC: DNA repair capacity, BMI: body mass index, BC: breast cancer.

For BC cases with low DRC levels, the mean expression of miR-628-5p was higher than the expression of miR-518f-3p (4.56% vs. 5.35%). The median of the low DRC BC cases shows a skewed distribution for both miRNAs (miR-518f-3p and miR-628-5p) which reveals the presence of biological outliers. In contrast, BC cases with high DRC had similar values for the median and the mean indicating a possible symmetric distribution (Figures 3(a) and 3(b)). The mean expression of these miRNAs in the control groups was similar independently of the DRC levels. In terms of the controls with low and high DRC, miR-299-5p, miR-302c-3p, miR-373-3p, and miR-331-5p showed a similar distribution in both groups (Figures 3(c), 3(e), 3(h), and 3(j)). In contrast, for miR-29b-3p, miR-323-3p, miR-367-3p, miR-636, and miR-597-5p, at least one of the control groups shows a slightly skewed distribution (Figures 3(d), 3(f), 3(g), 3(i), and 3(l)).

Relative miRNA expression was higher in BC cases than in controls for all miRNA candidates included in this analysis focused on DRC levels (Figures 3 and S2). Interestingly, some miRNAs were highly expressed in BC cases with high DRC such as miR-323-3p, miR-367-3p, and miR-363-3p (Figures 3(f), 3(g), and 3(k)). A different group of miRNAs had a higher expression in BC cases with low DRC levels, including miR-299-5p, miR-29b-3p, miR-302c-3p, miR-373-3p, miR-636, miR-331-5p, and miR-597-5p (Figures 3(c)–3(e), 3(h)–3(j), and 3(l)). When performing multiple comparison tests, significant differences in expression were found between BC cases and controls with low DRC for miR-299-5p ($p<0.05$), miR-302c-3p ($p<0.01$), miR-331-5p ($p<0.05$), miR-363-3p ($p<0.05$), miR-373-3p ($p<0.01$), and miR-597-5p ($p<0.01$) (Table 3 and Figure 3). Also, significant differences were observed between high DRC BC cases and low DRC controls for miR-29b-3p ($p<0.05$) and miR-518f-3p ($p<0.01$)

Table 2: Clinicopathological characteristics of BC cases with low and high levels of DNA repair capacity.

Clinicopathological Characteristics	Low DRC (<3.8%) n=18 (%)	High DRC (≥3.8%) n=9 (%)	p-value
Estrogen receptor status			
Positive	9 (33.3)	3 (11.1)	0.5698
Negative	6 (22.2)	3 (11.1)	
Missing	3 (11.1)	3 (11.1)	
Progesterone receptor status			
Positive	8 (29.6)	3 (11.1)	0.6121
Negative	7 (25.9)	3 (11.1)	
Missing	3 (11.1)	3 (11.1)	
HER2 status			
Positive	0 (0.0)	1 (3.7)	0.7160
Negative	12 (44.4)	5 (18.5)	
Missing	6 (22.2)	3 (11.1)	
Ki-67			
Low (≤10%)	1 (3.7)	1 (3.7)	0.9297
Borderline (11-20%)	0 (0.0)	0 (0.0)	
High (≥21%)	3 (11.1)	1 (3.7)	
Missing	15 (55.6)	6 (22.2)	
Grade			
I	4 (14.8)	0 (0.0)	0.4194
II	6 (22.2)	4 (14.8)	
III	5 (18.5)	4 (14.8)	
Missing	3 (11.1)	1 (3.7)	
Molecular Subtypes			
Luminal A	7 (25.9)	3 (11.1)	0.6923
Luminal B	0 (0.0)	0 (0.0)	
HER2+	0 (0.0)	1 (3.7)	
Triple-negative	5 (18.5)	2 (7.4)	
Missing	6 (22.2)	3 (11.1)	
Site			
Ductal	16 (59.3)	7 (25.9)	0.3522
Lobular	2 (7.4)	1 (3.7)	
Ductal + Lobular	0 (0.0)	1 (3.7)	
Type			
In situ	1 (3.7)	0 (0.0)	0.4712
Invasive	17 (63.0)	9 (33.3)	

Pearson's chi-square test was performed to assess significance among groups.
DRC: DNA repair capacity, BMI: body mass index, BC: breast cancer.

(Table 3 and Figure 3). Only for miR-636, significant differences were observed between the BC cases and controls with high DRC ($p<0.05$).

Other differentially expressed candidates were miR-155-5p, miR-194-5p, miR-222-3p, miR-372-3p, miR-483-5p, and miR-342-3p; however, the post hoc test did not yield statistically significant results ($p>0.05$) (Figure S2). BC cases with low DRC had the highest relative expression of miR-155-5p, miR-194-5p, miR-296-3p, and miR-483-5p among all study groups, followed by high DRC BC cases (Figures S2(a)–S2(c) and S2(e)). In contrast, low DRC BC cases had the highest relative expression among groups for miR-372-3p and miR-342-3p, followed by high DRC BC cases (Figure S2(d) and S2(f)). As for the control groups, similar expression of these miRNAs was observed in high and low DRC groups (Figure S2(a)–S2(f)).

3.4. Multivariate Analyses. The principal component (PC) matrix was constructed using the miRNAs that were detected in all the samples, excluding miRNAs with missing values. The aim of this analysis was to identify the miRNAs responsible for the variation in expression among samples, as illustrated in Figure S1. A second aim was to identify any clustering using different variables such as case or control classification, DRC levels, tumor grade, and BC subtype. Among the miRNAs that qualified for this analysis

Table 3: Breast cancer-related miRNAs and comparisons with women with low and high DRC levels.

miRNA ID	Case-Control Groups[1]	Regulation	DRC Groups[2]	Multiple Comparisons∗	*p-value*[3]
let-7b	0.0153	↑	0.1062	-	-
let-7c	0.0157	↑	0.0581	-	-
let-7e	0.0477	↑	0.2243	-	-
miR-101-3p	0.0389	↑	0.1517	-	-
miR-150-5p	0.0258	↑	0.1615	-	-
miR-155-5p	0.0043	↑	0.0329	NS	*p>0.05*
miR-18a-5p	0.0205	↓	0.1344	-	-
miR-194-5p	0.0083	↑	0.0465	NS	*p>0.05*
miR-204-5p	0.0337	↑	0.1175	-	-
miR-212-3p	0.0227	↑	0.0857	-	-
miR-222-3p	0.0330	↑	0.1847	-	-
miR-25-3p	0.0455	↑	0.1010	-	-
miR-296-3p	0.0440	↑	0.0322	NS	*p>0.05*
miR-299-5p	0.0143	↑	0.0362	BC LDRC vs. Controls LDRC	∗*p<0.05*
miR-29b-3p	0.0021	↑	0.0168	BC HDRC vs. Controls LDRC	∗*p<0.05*
miR-302a-3p	0.0163	↑	0.0616	-	-
miR-302c-3p	0.0022	↑	0.0040	BC LDRC vs. Controls LDRC	∗∗*p<0.01*
miR-30b-5p	0.0258	↑	0.1107	-	-
miR-320a-3p	0.0492	↑	0.2296	-	-
miR-323-3p	0.0002	↑	0.0014	BC cases LDRC vs. Controls (LDRC & HDRC)	∗*p<0.05*
miR-331-5p	0.0124	↑	0.0145	BC LDRC vs. Controls LDRC	∗*p<0.05*
miR-342-3p	0.0065	↑	0.0297	NS	*p>0.05*
miR-363-3p	0.0227	↑	0.0394	BC LDRC vs. Controls LDRC	∗*p<0.05*
miR-367-3p	0.0046	↑	0.0235	BC LDRC vs. Controls HDRC	∗*p<0.05*
miR-372-3p	0.0024	↓	0.0254	NS	*p>0.05*
miR-373-3p	0.0006	↑	0.0077	BC LDRC vs. Controls LDRC	∗∗*p<0.01*
miR-375-3p	0.0175	↑	0.1060	-	-
miR-383-5p	0.0135	↑	0.0849	-	-
miR-425-5p	0.0165	↑	0.0540	-	-
miR-483-5p	0.0121	↑	0.0386	NS	*p>0.05*
miR-486 -5p	0.0234	↑	0.1370	-	-
miR-509-5p	0.0226	↑	0.1330	-	-
miR-518f-3p	0.0002	↑	0.0011	BC cases LDRC vs. Controls (LDRC&HDRC)	∗∗*p<0.01*
miR-520b-3p	0.0084	↑	0.0615	-	-
miR-525-5p	0.0055	↑	0.0537	-	-
miR-597-5p	0.0029	↑	0.0073	BC LDRC vs. Controls LDRC	∗∗*p<0.01*
miR-628-5p	0.0003	↑	0.0026	BC cases LDRC vs. Controls (LDRC&HDRC)	∗*p<0.05*
miR-636	0.0205	↑	0.0266	BC cases LDRC vs. Controls HDRC	∗*p<0.05*
miR-652-3p	0.0423	↓	0.2382	-	-
miR-708-5p	0.0187	↑	0.1298	-	-

p-value[1]: obtained from Mann–Whitney test (BC case-control comparisons); *p-value*[2]: obtained from Kruskal–Wallis test (DRC stratifications); *p-value*[3]: obtained from Dunn's multiple comparisons post hoc test. NS: nonsignificant, BC: breast cancer, LDRC: low DNA repair capacity, HDRC: high DNA repair capacity. Arrows represent up- or downregulation in BC cases when compared to controls.
∗ means groups significantly different from post hoc analysis.

were miR-101-3p, miR-150-5p, miR-155-5p, miR-194-5p, miR-212-3p, miR-30b-5p, miR-320a-3p, miR-363-3p, miR-375-3p, miR-483-5p, and miR-597-5p. The eigen analysis of the correlation matrix was used to generate the new PC coordinates with a cumulative variance of 0.69 using the two components. A scree plot was also used to choose the PC using the Kaiser criterion (Figure 4(e)) [30]. The PC2 variance contribution was very small (9.5%), and the PC1 weights were stronger for almost all these candidates (59.5%). The biplot graph using the PC1 and PC2 coordinates was generated and further used to localize the samples that were stratified by case or control classification, DRC levels, tumor

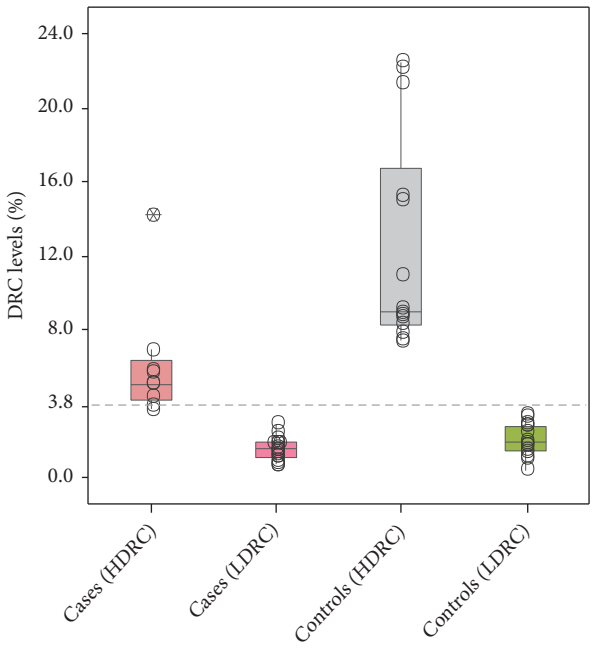

Figure 1: Distribution of DNA repair capacity levels among study participants including breast cancer cases and control. Groups were stratified into low (<3.8%) and high (≥3.8%) DRC based on a previously established cut-off (dotted line). Study groups were composed of BC cases with low (n=15) and high (n=14) DRC along with controls with low (n=18) and high (n=9) DRC levels. Box plots represent the data distribution of 26 breast cancer patients and 27 controls.

grade, and BC subtype, which are presented in a color-coded graph panel (Figures 4(a)–4(f)). In order to discriminate among the miRNAs that were responsible for these clusters, a loading plot was generated using the PC axis (Figure 4(f)). Among the identified miRNAs with greater contribution to the PC1 were miR-101-3p, miR-150-5p, miR-320a-3p, miR-483-5p, miR-212-3p and miR-597-5p. The PC2 was below zero for miR-320a-3p and miR-597-5p. MiR-483-5p and miR-212-3p had a negative value on the PC2. The minor contributors for the PC1 were miR-155-5p, miR-194-5p, miR-30b-5p, miR-363-3p, and miR-375-3p. MiR-155-5p and miR-194-5p had the largest values on the PC2, followed by miR-101-3p and miR-150-5p. Thus, these miRNAs were also the ones with the highest degree of accumulative variance.

The PC analysis revealed that BC cases with high DRC were similar to the controls (independently of their DRC levels) and slightly different from the BC cases with low DRC on the PC1 axis. In Figure 4(b), an overlap can be seen between high DRC BC cases and controls showing that these samples are similar in terms of miRNA expression. The clinicopathological variables that were evaluated to possibly explain the data variation exposed in the mean comparison analyses and on the hierarchical heatmap were tumor site (ductal, lobular, or mixed), type of cancer (in situ or invasive), tumor grade, and molecular subtype. Only three samples were classified as a lobular malignancy and one sample had mixed components (combination of ductal and lobular) (Table 2). Only one tumor sample was classified as in situ BC, which accounted for 3.7% of the BC cases included in this pilot study. However, no clustering was detected in the PC analysis for tumor site and type of cancer when these samples were localized in the PC plot (data not shown). No clustering was observed on the PC analysis by tumor grade. Samples identified as grade I were spread along the PC1 axis. In addition, no clusters were identified when stratifiying samples by molecular BC subtype. However, the sample cohort did not have representation of the luminal B and HER2 subtypes.

4. Discussion

Although the role of miRNAs in BC has been extensively investigated and published, this pilot study is the first, to our knowledge, to establish a link between miRNA expression and overall DRC levels in BC cases. This study also represents one of the few assessing miRNA expression changes in Hispanic women with BC. Although a vast number of studies have been published regarding aberrant expression of miRNAs once the BC malignancy is developed, emerging evidence suggests that differences in miRNA expression profiles are partly influenced by ethnicity [19, 31, 32]. This pilot study provides new data on the miRNA expression profile of Hispanic women with BC and a basis for comparison of miRNAs profiles of women with BC from other populations. In addition, since the 27 women with BC studied were recently diagnosed and treatment naïve, treatment can be eliminated as a potential confounder.

4.1. Epidemiological and Clinicopathological Variables. The study cohort was composed of 56 Hispanic women from Puerto Rico where 51.8% were controls and 48.2% were BC cases. Epidemiological variables were categorized by DRC levels to assess differences among groups. Although no differences were observed for various epidemiological variables, a low DRC level was frequently observed in BC cases as we have previously published [19, 22, 33]. Overall, in our cohort, controls were younger than BC cases, as has been previously reported in many BC studies [1, 34]. Body mass index (BMI) has been reported to vary depending on age and ethnicity [19, 22, 35, 36]; however, in this study no association was found between BMI and having BC. Most of the participants reported having at least one pregnancy in the age range between 20 and 29 years. An equal proportion of the BC cases and controls (5.4%) reported being nulliparous. Early menarche (before age 12) is also a known BC risk factor [37]. Consistent with previous studies, we found an association between having the first menstrual period before 12 years old and having BC. Some surgical procedures have also been linked to decreasing BC risk (i.e., hysterectomy and oophorectomy); however, no association was found for any of these variables in our study group [38]. Lifestyle habits known to affect BC risk (i.e., smoking and alcohol consumption) were equally distributed in our cohort. No association with nonsporadic BC was found, based on the family history of BC and cancer in general.

Most of the BC cases were diagnosed with invasive ductal carcinoma including women with high and low DRC levels.

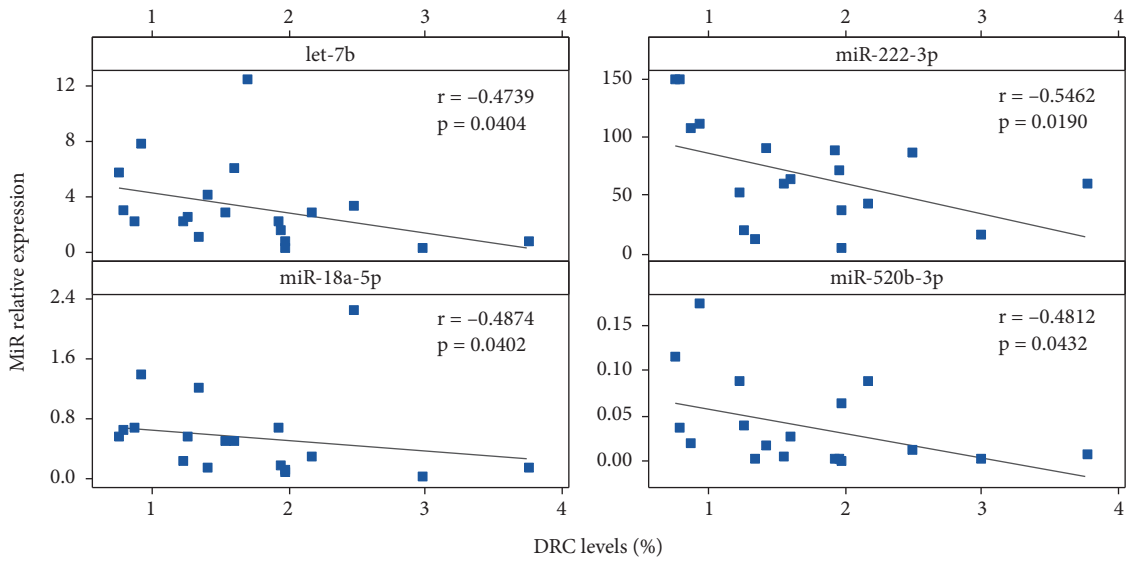

Figure 2: Correlation between selected microRNAs and DNA repair capacity levels. Linear regressions were performed to test for correlations between DRC levels and let-7b, miR-222-3p, miR-18a-5p, and miR-520-3p expression in BC patients (n=15). Blue squares represent BC patients with low DRC only. Correlations were tested using Spearman's rank correlation coefficient ($p<0.05$).

Invasive ductal carcinoma is the most commonly diagnosed type of BC worldwide and this is reflected in our cohort [1, 39]. The tumor grade data was based on TNM staging system to classify the tumors among the 0, I, II, or III, or IV grade. Most of the BC cases had stage II and III tumors, independently of DRC levels. Ki-67 expression is used along with the molecular BC subtype classification for prognosis and to determine BC aggressiveness [40, 41]. Unfortunately, not enough data regarding Ki-67 expression was available; therefore, no further comparisons could be performed. No differences were found when stratifying cases by receptor status (ER, PR, and HER2) and DRC levels. The lack of association found between DRC levels and molecular subtypes was probably the result of a small sample size. In a recent study, involving 267 BC cases, we reported substantial variability in four molecular BC subtypes when analyzed in terms of DRC levels [16]. Consistent with that study, most of the women in the triple-negative BC group had low DRC levels. In general, the clinicopathological characteristics were equally distributed among groups.

4.2. Breast Cancer-Related MicroRNAs. MicroRNA expression was significantly different between cases and controls. A similar pattern has been reported in several studies [42–47]. The hierarchical matrix also revealed a characteristic pattern for every woman with and without BC based on relative miRNA expression. These unique patterns are also responsible for the variability observed in the mean comparison analyses and may be a reflection of biological variability among BC cases. Variations in plasma miRNA expression in BC have been reported for some of the 40 candidates identified as BC-related, including let-7b [48, 49], miR-155-5p [44, 50–52], miR-194-5p [53], miR-373-3p [54], and miR-375-3p [53]. Similar to our results, these miRNAs were overexpressed in the plasma from BC cases when compared to controls. Of these 40 candidates, only three miRNAs were underexpressed in BC cases: miR-18a-5p, miR-372-3p, and miR-652-3p. As for miR-18a-5p, a study by Jurkovicova et al. (2017) assessed the expression of several miRNAs including this miRNA in invasive and noninvasive BC cases and controls [55]. Although no significant differences among groups were reported, their results show that women with noninvasive BC had the highest expression of miR-18a-5p while women with invasive BC and controls had similar expression [55]. As for miR-372-3p, no studies have elucidated its expression levels in plasma from women with BC. However, the role of this miRNA in BC has been studied in breast tumor tissues, where its expression is lower in tumors than in adjacent normal tissue [56]. As for miR-652-3p, a recent study by Cuk et al. (2017) reported a higher expression of this miRNA in the plasma from women with BC when compared to women without BC [43].

4.3. MicroRNAs and DNA Repair in Breast Cancer. MicroRNAs regulate multiple genes involved in different DNA repair mechanisms [57]. Our pilot study provides a link between specific miRNAs and DRC levels (low and high), specifically through the NER pathway measured in lymphocytes. Very few studies have been aimed at elucidating the relationship between plasma miRNA expression and DRC in BC. Most of the studies aimed at elucidating this relationship have been performed in tumor tissues or using in vitro models. Initially, we identified four miRNAs that were negatively correlated with DRC within the range of low DRC levels: let-7b, miR-18a-5p, miR222-3p, and miR-520-3p. High let-7b expression has been associated with BC patients with high DRC; this is the first time that a negative correlation is detected in patients with low DRC [19]. In contrast with our results and as previously mentioned, miR-18a has been found to be upregulated in BC [55] and other cancer types [58]. Also, mechanistic

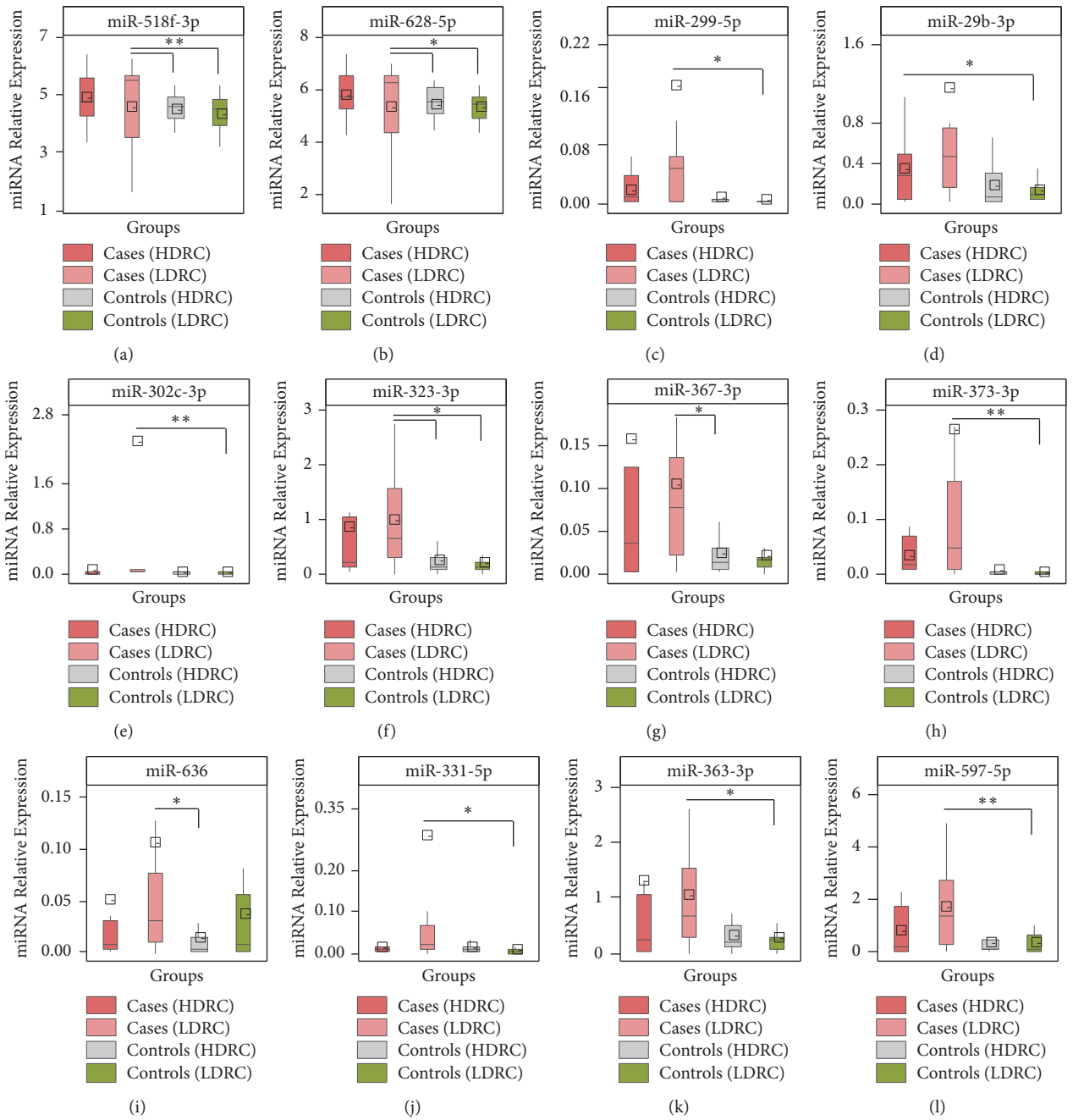

Figure 3: Comparison of relative microRNA expression between breast cancer cases and controls stratified by DRC. Groups were stratified into low (<3.8%) and high (≥3.8%) DRC based on a previously established cut-off. BC cases with low (n-=15) and high (n=14) DRC along with controls with low (n=18) and high (n=9) DRC levels were included in all panels. MicroRNAs were divided into 12 panels depending on their relative expression ranges. (a, b) miRNAs with extremely high relative expression were reported using a logarithmic scale. (c-l) miRNAs with a relative expression range 0-4. Each panel shows the miRNA relative expression distribution after normalization using the mammalian U6 endogenous control. Box plots represent the data distribution of 26 breast cancer cases and 27 controls. The point within the empty square represents the mean miRNA expression. DRC stratifications are represented by colors as can be seen in the legend (top). All miRNAs presented were differentially expressed among groups when mean comparisons were performed using KW test ($p<0.05$) followed by Dunn's multiple comparisons post hoc test (Table 3).

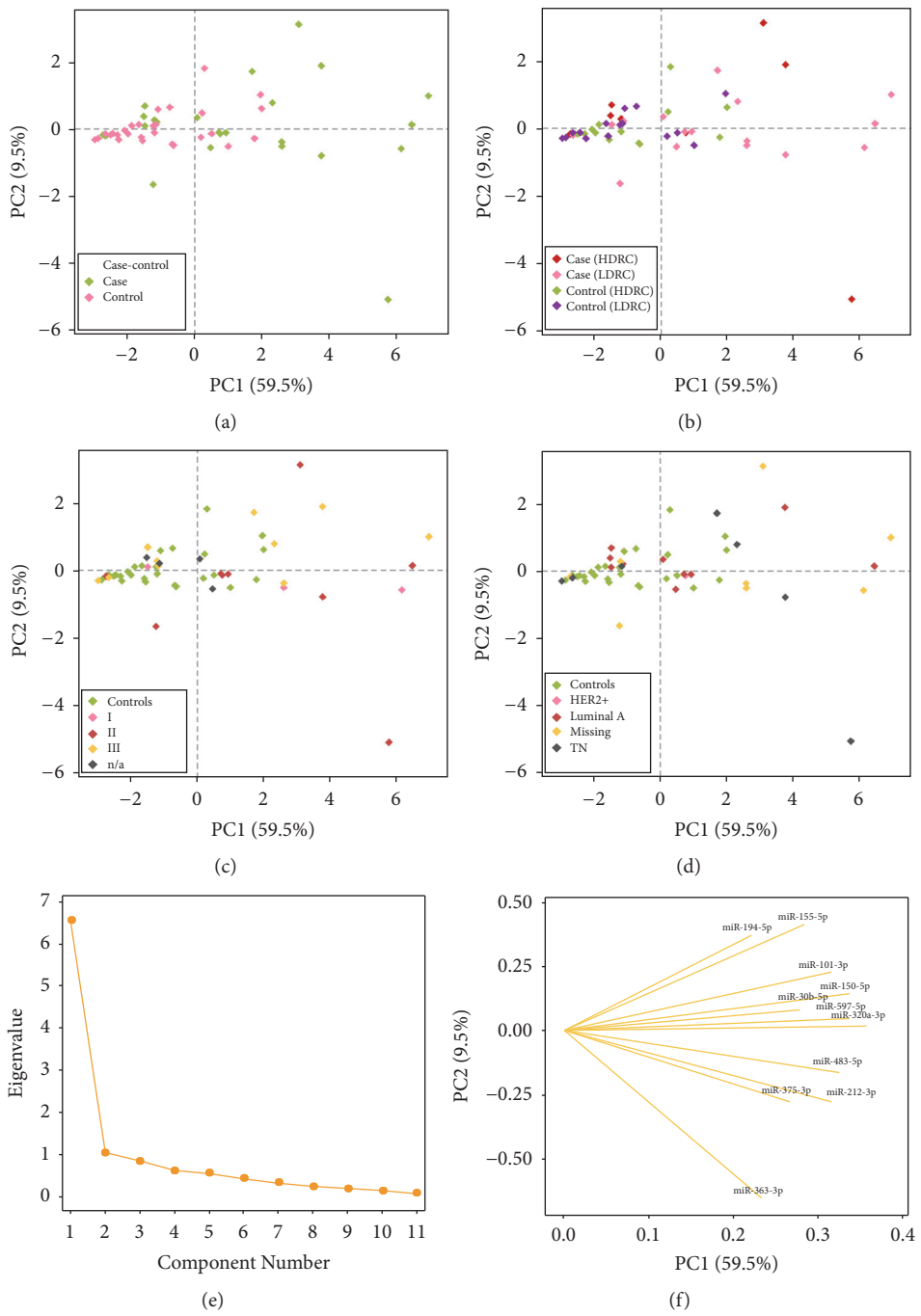

Figure 4: Population characteristics based on PCA matrix. The multivariate PCA matrix was used to localize the samples based on different stratifications: (a) case or control, (b) DRC (high and low), (c) tumor grade, and (d) BC subtypes. (e) PCA scree plot for the relative miRNAs expression of 26 BC cases and 27 controls. (f) Loading plot of miRNAs illustrating the PC1 and PC2 contribution to the variation among samples.

studies show that miR-18a has an important role in down-regulating ATM (Ataxia Telangiectasia Mutated), a DNA repair protein, in breast tumor tissues [59]. This can partially explain the negative correlation between miR-18a-5p and DRC levels. miR-222-3p has been widely studied in BC [60, 61] and tamoxifen resistance [62]. Moreover, this miRNA has been linked to DNA damage response by repressing RAD51 expression in ovarian cancer cells [63]. As for miR-520-3p, no reports on its expression changes in BC or any relationship with DRC were found. Among the 18 candidates found to be DRC-related, only miR-299-5p and miR-373 have been linked mechanistically to DNA repair. The study of Yan and coworkers shows that miR-299-5p expression is inversely correlated with RAD21 expression [64]. RAD21 is a protein involved in double-strand break repair [65]. A mechanistic study by Crosby and coworkers found that the forced

expression of miR-373 induces a reduction in NER proteins, RAD23B and RAD52, in the breast cancer cell line MCF-7 [66].

4.4. Multivariate Analyses. Due to the variation observed in the heatmap matrix, a multivariate analysis was performed to study data variability using the following stratifications: case or control classification, DRC levels (high and low), tumor grade, and molecular subtype classification. The DRC levels and case-control stratifications were the best variables to describe the data variability, as described in the Results. Other studies have been performed using the PC algorithm to explain and reduce the biological variability. Wei et al. (2018) used this model to study 1046 miRNAs in tumors from esophageal cancer patients. Their results showed the entire variation of the data using 6 components [67]. Sredni et al. (2011) also used this method to study miRNAs extracted from whole blood from women stratified by age. This group illustrated a PC analysis that covered 40.8% of the data variation [68]. However, our PC model accounts for 69.0% of the data variability, with only two components. Although, two components are not an accurate representation of this data because they do not cover the entire variability of the data, it is the best approximation based on the eigenvalue graph. It is also important to highlight the fact that the miRNAs included in the PC matrix were significantly expressed between the cases and controls and, thus, are BC-related in our cohort. The PC analysis demonstrated that the DRC levels can be related to the data variability. Our results indicate that miR-101-3p, miR-150-5p, miR-320a-3p, miR-483-5p, miR-212-3p, and miR-597-5p are responsible for this sample variability.

5. Conclusions

In conclusion, we identified 40 BC-related miRNAs that may have an important role in the epigenetics of Hispanic BC patients. This pilot study provides evidence of four miRNAs that are negatively regulated in BC cases with low DRC levels. Finally, the PC analysis suggested that the clinicopathological characteristics may not have a direct effect on specific miRNA expression. Additional studies are needed in order to have a complete framework regarding the overall DRC levels, miRNA expression profiles, and the tumor characteristics. When our results are validated with a larger sample size, this knowledge will become a pivotal force to study prognosis, recurrence, and treatment outcomes based on the overall DRC levels.

Data Availability

The data used to support the findings of this study are available from the corresponding author upon request.

Conflicts of Interest

The authors declare that there are no conflicts of interest regarding the publication of this paper.

Acknowledgments

This study was supported by grants from the NCI Center to Reduce Health Disparities and NIH-MBRS Program, grants #S06GM008239-20 (Jaime Matta, principal investigator), 9SC1CA182846-04 (Jarline Encarnación-Medina, corresponding author; Carmen Ortiz, coinvestigator; Jaime Matta, principal investigator), and 5SC1CA157250-02 to Ponce Health Sciences University (PHSU), and PHSU-Moffitt Cancer Center Partnership grant #5U54CA163071-04 (Jaime Matta, principal investigator). Additional support was provided by the 5R25GM096955-08 (Ralphdy Vergne, coinvestigator; Luis Padilla, coinvestigator), grant from NIH-NIGMS. Dr. Luisa Morales is gratefully acknowledged for performing the host-cell reactivation assay measurements. Mrs. Susan McCarthy at H. Lee Moffitt Cancer Center conducted the experiments to assess the miRNA expression.

Supplementary Materials

Figure S1: hierarchical MicroRNA clustering. After case-control comparisons using a Mann–Whitney U test, 40 candidate microRNAs were obtained. Left side (a) shows the expression profile for BC cases (X1-X.26). Right side (b) shows the miRNA expression for the controls (X2-X.29). Table S1: target sequences for the microRNAs included in this study. Figure S2: comparison of relative microRNA expression between breast cancer cases and controls stratified by DRC. BC cases with low (n-=15) and high (n=14) DRC along with controls with low (n=18) and high (n=9) DRC levels were included in all panels. Each panel shows the miRNA relative expression distribution after normalization using the mammalian U6 endogenous control. Box plots represent the data distribution of 26 breast cancer patients and 27 controls. The point within the empty square represents the mean miRNA expression. DRC stratifications are represented by colors. All miRNAs presented were differentially expressed among groups when mean comparisons were performed using KW test ($p<0.05$) only (Table 3). *(Supplementary Materials)*

References

[1] R. L. Siegel, K. D. Miller, and A. Jemal, "Cancer statistics, 2019," *CA: A Cancer Journal for Clinicians*, vol. 69, no. 1, pp. 7–34, 2019.

[2] ACS, "Cancer Facts and Figures 2017," Atlanta, American Cancer Society, 2017.

[3] PRCCC, "Puerto Rico Comprehensive Cancer Control Plan: 2015-2020," San Juan, PR, Puerto Rico Cancer Control Coalition and Puerto Rico Comprehensive Control Program, 2014.

[4] D. Hanahan and R. A. Weinberg, "Hallmarks of cancer: the next generation," *Cell*, vol. 144, no. 5, pp. 646–674, 2011.

[5] T. J. Klein and P. M. Glazer, "The tumor microenvironment and DNA repair," *Seminars in Radiation Oncology*, vol. 20, no. 4, pp. 282–287, 2010.

[6] Q. Wei, M. L. Frazier, and B. Levin, "DNA repair: A double-edged sword," *Journal of the National Cancer Institute*, vol. 92, no. 6, pp. 440-441, 2000.

[7] J. L. Matta, J. L. Villa, J. M. Ramos et al., "DNA repair and nonmelanoma skin cancer in Puerto Rican populations,"

Journal of the American Academy of Dermatology, vol. 49, no. 3, pp. 433–439, 2003.

[8] Q. Wei, G. M. Matanoski, E. R. Farmer, M. A. Hedayati, and L. Grossman, "DNA repair and aging in basal cell carcinoma: A molecular epidemiology study," *Proceedings of the National Acadamy of Sciences of the United States of America*, vol. 90, no. 4, pp. 1614–1618, 1993.

[9] J. M. Ramos, A. Ruiz, R. Colen, I. D. Lopez, L. Grossman, and J. L. Marta, "DNA Repair and Breast Carcinoma Susceptibility in Women," *Cancer*, vol. 100, no. 7, pp. 1352–1357, 2004.

[10] K. Milanowska, J. Krwawicz, G. Papaj et al., "REPAIRtoire-A database of DNA repair pathways," *Nucleic Acids Research*, vol. 39, no. 1, pp. D788–D792, 2011.

[11] R. D. Wood, M. Mitchell, and T. Lindahl, "Human DNA repair genes, 2005," *Mutation Research - Fundamental and Molecular Mechanisms of Mutagenesis*, vol. 577, no. 1-2, pp. 275–283, 2005.

[12] R. D. Wood, M. Mitchell, J. Sgouros, and T. Lindahl, "Human DNA repair genes," *Science*, vol. 291, no. 5507, pp. 1284–1289, 2001.

[13] N. S. Gavande, P. S. VanderVere-Carozza, K. S. Pawelczak, and J. J. Turchi, "Targeting the nucleotide excision repair pathway for therapeutic applications," in *DNA Repair in Cancer Therapy*, M. R. Kelley and M. L. Fishel, Eds., chapter 5, pp. 135–150, Academic Press, Boston, Massachusetts, Mass, USA, 2nd edition, 2016.

[14] J. J. Latimer, J. M. Johnson, C. M. Kelly et al., "Nucleotide excision repair deficiency is intrinsic in sporadic stage i breast cancer," *Proceedings of the National Acadamy of Sciences of the United States of America*, vol. 107, no. 50, pp. 21725–21730, 2010.

[15] J. Matta, L. Morales, J. Dutil et al., "Differential expression of DNA repair genes in Hispanic women with breast cancer," *Molecular Cancer Biology*, vol. 1, no. 1, article 54, 2013.

[16] J. Matta, C. Ortiz, J. Encarnación, J. Dutil, and E. Suárez, "Variability in DNA repair capacity levels among molecular breast cancer subtypes: triple negative breast cancer shows lowest repair," *International Journal of Molecular Sciences*, vol. 18, no. 7, 2017.

[17] S. P. Barros and S. Offenbacher, "Epigenetics: connecting environment and genotype to phenotype and disease," *Journal of Dental Research*, vol. 88, no. 5, pp. 400–408, 2009.

[18] D. L. Foley, J. M. Craig, R. Morley et al., "Prospects for epigenetic epidemiology," *American Journal of Epidemiology*, vol. 169, no. 4, pp. 389–400, 2009.

[19] J. Encarnación, C. Ortiz, R. Vergne, W. Vargas, D. Coppola, and J. L. Matta, "High DRC levels are associated with let-7b overexpression in women with breast cancer," *International Journal of Molecular Sciences*, vol. 17, no. 6, 2016.

[20] D. P. Bartel, "MicroRNAs: genomics, biogenesis, mechanism, and function," *Cell*, vol. 116, no. 2, pp. 281–297, 2004.

[21] R. Hamam, D. Hamam, K. A. Alsaleh et al., "Circulating microRNAs in breast cancer: novel diagnostic and prognostic biomarkers," *Cell Death and Disease*, vol. 8, no. 9, article e3045, 2017.

[22] J. Matta, M. Echenique, E. Negron et al., "The association of DNA Repair with breast cancer risk in women. A comparative observational study," *BMC Cancer*, vol. 12, article 490, 2012.

[23] P. Mendez, M. Taron, T. Moran, M. A. Fernandez, G. Requena, and R. Rosell, "A modified host-cell reactivation assay to quantify DNA repair capacity in cryopreserved peripheral lymphocytes," *DNA Repair*, vol. 10, no. 6, pp. 603–610, 2011.

[24] W. F. Athas, M. A. Hedayati, G. M. Matanoski, E. R. Farmer, and L. Grossman, "Development and field-test validation of an assay for DNA repair in circulating human lymphocytes," *Cancer Research*, vol. 51, no. 21, pp. 5786–5793, 1991.

[25] L. Wang, Q. Wei, Q. Shi, Z. Guo, Y. Qiao, and M. R. Spitz, "A modified host-cell reactivation assay to measure repair of alkylating DNA damage for assessing risk of lung adenocarcinom," *Carcinogenesis*, vol. 28, no. 7, pp. 1430–1436, 2007.

[26] J. Matta, M. Echenique, E. Negron et al., "The association of DNA Repair with breast cancer risk in women. A comparative observational study," *BMC Cancer*, vol. 12, no. 1, article 490, 2012.

[27] L. Morales, C. Alvarez-Garriga, J. Matta et al., "Factors associated with breast cancer in Puerto Rican women," *Journal of Epidemiology and Global Health*, vol. 3, no. 4, pp. 205–215, 2013.

[28] Y. Vergne, J. Matta, L. Morales et al., "Breast cancer and DNA repair capacity: association with use of multivitamin and calcium supplements," *Journal of Integrative Medicine*, vol. 12, no. 3, pp. 38–46, 2013.

[29] N. Gehlenborg and B. Wong, "Heat maps," *Nature Methods*, vol. 9, article 213, 2012.

[30] J. Braeken and M. A. L. M. Van Assen, "An empirical Kaiser criterion," *Psychological Methods*, vol. 22, no. 3, pp. 450–466, 2017.

[31] R. A. Rawlings-Goss, M. C. Campbell, and S. A. Tishkoff, "Global population-specific variation in miRNA associated with cancer risk and clinical biomarkers," *BMC Medical Genomics*, vol. 7, article 53, 2014.

[32] H. Zhao, J. Shen, L. Medico, D. Wang, C. B. Ambrosone, and S. Liu, "A pilot study of circulating miRNAs as potential biomarkers of early stage breast cancer," *PLoS ONE*, vol. 5, no. 10, article e13735, 2010.

[33] L. M. Hines, B. Risendal, M. L. Slattery et al., "Comparative analysis of breast cancer risk factors among hispanic and non-hispanic white women," *Cancer*, vol. 116, no. 13, pp. 3215–3223, 2010.

[34] C. K. Anders, R. Johnson, J. Litton, M. Phillips, and A. Bleyer, "Breast cancer before age 40 years," *Seminars in Oncology*, vol. 36, no. 3, pp. 237–249, 2009.

[35] M. J. Schoemaker, H. B. Nichols, L. B. Wright et al., "Association of body mass index and age with subsequent breast cancer risk in premenopausal women," *JAMA Oncology*, vol. 4, no. 11, article e181771, 2018.

[36] M. Wenten, F. D. Gilliland, K. Baumgartner, and J. M. Samet, "Associations of weight, weight change, and body mass with breast cancer risk in Hispanic and Non-Hispanic white women," *Annals of Epidemiology*, vol. 12, no. 6, pp. 435–444, 2002.

[37] Collaborative Group on Hormonal Factors in Breast Cancer, "Menarche, menopause, and breast cancer risk: individual participant meta-analysis, including 118 964 women with breast cancer from 117 epidemiological studies," *The Lancet Oncology*, vol. 13, no. 11, pp. 1141–1151, 2012.

[38] D. J. Press, J. Sullivan-Halley, G. Ursin et al., "Breast cancer risk and ovariectomy, hysterectomy, and tubal sterilization in the women's contraceptive and reproductive experiences study," *American Journal of Epidemiology*, vol. 173, no. 1, pp. 38–47, 2011.

[39] W. Böcker, "WHO classification of breast tumors and tumors of the female genital organs: pathology and genetics," *Journal of Clinical Pathology*, vol. 86, pp. 116–119, 2002.

[40] N. A. Soliman and S. M. Yussif, "Ki-67 as a prognostic marker according to breast cancer molecular subtype," *Cancer Biology & Medicine*, vol. 13, no. 4, pp. 496–504, 2016.

[41] E. C. Inwald, M. Klinkhammer-Schalke, F. Hofstädter et al., "Ki-67 is a prognostic parameter in breast cancer patients: Results of a large population-based cohort of a cancer registry," *Breast Cancer Research and Treatment*, vol. 139, no. 2, pp. 539–552, 2013.

[42] R. Hamam, A. M. Ali, K. A. Alsaleh et al., "microRNA expression profiling on individual breast cancer patients identifies novel panel of circulating microRNA for early detection," *Scientific Reports*, vol. 6, article 25997, 2016.

[43] K. Cuk, M. Zucknick, D. Madhavan et al., "Plasma microRNA panel for minimally invasive detection of breast cancer," *PLoS ONE*, vol. 8, no. 10, article e76729, 2013.

[44] M. Sochor, P. Basova, M. Pesta et al., "Oncogenic MicroRNAs: MiR-155, miR-19a, miR-181b, and miR-24 enable monitoring of early breast cancer in serum," *BMC Cancer*, vol. 14, no. 448, pp. 1471–2407, 2014.

[45] A. R. Kodahl, M. B. Lyng, H. Binder et al., "Novel circulating microRNA signature as a potential non-invasive multi-marker test in ER-positive early-stage breast cancer: A case control study," *Molecular Oncology*, vol. 8, no. 5, pp. 874–883, 2014.

[46] S. Zearo, E. Kim, Y. Zhu et al., "MicroRNA-484 is more highly expressed in serum of early breast cancer patients compared to healthy volunteers," *BMC Cancer*, vol. 14, no. 200, pp. 1471–2407, 2014.

[47] K. Zhang, Y.-W. Wang, Y.-Y. Wang et al., "Identification of microRNA biomarkers in the blood of breast cancer patients based on microRNA profiling," *Gene*, vol. 619, pp. 10–20, 2017.

[48] S. A. Joosse, V. Müller, B. Steinbach, K. Pantel, and H. Schwarzenbach, "Circulating cell-free cancer-testis MAGE-A RNA, BORIS RNA, let-7b and miR-202 in the blood of patients with breast cancer and benign breast diseases," *British Journal of Cancer*, vol. 111, no. 5, pp. 909–917, 2014.

[49] A. Qattan, H. Intabli, W. Alkhayal, C. Eltabache, T. Tweigieri, and S. B. Amer, "Robust expression of tumor suppressor miRNA's let-7 and miR-195 detected in plasma of Saudi female breast cancer patients," *BMC Cancer*, vol. 17, no. 1, p. 799, 2017.

[50] F. Wang, Z. Zheng, J. Guo, and X. Ding, "Correlation and quantitation of microRNA aberrant expression in tissues and sera from patients with breast tumor," *Gynecologic Oncology*, vol. 119, no. 3, pp. 586–593, 2010.

[51] C. Roth, B. Rack, V. Müller, W. Janni, K. Pantel, and H. Schwarzenbach, "Circulating microRNAs as blood-based markers for patients with primary and metastatic breast cancer," *Breast Cancer Research*, vol. 12, no. 6, article 3, 2010.

[52] Y. Sun, M. Wang, G. Lin et al., "Serum microRNA-155 as a potential biomarker to track disease in breast cancer," *PLoS ONE*, vol. 7, no. 10, article 10, 2012.

[53] D. Huo, W. M. Clayton, T. F. Yoshimatsu, J. Chen, and O. I. Olopade, "Identification of a circulating MicroRNA signature to distinguish recurrence in breast cancer patients," *Oncotarget* , vol. 7, no. 34, pp. 55231–55248, 2016.

[54] C. Eichelser, D. Flesch-Janys, J. Chang-Claude, K. Pantel, and H. Schwarzenbach, "Deregulated serum concentrations of circulating cell–free microRNAs miR-17, miR-34a, miR-155, and miR-373 in human breast cancer development and progression," *Clinical Chemistry*, vol. 59, no. 10, pp. 1489–1496, 2013.

[55] D. Jurkovicova, B. Smolkova, M. Magyerkova et al., "Down-regulation of traditional oncomiRs in plasma of breast cancer patients," *Oncotarget* , vol. 8, no. 44, pp. 77369–77384, 2017.

[56] Y.-X. Zhao, H.-C. Liu, W.-Y. Ying et al., "MicroRNA-372 inhibits proliferation and induces apoptosis in human breast cancer cells by directly targeting E2F1," *Molecular Medicine Reports*, vol. 16, no. 6, pp. 8069–8075, 2017.

[57] M. He, W. Zhou, C. Li, and M. Guo, "MicroRNAs, DNA damage response, and cancer treatment," *International Journal of Molecular Sciences*, vol. 17, no. 12, article 2087, 2016.

[58] S. Komatsu, D. Ichikawa, H. Takeshita et al., "Circulating miR-18a: a sensitive cancer screening biomarker in human cancer," *In Vivo*, vol. 28, no. 3, pp. 293–297, 2014.

[59] L. Song, C. Lin, Z. Wu et al., "miR-18a impairs DNA damage response through downregulation of ataxia telangiectasia mutated (ATM) kinase," *PLoS ONE*, vol. 6, no. 9, article e25454, 2011.

[60] S. Amini, A. Abak, M. A. Estiar, V. Montazeri, A. Abhari, and E. Sakhinia, "Expression analysis of MicroRNA-222 in breast cancer," *Clinical Laboratory*, vol. 64, no. 4, pp. 491–496, 2018.

[61] Y. Zong, Y. Zhang, X. Sun, T. Xu, X. Cheng, and Y. Qin, "MiR-221/222 promote tumor growth and suppress apoptosis by targeting lncRNA GAS5 in breast cancer," *Bioscience Reports*, 2018.

[62] T. E. Miller, K. Ghoshal, B. Ramaswamy et al., "MicroRNA-221/222 confers tamoxifen resistance in breast cancer by targeting p27Kip1," *The Journal of Biological Chemistry*, vol. 283, no. 44, pp. 29897–29903, 2008.

[63] S. Neijenhuis, I. Bajrami, R. Miller, C. J. Lord, and A. Ashworth, "Identification of miRNA modulators to PARP inhibitor response," *DNA Repair*, vol. 12, no. 6, pp. 394–402, 2013.

[64] M. Yan, H. Xu, N. Waddell et al., "Enhanced RAD21 cohesin expression confers poor prognosis in BRCA2 and BRCAX, but not BRCA1 familial breast cancers," *Breast Cancer Research*, vol. 14, no. 2, pp. R69–R69, 2012.

[65] C. Bauerschmidt, C. Arrichiello, S. Burdak-Rothkamm et al., "Cohesin promotes the repair of ionizing radiation-induced DNA double-strand breaks in replicated chromatin," *Nucleic Acids Research*, vol. 38, no. 2, pp. 477–487, 2009.

[66] M. E. Crosby, R. Kulshreshtha, M. Ivan, and P. M. Glazer, "MicroRNA regulation of DNA repair gene expression in hypoxic stress," *Cancer Research*, vol. 69, no. 3, pp. 1221–1229, 2009.

[67] L. Wei, S. Zhongyu, L. Wenshuang, L. Tianjia, and G. Pengcheng, "MicroRNA data reduction of esphageal cancer," *Journal of Physics*, vol. 1053, 2018.

[68] S. T. Sredni, S. Gadd, N. Jafari, and C. Huang, "A parallel study of mRNA and microRNA profiling of peripheral blood in young adult women," *Frontiers in Genetics*, vol. 2, article 49, 2011.

Hindawi
Journal of Oncology
Volume 2019, Article ID 2976373, 8 pages
https://doi.org/10.1155/2019/2976373

Research Article

RAD51 and *XRCC3* Polymorphisms Are Associated with Increased Risk of Prostate Cancer

Maria Nowacka-Zawisza,[1] **Agata Raszkiewicz**,[1] **Tomasz Kwasiborski**,[1] **Ewa Forma**,[1] **Magdalena Bryś**,[1] **Waldemar Różański**,[2] **and Wanda M. Krajewska**[1]

[1]*Department of Cytobiochemistry, Faculty of Biology and Environmental Protection, University of Lodz, Lodz, Poland*
[2]*Department of Urology 2, Faculty of Biomedical Sciences and Postgraduate Training, Medical University of Lodz, Lodz, Poland*

Correspondence should be addressed to Maria Nowacka-Zawisza; nmary@interia.pl

Received 21 January 2019; Revised 14 March 2019; Accepted 31 March 2019; Published 2 May 2019

Guest Editor: Zhihua Kang

Genetic polymorphisms in DNA repair genes may affect DNA repair efficiency and may contribute to the risk of developing cancer. The aim of our study was to investigate single nucleotide polymorphisms (SNPs) in *RAD51* (rs2619679, rs2928140, and rs5030789) and *XRCC3* (rs1799796) involved in DNA double-strand break repair and their relationship to prostate cancer. The study group included 99 men diagnosed with prostate cancer and 205 cancer-free controls. SNP genotyping was performed using the PCR-RFLP method. A significant association was detected between *RAD51* rs5030789 polymorphism and *XRCC3* rs1799796 polymorphism and an increased risk of prostate cancer. Our results indicate that *RAD51* and *XRCC3* polymorphism may contribute to prostate cancer.

1. Introduction

Prostate cancer is the second most commonly occurring cancer and the fifth leading cause of cancer death in men with an estimated 1.3 million new cases and 359.000 associated deaths worldwide in 2018. It is the most frequently diagnosed cancer among men in over one-half of the countries of the world [1, 2]. Prostate cancer is characterized by the highest dynamic of increase in the last decade, and in 2016, for the first time, it became the most common cancer among men in Poland [3]. This cancer is very rarely manifested before the age of 50, and more than half of patients at the time of diagnosis are at least 70 years old. Age-adjusted incidence rates of prostate cancer increased dramatically and this is largely because of the increased availability of screening for specific prostate antigen (PSA) in men without symptoms of the desease. PSA screening offers a potential benefit of reducing the chance of death from prostate cancer. However, the value of PSA screening is moderate. An increase in PSA over 4 ng/ml suggests cancer, but nearly 25% of men with elevated levels of PSA do not have cancer, and nearly 20% of patients with prostate cancer have normal serum PSA. Elevated PSA levels may be also associated with benign conditions such as inflammation and benign prostatic hypertrophy and procedures such as bladder catheterization, transrectal ultrasound, gland biopsy, cystoscopy, and transurethral endoscopy. The search for markers other than PSA, allowing for early diagnosis and prognosis of prostate cancer, seems to be justified [3, 4]. The factors associated with an increased risk of prostate cancer include family burden, race, ethnicity, obesity, high fat diet, smoking, and exposure to androgens [2]. Germline and somatic mutations appeared to be well-established risk factors for primary and metastaic prostate cancer. In addition, genome-wide association studies (GWAS) have identified approximately 170 SNPs associated with the development of prostate cancer. Pathogenic variants of high and moderate penetrance genes, such as *BRCA1* and *BRCA2*, mismatch repair genes, and *HOXB13* confer modest to high lifetime risk of prostate cancer. Some, such as *BRCA2*, have emerging clinical relevance in the treatment and screening for prostate cancer [5–8].

The process of tumorigenesis occurs in the absence of efficient DNA repair systems and this may, among others, result from genetic variations in the genes involved in them. The most deleterious form of DNA damage is the double-strand break (DSB). In order to maintain genomic

stability, double-strand breaks must be repaired by homologous recombination (HR) or nonhomologous end joining (NHEJ). Germline and somatic mutations in genes that promote homology-directed repair, especially *BRCA1* and *BRCA2*, are frequently observed in several cancers, in particular, breast and ovary, but also prostate and other cancers. The critical biochemical function of BRCA2 in homology-directed repair is to promote RAD51 filament assembly onto ssDNA that arises from end resection. BRCA2 directly interacts with RAD51 at multiple sites to facilitate RAD51 filament assembly. BRCA2 is shown to regulate both the intracellular localization and DNA-binding ability of RAD51. Loss of these controls may be a key event leading to genomic instability and tumorigenesis [9, 10]. The human *RAD51*, located on chromosome 15q15.1, plays a crucial role in DNA double-strand break repair [11]. The protein encoded by this gene is a member of RAD51 protein family. RAD51 family members are highly similar to bacterial RecA and *Saccharomyces cerevisiae* Rad51 and are known to be involved in the homologous recombination and repair of DNA. RAD51 binds to single- and double-stranded DNA and exhibits DNA-dependent ATPase activity. RAD51 catalyzes the recognition of homology and strand exchange between homologous DNA partners to form a joint molecule between a processed DNA break and the repair template. RAD51 binds to single-stranded DNA in an ATP-dependent manner to form nucleoprotein filaments which are essential for the homology search and strand exchange. RAD51 plays a role in regulating mitochondrial DNA copy number under conditions of oxidative stress in the presence of RAD51C and XRCC3 and is also involved in interstrand cross-link repair. At the site of DNA damage nuclear foci containing BRCA1, BRCA2, and RAD51, together with other proteins engaged in homologous recombination, are forming. The protein that binds to RAD51 is XRCC3. This combination facilitates formation of the nucleoprotein filament that represents primary vector for both homologous and heterologous recombination [12–16].

As we have previously shown the rs1801320 polymorphism in *RAD51* may contribute to prostate cancer susceptibility in Poland [17]. The purpose of the presented work was to investigate further selected single nucleotide polymorphisms (SNPs), i.e., rs2619679, rs2928140, and rs5030789 in *RAD51* and rs1799796 in *RAD51* paralog *XRCC3* and their relationship to prostate cancer.

2. Material and Methods

2.1. Patients. The study group included 99 men with prostate adenocarcinoma and 205 sex- and age-matched cancer-free subjects with low (<4 ng/ml) levels of PSA as a control group. Peripheral blood samples from the patients with prostate adenocarcinoma were obtained from the Department of Urology 2, Medical University of Lodz, Poland. Peripheral blood samples from the control group were obtained from the Urological Department of the Provincial M. Sklodowska-Curie Hospital in Zgierz, Poland. Table 1 presents clinicopathological characteristics of patients and the control group.

Table 1: Clinicopathological characteristics of studied material.

	Parameter
Control group (n=205)	
Age	
Range	43 - 84
Mean ± SD	63.33 ± 9.28
Median	64
PSAT (ng/ml)	
Range	0.004 – 3.94
Mean ± SD	1.09 ± 0.88
Median	0.95
Patients with prostate cancer (n=99)	
Age	
Range	49 - 85
Mean ± SD	70.38 ± 8.63
Median	71
PSAT (ng/ml)	
Range	4.01 – 1489.00
Mean ± SD	59.17 ± 184.59
Median	9.22
Free/total PSA (F/T PSA)	
Range	0.04-0.79
Mean ± SD	0.19±0.15
Median	0.16
< 0.16	48
≥ 0.16	51
PSA Density (PSAD, ng/ml)	
Range	0.07-56.4
Mean ± SD	2.57±8.44
Median	0.28
< 0.28	49
≥ 0.28	50
Prostate volume (ml)	
Range	20.7-191
Mean ± SD	59.5±39.0
Median	48.2
< 48	46
≥ 48	53
Gleason score	
< 7	28
≥ 7	71
Cancer stage	
T1-T2	58
T3-T4	41

2.2. DNA Isolation. DNA from peripheral blood was isolated by phenol extraction [18] or using AxyPrep Blood Genomic DNA Miniprep Kit (Axygen Biosciences) and stored in -70°C. DNA preparations were subjected to spectrophotometric analysis (Biophotometer Eppendorf AG, Germany) by measuring absorbance at 260 nm and 280 nm to determine the quantity and quality of the isolated nucleic acid. The A260/A280 ratio was in the range 1.8-2.1.

Table 2: Polymorphic sites in *RAD51* and *XRCC3* (according to NCBI).

Gene	SNP	Other names	Chromosome	SNP position
RAD51	rs2619679	g.3879T>A c.-1285T>A	15: 40694039	Promoter
	rs2928140	g.7995G>C, c.-2-602G>C	15: 40698155	Intron 1
	rs5030789	g.3997A>G, c.-1167A>G	15: 40694157	Promoter
XRCC3	rs1799796	g.20897A>G c.562A>G	14: 103699590	Intron 7

2.3. Genotyping. Single nucleotide polymorphism (SNP) was determined by PCR-RFLP (polymerase chain reaction-restriction fragment length polymorphism). Tested SNPs are shown in the Table 2.

The primers for studied SNPs were as follows: (F) 5′-CCGTGCAGGCCTTATATGAT-3′ and (R) 5′-AGATAAACCTGGCCAACGTG-3′ for rs2619679; (F) 5′-GCTTCTGGCTATTTTCAAGT-3′ and (R) 5′-TGAGGCAGGTAAATGGCTTC-3′ for rs2928140; (F) 5′-CCGTGCAGGCCTTATATGAT-3′ and (R) 5′-AGATAAACCTGGCCAACGTG-3′ for rs5030789; (F) 5′-CCGCATCCTGGCTAAAAATA-3′ and (R) 5′-CAGAGTATGGGCACTGTGAGC-3′ for rs1799796. The primers were synthesized at Sigma-Aldrich®. The polymerase chain reaction (PCR) was performed in an Applied Biosystems® 2720 thermocycler in total volume of 10 μl. The reaction mixture contained 10 ng of genomic DNA; 0.2 μmoles of primers (F) and (R); 3 HOT FIREPol® units of DNA polymerase (5 U/ml); 1 mM GeneAmp dNTPmix (10 mM); 2.5 mM magnesium chloride (25 mM); and 1 x Solis BioDyne buffer B1 (10x concentrated). The components of the PCR reaction mixture were from Solis BioDyne (Estonia) and Applied Biosystem (USA).

The temperature-time profile of PCR was as follows: Pre-PCR: 95°C for 12 min; PCR (30 cycles): 95°C for 0.5 min, 63°C (rs2928140) or 64°C (for rs2619679 and rs1799796) or 65°C (rs5030789) for 0.5 min, 72°C for 1 min; Post-PCR at 72°C for 5min.

The amplification products were digested with restriction enzymes: *Hinf*I (rs2619679), *Ear*I (rs2928140), *Nla*III (rs5030789), or *Alu*I (rs1799796) at 37°C for 16 hours. Enzyme inactivation lasted 20 minutes at 65°C for *Ear*I and at 80°C for *Hinf*I, *Nla*III, and *Alu*I. The enzymes came from New England BioLabs Inc. DNA fragments were separated in a 3% agarose gel with ethidium bromide for UV visualization. Electrophoresis was performed in 1x TBE buffer (10x TBE: 89 mM Tris, 89 mM boric acid, 2 M EDTA pH 8.0) and 100V. Examples of the obtained restriction patterns are shown in Figure 1.

2.4. Statistical Analysis. The compatibility of the genotype distribution with the Hardy-Weinberg law in the control group and in study group was checked by the χ^2 test. Significance of differences between the distribution of genotypes/alleles in the control and study group was assessed by the χ^2 test. The risk of comorbidity of genotypes/alleles with the disease was assessed based on odds ratio (OR) together with a 95% confidence interval. All results were considered statistically significant at p values <0.05. Statistical calculations were made using spreadsheets available on the websites: quantpsy.org/chisq/chisq.htm and vassarstats.net/odds2x2.html.

3. Results

Table 3 presents results of studied polymorphisms in *RAD51* and *XRCC3* using the PCR-RFLP method. The distribution of genotypes and alleles in the control group and in patients with prostate cancer was consistent with Hardy-Weinberg law (p>0.05). Statistically significant differences were found in the distribution of genotypes and alleles for rs5030789 and rs1799796 polymorphism in *RAD51* and *XRCC3*, respectively, between control group and prostate cancer patients.

The odds ratio (OR) analysis showed that rs5030789 polymorphism in *RAD51* and rs1799796 polymorphism in *XRCC3* are associated with susceptibility to prostate cancer (Table 4). The presence of the GG genotype in both polymorphic sites of *RAD51* and *XRCC3* increases the risk of prostate cancer (OR = 2.782, p = 0.038 for rs5030789; OR = 1.986, p = 0.041 for rs1799796). Also, the presence of the G allele increases the risk of developing prostate cancer in both above polymorphisms (OR = 1.571 for rs5030789 and OR = 1.441 for rs1799796, p<0.05).

Because the polymorphism rs5030789 in *RAD51* and polymorphism rs1799796 in *XRCC3* increase the risk of prostate cancer, the correlation of these polymorphisms with age and clinicopathological characteristcs of prostate cancer patients was examined (Table 5). It was revealed that there is a relationship between rs1799796 polymorphism in *XRCC3* and the age of patients over 71 years (OR = 1.916, p = 0.033) and Gleason score of cancer equal to or higher than 7 (OR = 2.373, p = 0.012). No association was found with the level of PSAT, nor with rs5030789 in *RAD51* nor rs1799796 in *XRCC3*.

4. Discussion

Prostate specific antigen (PSA) is a blood-based biomarker used for the detection and surveillance of prostate cancer. However, PSA levels can also be affected by benign prostatic hyperplasia (BPH), local inflammation or infection, prostate volume, age, and genetic factors. In this regard, PSA seems to be an organ but not cancer specific biomarker [19]. Seeking the molecular mechanisms underlying prostate

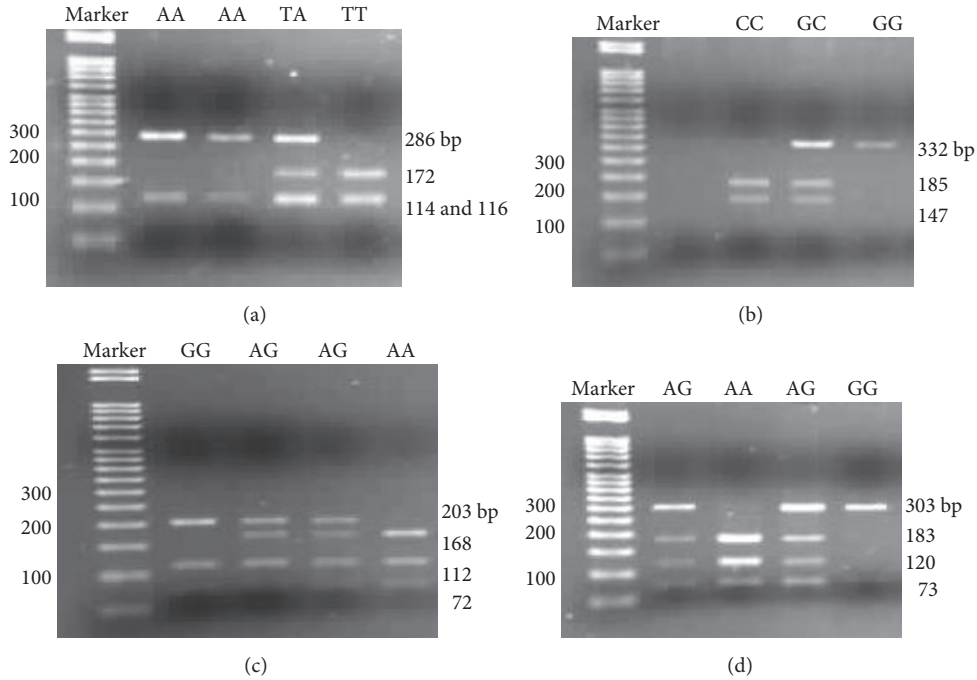

Figure 1: PCR-RFLP genotyping of (a) *RAD51* rs2619679 polymorphism; (b) *RAD51* rs2928140 polymorphism; (c) *RAD51* rs5030789 polymorphism; (d) *XRCC3* rs1799796 polymorphism.

Table 3: Distribution of genotypes and allele frequency of studied SNPs in *RAD51* and *XRCC3* in prostate cancer patients and control group.

Gene	rs	Genotype/allele	Control group (n=205)	Prostate cancer patients (n=99)
RAD51	rs2619679	TT	48	30
		TA	101	51
		AA	56	18
			$\chi^2 = 3.59$, $p = 0.17$	
		T	197	111
		A	213	87
			$\chi^2 = 3.43$, $p = 0.06$	
	rs2928140	GG	95	43
		GC	63	36
		CC	47	20
			$\chi^2 = 1.00$, $p = 0.61$	
		G	253	122
		C	157	76
			$\chi^2 = 0$, $p = 1.00$	
	rs5030789	AA	29	7
		AG	106	45
		GG	70	47
			$\chi^2 = 6.43$, $p = 0.04$	
		A	164	59
		G	246	139
			$\chi^2 = 5.98$, $p = 0.01$	
XRCC3	rs1799796	AA	77	28
		AG	92	45
		GG	36	26
			$\chi^2 = 4.15$, $p = 0.13$	
		A	246	101
		G	164	97
			$\chi^2 = 4.40$, $p = 0.04$	

Table 4: Prostate cancer risk and *RAD51* and *XRCC3* polymorphism.

Gene	rs	Genotype/allele	Control group (n=205)	Prostate cancer patients (n=99)	OR (95% Cl)	*p* value
RAD51	rs2619679	TT	48	30	1 (Ref.)	
		TA	101	51	0.808 (0.459-1.424)	0.554
		AA	56	18	0.514 (0.255-1.036)	0.089
		T	197	111	1 (Ref.)	
		A	213	87	0.725 (0.515-1.020)	0.077
	rs2928140	GG	95	43	1 (Ref.)	
		GC	63	36	1.262 (0.732-2.178)	0.484
		CC	47	20	0.940 (0.498-1.775)	0.841
		G	253	122	1 (Ref.)	
		C	157	76	1.004 (0.708-1.423)	0.526
	rs5030789	AA	29	7	1 (Ref.)	
		AG	106	45	1.759 (0.718-4.309)	0.299
		GG	70	47	*2.782 (1.126-6.872)*	*0.038*
		A	164	59	1 (Ref.)	
		G	246	139	*1.571 (1.093-2.228)*	*0.018*
XRCC3	rs1799796	AA	77	28	1 (Ref.)	
		AG	92	45	1.345 (0.768-2.356)	0.371
		GG	36	26	*1.986 (1.022-3.860)*	*0.041*
		A	246	101	1 (Ref.)	
		G	164	97	*1.441 (1.024-2.027)*	*0.044*

cancer, many mutations and polymorphisms of a single nucleotide have been identified, especially in DNA repair genes, which increase the risk of developing prostate cancer. Polymorphic genes of DNA repair are in great part included in low penetrance genes, which means that single gene product most often slightly affects the disease occurrence risk, but accumulation of changed alleles can have essential significance for its development. RAD51, which is a critical protein involved in the homologous recombination repair pathway, interacts with XRCC2, XRCC3, and other proteins to form a complex that is crucial for repairing the double-strand breaks and maintaining chromosome stability [12, 16, 20].

To our knowledge, genetic abnormalities in RAD51 paralogs, i.e., RAD51C and RAD51D, have been identified in prostate cancer, but not in RAD51 [5–10]. Our study has shown the importance of *RAD51* and its paralog *XRCC3* polymorphism in prostate cancer. Single nucleotide polymorphism within these genes may affect DNA double-strand break repair capacity, hence the increased susceptibility to neoplastic transformation. There is growing body of evidence which suggests that polymorphic variants of these genes have impact on developing different cancers. A meta-analysis conducted by Zeng et al. [11] suggests that *RAD51* rs1801320 (135G/C) polymorphism is a risk factor for three common gynecological tumors, i.e., breast, endometrial, and ovarian cancers, and especially for endometrial cancer. Al-Zoubi et al. [21] in their studies demonstrated that the homozygous variant T172T (rs1803121) is significantly associated with breast cancer risk (OR 3.717, 95% CI 2.283-6.052, $p < 0.0001$), while the heterozygous variant G135C (rs1801320) has no significant relationship with the risk of sporadic breast cancer (OR 1.598, 95% CI 0.5638-4.528, $p > 0.05$). However, both variants homozygous T172T and heterozygous G135C together showed a significant association with sporadic breast cancer susceptibility. Michalska et al. [22] found that the polymorphism of *RAD51* may be positively associated with the incidence of triple-negative breast carcinoma while Sekhar et al. [23] indicated that *RAD51* 135G > C substitution in the homozygous form (CC) increases the risk of breast cancer in an ethnic-specific manner. Söderlund et al. [24] suggest that *RAD51* 135G>C polymorphism predicts cyclophosphamide/methotrexate/5-fluorouracil chemotherapy effect in early breast cancer.

Polymorphism of the *RAD51* also seems to play a role in other types of cancer. In our previous study we found a significant relationship between *RAD51* polymorphism rsl801320 and an increased risk of prostate cancer [17]. It has been shown that subjects carrying *RAD51* rs1801320 GC genotype also have an increased risk of glioblastoma (GC vs GG, $\chi(2) = 10.75$; OR 3.0087; $p = 0.0010$). In addition, *RAD51* rs1801320 C allele increased the risk of developing glioblastoma also in combination with the *XRCC1* rs25487 G allele and *XRCC3* rs861539 C allele ($\chi(2) = 6.558$; $p = 0.0053$) [25]. Trang et al. [26] showed that the combination of *Helicobacter pylori* infection and *RAD51* G135C genotype of the host leads to an increased score for intestinal metaplasia. This suggests that *RAD51* G135C may be an important predictor for gastric cancer of *Helicobacter pylori*-infected patients. Mucha et al. [27] study revealed a statistically significant association also between rs5030789 polymorphism in *RAD51* and the risk of colorectal cancer. In turn in the case of rs2619679 polymorphism in *RAD51*, it was shown that it does not correlate with the risk of head and neck cancer [28].

Table 5: Relationship between G allele for rs5030789 in *RAD51* and rs1799796 in *XRCC3* and clinicopathological characteristics of prostate cancer patients.

Clinicopathological parameter	rs5030789		rs1799796	
	A	G	A	G
Age				
≤ 71	35	67	60	42
> 71	24	72	41	55
	OR = 1.567 (0.846-2.902)		*OR = 1.916 (1.089-3.371)*	
	$p = 0.202$		*$p = 0.033$*	
PSAT (ng/ml)				
< 4-10	34	68	53	49
> 10	25	71	48	48
	OR = 1.420 (0.768-2.624)		OR = 1.082 (0.619-1.889)	
	$p = 0.335$		$p = 0.887$	
Free/total PSA (F/T PSA)				
< 0.16	25	71	44	52
≥ 0.16	34	68	57	45
	OR = 0.704 (0.381-1.301)		OR = 0.668 (0.381-1.170)	
	$p = 0.335$		$p = 0.203$	
PSA Density (PSAD, ng/ml)				
< 0.28	26	72	49	49
≥ 0.28	33	67	52	48
	OR = 0.733 (0.397-1.352)		OR = 0.923 (0.529-1.612)	
	$p = 0.399$		$p = 0.888$	
Prostate volume (ml)				
< 48	31	61	52	40
≥ 48	28	78	49	57
	OR = 1.416 (0.768-2.608)		OR = 1.512 (0.862-2.652)	
	$p = 0.337$		$p = 0.192$	
Gleason score				
< 7	19	37	37	19
≥ 7	40	102	64	78
	OR = 1.309 (0.675-2.541)		*OR = 2.373 (1.246-4.521)*	
	$p = 0.532$		*$p = 0.012$*	
Cancer stage				
T1-T2	35	81	58	58
T3-T4	24	58	43	39
	OR = 1.224 (0.664-2.256)		OR = 0.907 (0.515-1.597)	
	$p = 0.624$		$p = 0.841$	

Avadanei et al. [29] findings suggest that *XRCC3* polymorphism in hepatocellular carcinoma may affect the aggressiveness of the tumor expressed by tumor grade. Statistically significant differences were shown for rs1799796 A>G and tumor grade, between wild type (AA) and heterozygote (AG) genotypes, and wild type (AA) and heterozygote and homozygote (AG and GG) genotypes. The logistic regression analysis found an OR of rs1799796 polymorphism occurrence in hepatocellular carcinoma related to tumor grade. In the case of rs861539 C>T polymorphism, statistical analysis showed better survival only for the homozygote (TT) compared to the heterozygote (CT) genotype, and in the case of rs1799796 A>G polymorphism, a longer survival for wild type (AA) compared to heterozygote (AG) and to heterozygote and homozygote (AG and GG) genotypes, respectively. The results presented by Ali et al. [30] suggest that the polymorphism rs1799794 in *XRCC3* is strongly associated with the development of breast cancer in Saudi women while genotype and allele frequencies of rs861539 C>T and rs1799796 A>G did not show a significant difference. However, the frequency of rs1799796 differed significantly in patients depending on the age of the diagnosis, tumor grade, and ER and HER2 status. The wild type A allele occurred more frequently in the ER- and HER2- group. It was also found that the presence of the polymorphism rs1799796 in *XRCC3* may reduce the risk of oral premalignant lesions [31]. On the other hand, Mandal et al. [32] showed no significant association between rs1799796 and rs861539 polymorphism

in *XRCC3* and the risk of prostate cancer. In the case of studies conducted by Mittal et al. [33], no direct relationship was found between the occurrence of rs1799796 polymorphism in *XRCC3* and the incidence of bladder cancer. In addition, the studied polymorphism seems to be not related to the incidence of nasopharyngeal cancer as well as head and neck cancer [27, 34]. However, a meta-analysis of 5302 cases of ovarian cancer compared to 8075 control cases revealed statistically significant correlation of rs1799794 and rs1799796 polymorphism in *XRCC3* and an increased risk of developing ovarian cancer in Caucasians, Asian, and African population [35]. It is also worth pointing out that Vral et al. [36] have demonstrated the combined effect of polymorphisms in *RAD51* and *XRCC3* on breast cancer risk.

5. Conclusion

Our study showed that rs5030789 polymorphism in *RAD51* and rs1799796 in *XRCC3* are associated with the occurrence of prostate cancer in Polish men. We have demonstrated correlation between the rs1799796 polymorphism in *XRCC3* and the age of patients over 71 years and Gleason score of tumor higher than 7. Our findings indicate the importance of *RAD51* and *XRCC3* polymorphisms in the development of prostate cancer. Based on the results presented, we suggest considering genetic testing for *RAD51* and *XRCC3* to identify those men who have DNA repair deficiency and who have not responded to standard treatment.

Data Availability

The data used to support the findings of the study are included within article.

Ethical Approval

The study was conducted in accordance with the ethical standards of the 1975 Helsinki Declaration and its later amendments and approved by institutional ethics committees (University of Lodz, Poland, KBBN-UL/25/2012; Medical University of Lodz, Poland, RNN/59/089/KE).

Consent

Informed consent was obtained from the patients.

Conflicts of Interest

The authors declare that there are no conflicts of interest.

Authors' Contributions

M. Nowacka-Zawisza, A. Raszkiewicz, T. Kwasiborski, and E. Forma performed the experiments. M. Nowacka-Zawisza analyzed data. M. Nowacka-Zawisza, M. Bryś, and W. Różański collected study samples. M. Nowacka-Zawisza and W. M. Krajewska designed the research study and wrote the paper.

References

[1] F. Bray, J. Ferlay, I. Soerjomataram, R. L. Siegel, L. A. Torre, and A. Jemal, "Global cancer statistics 2018: globocan estimates of incidence and mortality worldwide for 36 cancers in 185 countries," *CA: A Cancer Journal for Clinicians*, vol. 68, no. 6, pp. 394–424, 2018.

[2] C. H. Pernar, E. M. Ebot, K. M. Wilson, and L. A. Mucci, "The epidemiology of prostate cancer," *Cold Spring Harbor Perspectives in Medicine*, vol. 8, no. 12, Article ID a030361, 2018.

[3] U. Wojciechowska, K. Czaderny, A. Ciuba, P. Olasek, and J. Didkowska, "Cancer in Poland in 2016," *The Maria Sklodowska-Curie Memorial Cancer Center and Institute of Oncology, Polish National Cancer Registry*, 2018, Warsaw, Poland, http://onkologia.org.pl/publikacje/.

[4] H. E. Taitt, "Global trends and prostate cancer: a review of incidence, detection, and mortality as influenced by race, ethnicity, and geographic location," *American Journal of Men's Health*, vol. 12, no. 6, pp. 1807–1823, 2018.

[5] R. Eeles and H. N. Raghallaigh, "Men with a susceptibility to prostate cancer and the role of genetic based screening," *Translational Andrology and Urology*, vol. 7, no. 1, pp. 61–69, 2018.

[6] S.-H. Tan, G. Petrovics, and S. Srivastava, "Prostate cancer genomics: Recent advances and the prevailing underrepresentation from racial and ethnic minorities," *International Journal of Molecular Sciences*, vol. 19, no. 4, 2018.

[7] H. H. Cheng, C. C. Pritchard, B. Montgomery, D. W. Lin, and P. S. Nelson, "Prostate cancer screening in a new era of genetics," *Clinical Genitourinary Cancer*, vol. 15, no. 6, pp. 625–628, 2017.

[8] D. Robinson, E. M. Van Allen, Y.-M. Wu et al. et al., "Integrative Clinical Genomics of Advanced Prostate Cancer," *Cell*, vol. 161, no. 5, pp. 1215–1228, 2015.

[9] C. Chen, W. Feng, P. X. Lim, E. M. Kass, and M. Jasin, "Homology-directed repair and the role of BRCA1, BRCA2, and related proteins in genome integrity and cancer," *Annual Review of Cancer Biology*, vol. 2, no. 1, pp. 313–336, 2018.

[10] B. R. Potugari, J. M. Engel, and A. A. Onitilo, "Metastatic prostate cancer in a RAD51C mutation carrier," *Clinical Medicine and Research*, vol. 16, no. 3-4, pp. 69–72, 2018.

[11] X. Zeng, Y. Zhang, L. Yang et al., "Association between RAD51 135 G/C polymorphism and risk of 3 common gynecological cancers: a meta-analysis," *Medicine*, vol. 97, no. 26, p. e11251, 2018.

[12] W. D. Wright, S. S. Shah, and W.-D. Heyer, "Homologous recombination and the repair of DNA double-strand breaks," *Journal of Biological Chemistry*, vol. 293, no. 27, pp. 10524–10535, 2018.

[13] S. Inano, K. Sato, Y. Katsuki et al., "RFWD3-mediated ubiquitination promotes timely removal of both RPA and RAD51 from DNA damage sites to facilitate homologous recombination," *Molecular Cell*, vol. 66, no. 5, pp. 622–634.e8, 2017.

[14] N. Ameziane, P. May, A. Haitjema et al., "A novel Fanconi anaemia subtype associated with a dominant-negative mutation in RAD51," *Nature Communications*, vol. 18, no. 6, p. 8829, 2015.

[15] A. T. Wang, T. Kim, J. E. Wagner et al., "A dominant mutation in human RAD51 reveals its function in DNA interstrand crosslink repair independent of homologous recombination," *Molecular Cell*, vol. 59, no. 3, pp. 478–490, 2015.

[16] M. A. Brenneman, B. M. Wagener, C. A. Miller, C. Allen, and J. A. Nickoloff, "XRCC3 controls the fidelity of homologous

recombination: Roles for XRCC3 in late stages of recombination," *Molecular Cell*, vol. 10, no. 2, pp. 387–395, 2002.

[17] M. Nowacka-Zawisza, E. Wiśnik, A. Wasilewski et al., "Polymorphisms of Homologous recombination RAD51, RAD51B, XRCC2, and XRCC3 genes and the risk of prostate cancer," *Analytical Cellular Pathology*, vol. 2015, Article ID 828646, 9 pages, 2015.

[18] J. Sambrook and D. W. Russell, *Molecular Cloning: A Laboratory Manual*, Cold Spring Harbor Laboratory Press, Cold Spring Harbor, NY, USA, 2001.

[19] T. J. Hoffmann, M. N. Passarelli, R. E. Graff et al., "Genome-wide association study of prostate-specific antigen levels identifies novel loci independent of prostate cancer," *Nature Communications*, vol. 8, p. 14248, 2017.

[20] Z. Qureshi, I. Mahjabeen, R. M. Baig, and M. A. Kayani, "Correlation between selected XRCC2, XRCC3 and RAD51 gene polymorphisms and primary breast cancer in women in Pakistan," *Asian Pacific Journal of Cancer Prevention*, vol. 15, no. 23, pp. 10225–10229, 2014.

[21] M. S. Al-Zoubi, C. M. Mazzanti, K. Zavaglia et al., "Homozygous T172T and heterozygous G135C variants of homologous recombination repairing Protein RAD51 are related to sporadic breast cancer susceptibility," *Biochemical Genetics*, vol. 54, no. 1, pp. 83–94, 2016.

[22] M. M. Michalska, D. Samulak, H. Romanowicz, and B. Smolarz, "Single nucleotide polymorphisms (SNPs) of RAD51-G172T and XRCC2-41657C/T homologous recombination repair genes and the risk of triple- negative breast cancer in polish women," *Pathology & Oncology Research*, vol. 21, no. 4, pp. 935–940, 2015.

[23] D. Sekhar, S. Pooja, S. Kumar, and S. Rajender, "RAD51 135G>C substitution increases breast cancer risk in an ethnic-specific manner: a meta-analysis on 21,236 cases and 19,407 controls," *Scientific Reports*, vol. 5, no. 11588, pp. 1–10, 2015.

[24] K. Söderlund Leifler, A. Asklid, T. Fornander, and M. Stenmark Askmalm, "The RAD51 135G>C polymorphism is related to the effect of adjuvant therapy in early breast cancer," *Journal of Cancer Research and Clinical Oncology*, vol. 141, no. 5, pp. 797–804, 2015.

[25] S. Franceschi, S. Tomei, C. M. Mazzanti et al., "Association between RAD51 rs1801320 and susceptibility to glioblastoma," *Journal of Neuro-Oncology*, vol. 126, no. 2, pp. 265–270, 2016.

[26] T. T. H. Trang, H. Nagashima, T. Uchida et al., "RAD51 G135C genetic polymorphism and their potential role in gastric cancer induced by Helicobacter pylori infection in Bhutan," *Epidemiology and Infection*, vol. 144, no. 2, pp. 234–240, 2016.

[27] B. Mucha, J. Kabzinski, A. Dziki et al., "Polymorphism within the distal RAD51 gene promoter is associated with colorectal cancer in a Polish population," *International Journal of Clinical and Experimental Pathology*, vol. 8, no. 9, pp. 11601–11607, 2015.

[28] P. Gresner, J. Gromadzinska, K. Polanska, E. Twardowska, J. Jurewicz, and W. Wasowicz, "Genetic variability of Xrcc3 and Rad51 modulates the risk of head and neck cancer," *Gene*, vol. 504, no. 2, pp. 166–174, 2012.

[29] E.-R. Avadanei, S.-E. Giusca, L. Negura, and I.-D. Caruntu, "Single nucleotide polymorphisms of XRCC3 gene in hepatocellular carcinoma - relationship with clinicopathological features," *Polish Journal of Pathology*, vol. 69, no. 1, pp. 73–81, 2018.

[30] A. M. Ali, H. Abdulkareem, M. Al Anazi et al., "Polymorphisms in DNA repair gene XRCC3 and susceptibility to breast cancer in saudi females," *BioMed Research International*, vol. 2016, Article ID 8721052, 9 pages, 2016.

[31] C. Yuan, X. Liu, S. Yan, C. Wang, and B. Kong, "Analyzing association of the XRCC3 gene polymorphism with ovarian cancer risk," *BioMed Research International*, vol. 2014, Article ID 648137, pp. 1–9, 2014.

[32] R. K. Mandal, R. Kapoor, and R. D. Mittal, "Polymorphic variants of DNA repair gene XRCC3 and XRCC7 and risk of prostate cancer: a study from North Indian population," *DNA and Cell Biology*, vol. 29, no. 11, pp. 669–674, 2010.

[33] R. D. Mittal, R. Gangwar, R. K. Mandal, P. Srivastava, and D. K. Ahirwar, "Gene variants of XRCC4 and XRCC3 and their association with risk for urothelial bladder cancer," *Molecular Biology Reports*, vol. 39, no. 2, pp. 1667–1675, 2012.

[34] J. C. Liu, C. W. Tsai, C. M. Hsu et al., "Contribution of double strand break repair gene XRCC3 genotypes to nasopharyngeal carcinoma risk in taiwan," *Chinese Journal of Physiology*, vol. 58, no. 1, pp. 64–71, 2015.

[35] H. Yang, S. M. Lippman, M. Huang et al., "Genetic polymorphisms in double-strand break DNA repair genes associated with risk of oral premalignant lesions," *European Journal of Cancer*, vol. 44, no. 11, pp. 1603–1611, 2008.

[36] A. Vral, P. Willems, K. Claes et al., "Combined effect of polymorphisms in Rad51 and XRCC3 on breast cancer risk and chromosomal radiosensitivity," *Molecular Medicine Reports*, vol. 4, no. 5, pp. 901–912, 2011.

Hindawi
Journal of Oncology
Volume 2019, Article ID 9218251, 15 pages
https://doi.org/10.1155/2019/9218251

Research Article

Genotypic and Phenotypic Variables Affect Meiotic Cell Cycle Progression, Tumor Ploidy, and Cancer-Associated Mortality in a *brca2*-Mutant Zebrafish Model

L. Mensah, J. L. Ferguson, and H. R. Shive

Department of Population Health and Pathobiology, North Carolina State University, College of Veterinary Medicine, 1060 William Moore Drive, Raleigh, Raleigh, NC, USA

Correspondence should be addressed to H. R. Shive; hrshive@ncsu.edu

Received 26 November 2018; Revised 10 January 2019; Accepted 28 January 2019; Published 26 February 2019

Guest Editor: Zhihua Kang

Successful cell replication requires both cell cycle completion and accurate chromosomal segregation. The tumor suppressor BRCA2 is positioned to influence both of these outcomes, and thereby influence genomic integrity, during meiotic and mitotic cell cycles. Accordingly, mutations in *BRCA2* induce chromosomal abnormalities and disrupt cell cycle progression in both germ cells and somatic cells. Despite these findings, aneuploidy is not more prevalent in *BRCA2*-associated versus non-*BRCA2*-associated human cancers. More puzzlingly, diploidy in *BRCA2*-associated cancers is a negative prognostic factor, unlike non-*BRCA2*-associated cancers and many other human cancers. We used a *brca2*-mutant/*tp53*-mutant cancer-prone zebrafish model to explore the impact of *BRCA2* mutation on cell cycle progression, ploidy, and cancer-associated mortality by performing DNA content/cell cycle analysis on zebrafish germ cells, somatic cells, and cancer cells. First, we determined that combined *brca2*/*tp53* mutations uniquely disrupt meiotic progression. Second, we determined that sex significantly influences ploidy outcome in zebrafish cancers. Third, we determined that *brca2* mutation and female sex each significantly reduce survival time in cancer-bearing zebrafish. Finally, we provide evidence to support a link between *BRCA2* mutation, tumor diploidy, and poor survival outcome. These outcomes underscore the utility of this model for studying *BRCA2*-associated genomic aberrations in normal and cancer cells.

1. Introduction

Generation of cell progeny lies at the heart of virtually all biological processes. Successfully performing this fundamental cell behavior requires both completion of the cell cycle and faithful replication and segregation of chromosomal content. Both meiotic and mitotic cell cycles are governed by these principles, although clear mechanistic differences exist (reviewed by Duro E and Marston AL [1]). If cell cycle progression is disturbed during mitotic or meiotic cell cycles, potential adverse outcomes include cell cycle arrest, chromosomal aberrations, and/or missegregation; the latter outcomes may cause chromosomal instability and aneuploidy.

The tumor suppressor gene *BRCA2* functions in multiple pathways that affect both meiotic and mitotic cell cycles, and thereby genomic stability. These include homology-directed repair (HDR), replication fork maintenance, spindle assembly checkpoint (SAC), cytokinesis, and telomere homeostasis (reviewed by Venkitaraman AR [2]). Figure 1(a) indicates phases of the meiotic and mitotic cell cycles during which BRCA2 is known to function and the corresponding cellular DNA content in each phase. In meiosis, BRCA2 functions in prophase I of meiosis I; cells enter meiosis I with 4C DNA content and exit meiosis I with 2C DNA content following the first meiotic division. In mitosis, BRCA2 participates in multiple processes that span from the G2 checkpoint in late G2 phase to cytokinesis in M phase, as described below. Cells enter G2 phase with 4C DNA content and exit M phase with 2C DNA content.

In mammalian germ cells, loss of functional Brca2 resulted in cell cycle arrest in meiotic prophase I and persistent DNA damage [3, 4]. Additionally, aberrant chromosomal segregation during meiosis was described in *brca2*-mutant *Arabidopsis* gametophytes [5]. In primary somatic cells (mouse embryonic fibroblasts), loss of functional Brca2 caused cell cycle arrest and both structural and numerical

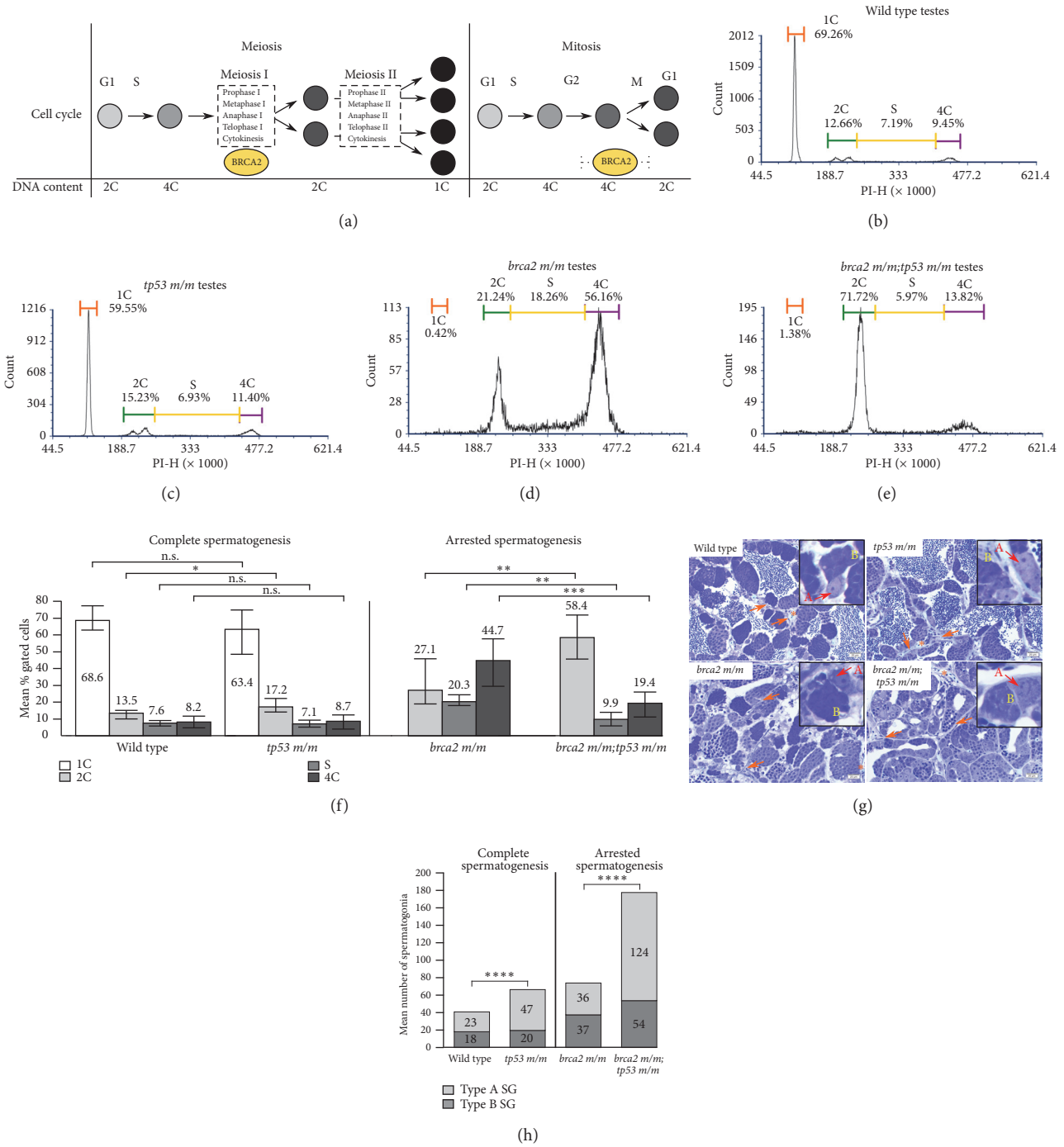

Figure 1: *brca2* and *tp53* mutations alter distribution of cells according to DNA content in adult zebrafish testes. (a) Comparison of cell progression through meiosis and mitosis with corresponding DNA content (designated as 1C, 2C, or 4C). BRCA2 participates in DNA repair during prophase I of meiosis I and performs multiple functions between late G2 and M phases of mitosis, as indicated by the positions of the yellow ovals. ((b)–(e)) Propidium iodide (PI) fluorescence histograms of testes derived from wild type (b), *tp53 m/m* (c), *brca2 m/m* (d), and *brca2 m/m;tp53 m/m* zebrafish testes (e). (f) Mean percent of gated cells clustered by DNA content for wild type, *tp53 m/m*, *brca2 m/m*, and *brca2 m/m;tp53 m/m* zebrafish testes. The mean percent of gated cells for each DNA content category is indicated. (g) Comparison of testicular morphology in wild type, *tp53 m/m*, *brca2 m/m*, and *brca2 m/m;tp53 m/m* zebrafish, Toluidine blue stain. Insets show type A (A, red) and type B (B, yellow) spermatogonia. Orange arrows indicate representative regions of stromal tissue and orange asterisks indicate examples of blood vessels within the stroma. (h) Comparison of the mean number of spermatogonia per 400X field (see Materials and Methods) in wild type, *tp53 m/m*, *brca2 m/m*, and *brca2 m/m;tp53 m/m* zebrafish testes. The mean numbers of type A and type B spermatogonia are shown in the appropriate portion of each column. SG, spermatogonia; ∗, p = 0.01-0.05; ∗∗, p = 0.001–0.01; ∗ ∗ ∗, p = 0.0001–0.01; ∗ ∗ ∗∗, p < 0.0001. Error bars represent the range of the data. See Table S1 for specific p-values.

chromosomal abnormalities [6, 7]. Additionally, disrupted interaction between Brca2 and the SAC mediator BubR1 resulted in both genomic instability and aneuploidy [8], and BRCA2 deficiency has been linked to defects in cytokineses [9, 10]. BRCA2 may also participate in regulation of entry into mitosis after the G2 checkpoint [11, 12] and was found to be essential for protection of stalled replication forks [13]. These findings indicate that loss of functional BRCA2 severely disrupts both meiotic and mitotic cell cycles and has significant potential to destabilize genomic integrity.

The above studies predict that *BRCA2*-associated human cancers might exhibit a high prevalence of aneuploidy. However, comparison of *BRCA2*-associated and non-*BRCA2*-associated human breast cancers has shown that *BRCA2* mutation does not increase aneuploidy in human cancer [14–16]. Instead, diploid and aneuploid cancers occurred in roughly equal proportions in *BRCA2* mutation carriers and noncarriers. Moreover, diploidy was identified as an independent negative prognostic indicator for *BRCA2* mutation carriers that was linked to decreased survival time [16]. In contrast, diploidy was a positive prognostic indicator for noncarriers [16]. This observation is at odds with the fact that aneuploidy is generally considered to be a poor prognostic indicator for many human cancers [17–22]. These unexpected findings suggest an unusual and complex relationship between *BRCA2* mutation, ploidy, and survival outcome.

In the current study, we used a zebrafish model to investigate the impact of *BRCA2* mutation on meiotic and mitotic cell cycle outcomes and to assess the relationship between *brca2* mutation, ploidy, and survival in cancer-bearing zebrafish. The zebrafish $brca2^{Q658X}$ mutation is a nonsense mutation that is similar in location and type to pathologic *BRCA2* mutations in humans [23]. The *brca2*-mutant zebrafish line is fully viable [23], unlike most *Brca2*-mutant mouse models (summarized by Evers B and Jonkers J) [24], and thus is useful for *in vivo* studies with adult animals. In human *BRCA2*-associated cancers, *TP53* is frequently mutated, which is thought to be an early and essential step in survival of transformed cells [25–28]. Similarly, we previously showed that the zebrafish $tp53^{M214K}$ mutation [29] exerts a collaborative effect on tumorigenesis in *brca2*-mutant zebrafish [23, 30]. In the current study, we analyzed zebrafish siblings with and without *brca2* mutation on a *tp53*-mutant background, enabling us to assess the specific impact of *brca2* mutation on ploidy outcome.

First, we determined the effect of *brca2* and *tp53* mutations on meiotic cell cycle progression in zebrafish testes by paired flow cytometry and histologic assessment. Second, we determined the influence of *brca2* and *tp53* mutations on ploidy in zebrafish somatic cells and cancer cells and evaluated the contributions of other variables (sex, tumor location) to ploidy outcome. Finally, we identified the individual and combined impacts of *brca2* genotype, sex, and tumor ploidy on survival outcome in cancer-bearing zebrafish.

2. Materials and Methods

2.1. Zebrafish Study Cohorts. Experiments were performed with adult wild type (AB) zebrafish and adult zebrafish from the $brca2^{hg5}$ and $tp53^{zdf1}$ mutant zebrafish lines, corresponding to the $brca2^{Q658X}$ and $tp53^{M214K}$ mutations, respectively [23, 29]. Mutant alleles for *brca2* and *tp53* are referred to as "m"; individual zebrafish within each genotypic group were siblings. For studies assessing zebrafish with or without $brca2^{Q658X}$ mutation on the $tp53^{M214K}$ background, the compared study populations were composed of siblings. Thus, reference to *tp53 m/m* zebrafish indicates siblings of *brca2 m/m;tp53 m/m* zebrafish that do not carry the $brca2^{Q658X}$ mutation. The study group used for analysis of tumor ploidy was composed of two related cohorts derived from two clutches in order to achieve a target of 50 individuals per genotype. As this target was not achieved with the first cohort, part of a second cohort was included in the study. All animal studies were approved by the Institutional Animal Care and Use Committee, North Carolina State University, Raleigh, NC, and the methods were carried out in accordance with relevant guidelines and regulations.

2.2. Zebrafish Husbandry and Genotyping. Zebrafish used in this study were reared in a multirack recirculating containment system. From five to nine days of age, zebrafish larvae received live cultured *Brachionus plicatilis* (L-type rotifers), and, from ten to thirty days of age, zebrafish fry received commercially available, appropriately sized powder diets supplemented with live cultured *Artemia* sp. (brine shrimp). Juvenile and adult zebrafish received commercially available dry zebrafish diets supplemented with live cultured *Artemia* sp. Pathogen testing is performed on a biannual basis with the IDEXX Zebrafish Essential PCR Profile using zebrafish exposed to prefiltration water and swabs of detritus.

Zebrafish were monitored for clinical and gross evidence of tumor development and were collected in chronological order as tumors arose. Zebrafish were humanely euthanized with Tricaine methanesulfonate (300 mg/L) in system water buffered with Sodium Bicarbonate to a pH of ~ 7.0. Live adult zebrafish were genotyped for the $brca2^{Q658X}$ mutation by sequencing over the mutation site as described previously [31]. Zebrafish on the $tp53^{M214K}$ background were maintained as a homozygous mutant line.

2.3. Tissue Collection and Histologic Analysis. Normal and tumor tissues were identified and collected by dissection using a stereomicroscope. For DNA content analysis, tissue samples were prepared as described below. For histologic analysis of tumor-bearing zebrafish, a sample of tumor tissue and the coelomic viscera were collected and fixed in 4% Paraformaldehyde. Fixed tissues were routinely processed for decalcification as needed, paraffin embedding, and preparation of hematoxylin- and eosin-stained sections. For histologic analysis of zebrafish testes, fixed tissues were embedded in glycol methacrylate, sectioned at 2.5 μm thickness, and stained with Toluidine blue stain (0.01 g/ml Toluidine blue and 0.01 g/ml sodium tetraborate in distilled water).

Histologic sections were analyzed with an Olympus BX43 microscope and imaged with a DP26 digital camera and cellSens entry microscope imaging software, version 1.5. Histologic images were minimally and globally

processed for exposure, contrast, and/or color balance with the GNU Image Manipulation Program, version 2.8.6 (http://www.gimp.org/).

For quantification of spermatogonia in zebrafish testes, three representative images were captured at 400X from the testes of five zebrafish from each genotypic group for a total of 15 histologic sections per genotypic group. For one *brca2 m/m;tp53 m/m* zebrafish, only two representative images were quantified due to insufficient tissue for capturing three high-quality images; thus, a total of 14 histologic sections were evaluated for this genotypic group. Spermatogonia were manually counted in each digital image using the ImageJ Fiji Cell Counter tool [32]. Spermatogonia were identified by histologic characteristics as previously described [33], and type A and type B spermatogonia were counted separately.

2.4. DNA Content Analysis. For preparation of dissociated zebrafish testes, both testes from each zebrafish were collected, minced, and incubated in 500 U/ml Collagenase (Collagenase type I in 1X Hank's Balanced Salt Solution in L15 medium) at 28°C for 2 hours with gentle pipetting every 20 minutes. For preparation of dissociated nonneoplastic somatic cells and cancer cells, matched normal and tumor tissues samples from each individual zebrafish were collected and dissociated as described above. Dissociated cells were washed with 1X phosphate-buffered saline (PBS), filtered with a 35 μm filter and fixed with ice-cold 70% ethanol. Cell suspensions were maintained at -20°C for a minimum of 24 hours. After fixation, cell suspensions were washed with 1X PBS and stained with Propidium Iodide staining solution containing RNase (Cellometer PI Cell Cycle Kit, CSK-0112, Nexcelom, Lawrence, MA).

Cell suspensions were analyzed for DNA content with a Beckman Coulter CytoFLEX flow cytometer. The CytoFLEX was maintained and calibrated daily according to the manufacturer's recommendations. Up to 10,000 events were recorded per sample at a flow rate of 10–30 μl/min (up to 300 events/second). Matched normal and cancer specimens from individual zebrafish were analyzed during the same experiment.

Flow cytometry data were analyzed with DeNovo FCS Express 6 Flow Research Edition. For DNA content analysis of testes, the gating strategy was based on the method described by Rotgers et al. [34]. Cell suspensions from zebrafish testes were gated on forward scatter-A (FSC-A) versus FSC-H, followed by gating on Propidium Iodide-A (PI-A) versus FSC-A (Figure S1A). DNA histograms were generated using PI-H, and haploid (1C), diploid (2C), S-phase, and tetraploid (4C) populations were identified as previously described [34]. Percentages of each cell populations identified by DNA content were acquired by defining marker gates for each population (Figure S1A).

For DNA content analysis of cell suspensions from nonneoplastic somatic tissues and cancer tissues, cells were gated on PI-H versus PI-A. DNA histograms were generated using PI-H with the FCS Express 6 Multicycle AV Professional Version (Figure S1B). Cell cycles were modeled with the SL S0 model (sliced nuclei background modeling with zero order S phase). At least 1,000 events were analyzed to generate the cell cycle for all but one nonneoplastic somatic tissue specimen, for which 632 events were analyzed.

2.5. Criteria for Exclusion of Samples. DNA content analysis was attempted on testes from age-matched zebrafish in order to meet a target of at least five individuals per genotypic group. Individual results were excluded from the study under the following criteria: insufficient cell number to generate cell cycle profile.

DNA content analysis was attempted on normal and tumor specimens from zebrafish in chronological order, as cancers arose, in order to meet a target of 50 individuals per genotype. Individuals were excluded from the study under the following criteria: (1) found dead; (2) no grossly identifiable tumor tissue; (3) insufficient cell number to generate cell cycle profile; (4) coefficient of variance (CV) of the sample from nonneoplastic somatic tissue > 6.0; (5) inability to define the diploid population in the nonneoplastic somatic tissue specimen.

2.6. Calculation of Tumor Ploidy. Tumor ploidy was defined by calculating the DNA index (Table S1) [35]. For tumor samples that contained an internal diploid population with a CV ≤ 6.0, the DNA index was calculated using the G0/G1 peak fluorescence intensity value of the internal diploid population. The internal diploid population was confirmed to be diploid by comparing the G0/G1 peak fluorescence intensity value of this population to the G0/G1 peak fluorescence intensity value of the matched nonneoplastic somatic tissue specimen. For tumor samples that did not contain an internal diploid population or contained an internal diploid population with a CV > 6.0, the DNA index was calculated using the G0/G1 peak fluorescence intensity value of the matched nonneoplastic somatic tissue specimen. Tumors that exhibited multiple peaks were defined as complex aneuploid and a DNA index was not calculated.

For five zebrafish cancers (4 *brca2 m/m;tp53 m/m* and 1 *tp53 m/m*), an aneuploid population was inconsistently modeled or constituted ≤ 20% of the total population. For eight zebrafish cancers (5 *brca2 m/m;tp53 m/m* and 3 *tp53 m/m*), a subpopulation of cells was inconsistently modeled as either an aneuploid population or as the G2/M population. For these thirteen cancers, the G0/G1 peak fluorescence intensity value of the predominant diploid population was used to calculate DNA index.

2.7. Statistical Analyses. Statistical analyses were performed using JMP Pro 13.2.1 (SAS Institute Inc.). Statistical significance was set at an alpha value of $p \leq 0.05$. Comparisons of zebrafish testes were performed between zebrafish exhibiting complete spermatogenesis (wild type and *tp53 m/m*) and incomplete spermatogenesis (*brca2 m/m* and *brca2 m/m;tp53 m/m*). The percentages of cells by DNA content category in zebrafish testes and nonneoplastic somatic tissues were compared by t-test corrected for unequal variances. The four samples from nonneoplastic tissues that exhibited a small aneuploid peak, described above, were excluded from comparison of the percent gated cells in G0/G1, S, and G2/M phases. The numbers of spermatogonia in zebrafish

testes were compared by unpaired t-test assuming unequal variances. Comparison of G1 peak PI fluorescence intensity values were tested for normality by fitting a normal distribution and analyzing goodness-of-fit (Shapiro-Wilk W test). Samples from Experiment Seven that exhibited anomalously high G0/G1 peak PI fluorescence intensity values, described below, were excluded from this analysis (5 samples from *brca2 m/m;tp53 m/m* zebrafish, 1 sample from *tp53 m/m* zebrafish). The Chi-square test was used to test for associations in pairwise comparisons of genotype, tumor location, ploidy outcome, and sex. The median survival times were obtained using the Kaplan-Meier test and differences in survival curves were assessed by the log-rank test and Cox's Proportional Hazard Model. Cox's Proportional Hazard Model was used to determine contribution to survival by the purported risk variables (i.e., *brca2* mutation status, sex, and tumor ploidy).

3. Results

3.1. Combined brca2 and tp53 Mutations Induce Meiotic Arrest and Spermatogonial Expansion in Zebrafish. We previously showed that zebrafish with homozygous $brca2^{Q658X}$ mutation (*brca2 m/m*) develop exclusively as males and exhibit incomplete spermatogenesis with extensive spermatocyte apoptosis, reflecting a conserved role for *BRCA2* in germ cell development [23]. In comparison, homozygous $tp53^{M214K}$ mutation (*tp53 m/m*) was not reported to impact sex ratios or fertility in zebrafish [29]. In the following studies, comparisons were performed between testes with complete spermatogenesis (wild type and *tp53 m/m*) and between testes with incomplete spermatogenesis (*brca2 m/m* and *brca2 m/m;tp53 m/m*).

Similar to *brca2 m/m* zebrafish, *brca2 m/m;tp53 m/m* males are sterile and exhibit incomplete spermatogenesis, with only spermatogonia and primary spermatocytes present in testes (Figure S2A). In comparison, *tp53 m/m* male zebrafish are fertile and exhibit complete spermatogenesis, with no histologic abnormalities observed in testes (Figure S2B). To further investigate this phenotype, we analyzed dissociated testes from age-matched wild type (n = 5), *tp53 m/m* (n = 7), *brca2 m/m* (n = 9), and *brca2 m/m;tp53 m/m* (n = 5) male zebrafish by flow cytometry (Figure 1 and Figure S1A). Testes from wild type and *tp53 m/m* zebrafish had similar cell cycle profiles and exhibited a predominance of cells with 1C DNA content, representing mature spermatozoa (Figures 1(b), 1(c), and 1(f)). The proportions of cells in each DNA content category (1C, 2C, S, and 4C) were not significantly different in testes from wild type and *tp53 m/m* zebrafish, with the exception of the 2C population ($p = 0.0405$, unpaired t-test; Figure 1(f) and Table S1).

In contrast, testes from *brca2 m/m* and *brca2 m/m;tp53 m/m* zebrafish did not contain an appreciable cell population with 1C DNA content (< 2% of gated cells), indicating arrested spermatogenesis in males from these genotypic groups. Seven of 9 testes from *brca2 m/m* zebrafish exhibited a predominance of cells with 4C DNA content (Figures 1(d) and 1(f)), while all testes from *brca2 m/m;tp53 m/m* zebrafish exhibited a predominance of cells with 2C DNA content (Figures 1(e) and 1(f)). Testes from *brca2 m/m* zebrafish additionally exhibited an increased proportion of cells in S phase. The proportions of cells in each DNA content category (2C, S, and 4C) were significantly different in testes from *brca2 m/m* and *brca2 m/m;tp53 m/m* zebrafish (Figure 1(f) and Table S1).

We next sought to determine a cause for the difference in the proportions of cells with 2C versus 4C DNA content in testes from *brca2 m/m* versus *brca2 m/m;tp53 m/m* zebrafish. The 2C population identified by flow cytometry in dissociated testes includes spermatogonia, secondary spermatocytes, and somatic cells (stromal component). However, secondary spermatocytes are rarely observed in zebrafish testes due to rapid entry into meiosis II [33]. We performed quantitative histologic analysis on thin sections of testes to determine the prevalence of spermatogonia. We analyzed testes from age-matched wild type (n = 5), *tp53 m/m* (n = 5), *brca2 m/m* (n = 5), and *brca2 m/m;tp53 m/m* (n = 5) male zebrafish (Figure 1(g)). Because testes from *brca2 m/m* and *brca2 m/m;tp53 m/m* zebrafish do not contain spermatozoa, testicular tubules are generally smaller and closer together than in testes from wild type and *tp53 m/m* zebrafish (Figure 1(g)). We therefore compared the numbers of spermatogonia between genotypic groups with complete spermatogenesis (wild type and *tp53 m/m*) and between genotypic groups with arrested spermatogenesis (*brca2 m/m* and *brca2 m/m;tp53 m/m*) (Figure 1(h) and Table S1).

In mammals [36] and zebrafish [33], spermatogonia can be identified as type A or type B based on nuclear morphology, with type A representing a less differentiated population than type B. *tp53 m/m* testes exhibited a significantly increased number of spermatogonia compared to wild type testes that was attributable to expansion of the type A spermatogonial population ($p < 0.0001$, unpaired t-test; Figure 1(h) and Table S1). *brca2 m/m;tp53 m/m* testes exhibited a significantly increased number of spermatogonia compared to *brca2 m/m* testes. This increase was largely attributable to expansion of the type A spermatogonial population, although the type B spermatogonial populations were also significantly increased (type A, $p < 0.0001$, unpaired t-test; type B, $p = 0.0061$, unpaired t-test; Figure 1(h) and Table S1). In *brca2 m/m;tp53 m/m* testes, we observed occasional giant spermatogonia (Figure S2C) and germ cells that were morphologically consistent with perinucleolar oocytes (Figure S2D). We did not observe these cell types in any other genotypic group. The stromal component of the testes (containing various types of somatic cells) appeared similar between zebrafish of different genotypes (Figure 1(g)).

3.2. brca2 Mutation Does Not Alter Ploidy or Cell Cycle Progression in Nonneoplastic Zebrafish Somatic Cells. In preparation for analyzing ploidy in zebrafish cancers, we collected matched nonneoplastic somatic tissue from each cancer-bearing zebrafish. This enabled us to define the diploid population for calculation of tumor ploidy for each cancer specimen and also allowed us to assess the impact of *brca2* mutation on DNA content and cell cycle progression in nonneoplastic somatic cells. We analyzed somatic tissues from 49 *brca2 m/m;tp53 m/m* zebrafish and 50 *tp53 m/m*

Table 1: Characteristics of the study population used for analysis of somatic and cancer cells.

	brca2 m/m;tp53 m/m	*tp53 m;m*
Total zebrafish	49	50
Males	22 (45%)	25 (50%)
Females	26 (53%)	25 (50%)
Sex not determined	1 (2%)	0 (0%)
Total tumors[a]	52	51
Age at tumor diagnosis (mo)		
Median age (total population)	8.2	10.8
Range (total population)	6.0 – 13.1	7.1 – 13.9
Median age (males)	9.0	11.3
Range (males)	6.2 – 13.1	7.1 – 13.9
Median age (females)	7.4	9.7
Range (females)	6.0 – 10.1	7.1 – 13.6
Tumor location		
Coelom	30 (58%)	40 (78%)
Ocular region	19 (37%)	9 (18%)
Other	3 (6%)	2 (4%)

[a] Two anatomically distinct tumors were independently analyzed for three *brca2 m/m;tp53 m/m* zebrafish and one *tp53 m/m* zebrafish.

zebrafish for DNA content (Table 1 and Figure S2B). 46 tissue samples from *brca2 m/m;tp53 m/m* zebrafish and 49 samples from *tp53 m/m* zebrafish exhibited a single diploid cell cycle. Four nonneoplastic somatic tissues exhibited a small aneuploid peak (ranging from 8.8 to 16.0% of gated cells) in addition to a predominant diploid cell cycle. These tissues were derived from three *brca2 m/m;tp53 m/m* zebrafish and one *tp53 m/m* zebrafish.

Comparison of the individual diploid G0/G1 peak propidium iodide (PI) fluorescence intensity values for nonneoplastic somatic cells demonstrated tight clustering of individual values within and between each independent flow cytometry analysis, designated as Experiments 1–23 (Figure 2(a), upper panel). Samples analyzed in one flow cytometry analysis (Experiment 7) showed anomalously high G0/G1 peak PI fluorescence intensity values compared to other samples but were highly similar to one another. Overall, the distributions of G0/G1 peak PI fluorescence intensity values were similar for nonneoplastic somatic cells derived from *brca2 m/m;tp53 m/m* and *tp53 m/m* zebrafish, both within and between each independent flow cytometry analysis. In contrast, the distributions of G0/G1 peak PI fluorescence intensity values for cancer cells derived from *brca2 m/m;tp53 m/m* and *tp53 m/m* zebrafish were highly variable (Figure 2(a), lower panel).

We analyzed the individual G0/G1 peak PI fluorescence intensity values for nonneoplastic somatic cells derived from *brca2 m/m;tp53 m/m* and *tp53 m/m* zebrafish for a normal distribution (Figure 2(b)). For both genotypic groups, the G0/G1 peak PI fluorescence intensity values followed a normal distribution, and the median G0/G1 peak PI fluorescence intensity values were similar (Figure 2(b)).

We assessed cell cycle progression in nonneoplastic somatic tissues based on DNA content distribution by comparing the percent gated cells in G0/G1, S, and G2/M phases (Figure S3). The mean percentages of cells in G0/G1, S, and G2/M phases were similar for *brca2 m/m;tp53 m/m* and *tp53 m/m* zebrafish (Figure S3A).

3.3. Tumor Ploidy Is Not Significantly Different in brca2-Associated and Non-brca2-Associated Zebrafish Cancers. We performed DNA content analysis on cancers derived from 49 *brca2 m/m;tp53 m/m* zebrafish and 50 *tp53 m/m* zebrafish siblings (Figures 3(a)–3(d) and Table 1). Cancer-bearing zebrafish in these studies were siblings that were distinguished by presence or absence of the *brca2* mutation. Therefore, cancers arising in *brca2 m/m;tp53 m/m* zebrafish are referred to as *brca2*-associated cancers and cancers arising in *tp53 m/m* zebrafish are referred to as non-*brca2*-associated cancers. Cancers were predominantly soft tissue sarcomas that showed variable histologic differentiation toward malignant peripheral nerve sheath tumor (MPNST), as we have previously described in zebrafish of these genotypes [31]. We have previously shown that *brca2* genotype was not correlated to degree of histologic differentiation (poorly differentiated sarcoma versus well-differentiated MPNST) [31]. In comparison, we have previously shown that *brca2 m/m* zebrafish without concurrent *tp53* mutation exhibit a relative increase in the incidence of benign testicular tumors [23, 30].

For each cancer-bearing zebrafish, matched nonneoplastic somatic tissues were simultaneously analyzed as described above. In three *brca2 m/m;tp53 m/m* zebrafish and one *tp53 m/m* zebrafish, there were two anatomically distinct tumors (e.g., both an ocular and a coelomic tumor in one individual) that were collected and analyzed independently. In total, 52 cancers from *brca2 m/m;tp53 m/m* zebrafish and 51 cancers from *tp53 m/m* zebrafish were analyzed. Ploidy was determined by calculating the DNA index based on G0/G1 peak PI fluorescence intensity values (Table S2 and Methods).

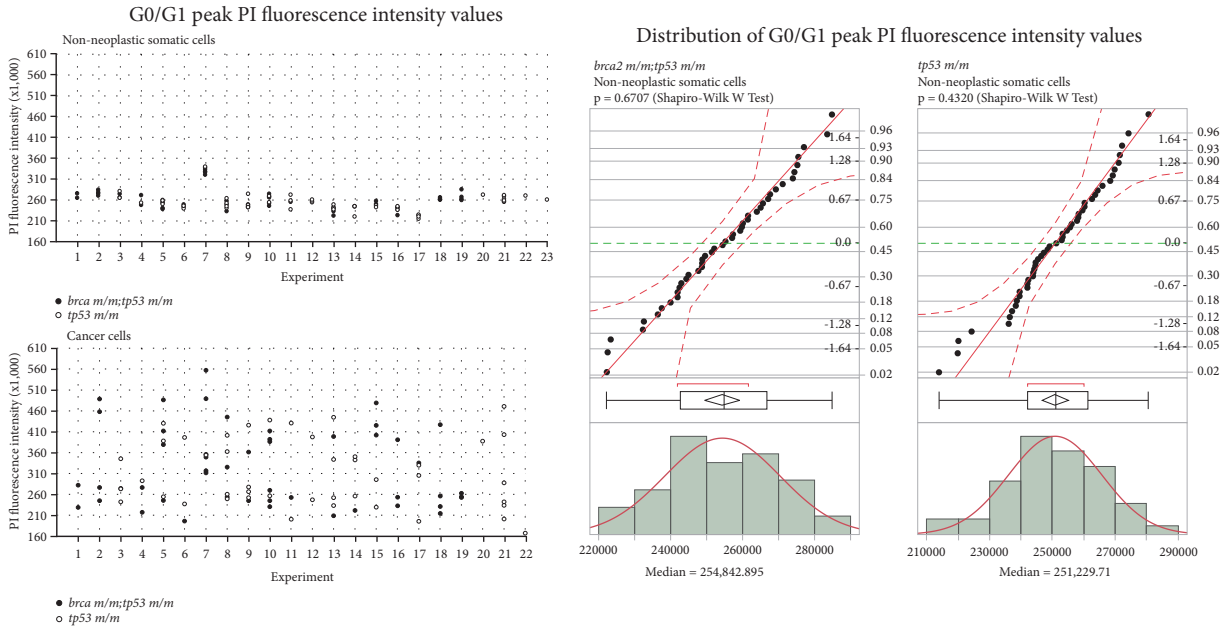

(a) (b)

FIGURE 2: *brca2* mutation does not alter DNA content of nonneoplastic somatic zebrafish tissue. (a) Comparison of G0/G1 peak propidium iodide (PI) fluorescence intensity values for nonneoplastic somatic cells (upper panel) and cancer cells (lower panel) derived from 49 *brca2 m/m;tp53 m/m* (black circles) and 50 *tp53 m/m* (white circles) cancer-bearing zebrafish. Each circle indicates the G0/G1 peak value for a single sample. Two matched samples (nonneoplastic somatic cells and cancer cells) were analyzed from each individual zebrafish. For every individual zebrafish, the matched nonneoplastic somatic cell sample and cancer cell sample were analyzed in the same experiment. The experiment number indicated on the *x*-axis refers to each independent cell cycle analysis. In experiment 23, the cancer cell sample was excluded (see Materials and Methods), and the G0/G1 peak is only reported for the matched nonneoplastic somatic cell sample. (b) Normal distribution of G0/G1 peak PI fluorescence intensity values for nonneoplastic somatic cells derived from *brca2 m/m;tp53 m/m* and *tp53 m/m* zebrafish. In the normal quantile plot, filled black circles represent individual data points and dashed red lines indicate the Lilliefores confidence bounds. In the outlier box plot, the vertical line represents the median sample value; the diamond contains the mean and upper and lower 95% of the mean; the box ends represent the 25th and 75th quantiles; the whiskers extend to the outermost data points; and the red bracket indicates the shortest half (most dense 50% of observations). In the histogram, vertical bars represent G0/G1 peak intensity values by bin and the overlying red curve fits a smooth curve using nonparametric density estimation.

Based on DNA index, zebrafish cancers were classified as diploid or aneuploid, and aneuploid tumors were further categorized by type of aneuploidy (Table S2 and Table 2). *brca2* genotype influenced the relative proportions of cancers in diploid and aneuploid categories (Figure 3(b) and Table 2). For *brca2*-associated cancers, approximately equal proportions of cancers were diploid versus aneuploid (48% and 52%, respectively). In contrast, for non-*brca2*-associated cancers the proportion of diploid cancers was almost half the proportion of aneuploid cancers (35% and 65%, respectively). However, the association between *brca2* genotype and ploidy outcome (diploid versus aneuploid) was not statistically significant ($p = 0.1877$, Chi-square test). For both *brca2*-associated and non-*brca2*-associated cancers, hyperdiploid aneuploidy was the most common nondiploid categorization (Table 2).

Four zebrafish (three *brca2 m/m;tp53 m/m* and one *tp53 m/m* zebrafish) developed two cancers in anatomically distinct locations that were analyzed independently (Figure S4). In three of four individuals, the two cancers did not exhibit the same ploidy (aneuploid versus diploid). In one of four individuals, the two cancers exhibited the same ploidy (both aneuploid).

We assessed cell cycle progression in zebrafish cancers based on DNA content distribution (Figure S3). The mean percentage of cells in G0/G1, S, and G2/M phases were similar for diploid cancers from *brca2 m/m;tp53 m/m* and *tp53 m/m* zebrafish (Figure S3B) and for aneuploid cancers from *brca2 m/m;tp53 m/m* and *tp53 m/m* zebrafish (Figure S3C).

3.4. Sex, But Not Tumor Location, Significantly Influences Ploidy Outcome in Zebrafish Cancers. We have previously shown that the coelom and ocular region are the most common sites for cancer development in zebrafish with *brca2* and *tp53* mutations [23, 31], similar to the *tp53*^{M214K} line [29]. In the current study populations, the majority of analyzed cancer specimens arose in coelomic or ocular locations, with a small number arising in other locations (Table 1). We observed approximately twice as many ocular cancers in *brca2 m/m;tp53 m/m* zebrafish as occurred in *tp53 m/m* zebrafish (Table 1). The association between *brca2* genotype

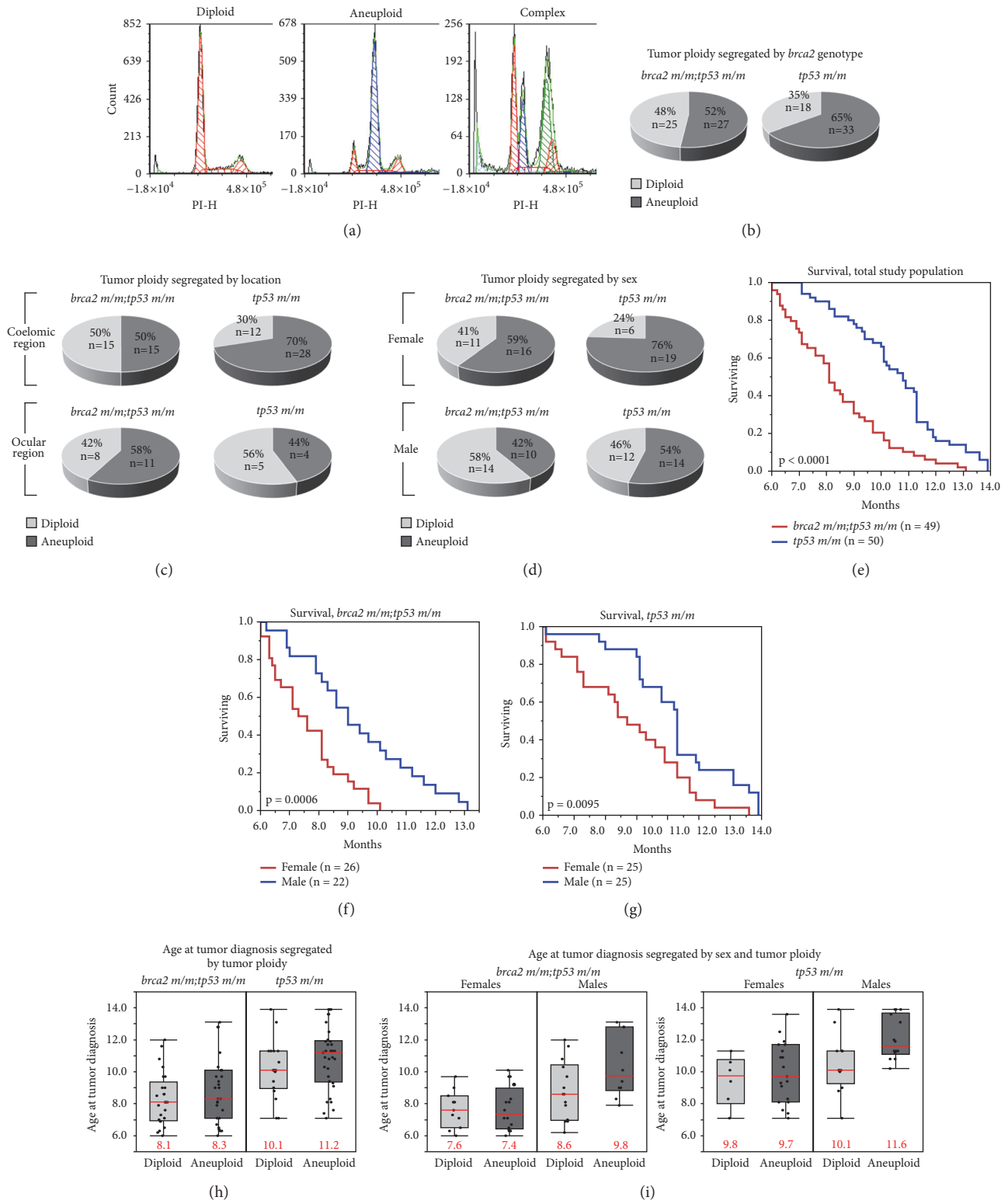

Figure 3: *brca2* mutation status and sex alter ploidy outcomes in zebrafish cancers. (a) Representative propidium iodide (PI) fluorescence histograms from cancers that are diploid or aneuploid or exhibit complex aneuploidy. Software-identified diploid populations are depicted in red; aneuploid populations are depicted in blue and green. ((b)–(d)) Ploidy outcomes segregated by *brca2* genotype alone (b) and in combination with tumor location (c) or sex (d). ((e)–(g)) Kaplan-Meier survival curves for the total study population (e), the *brca2 m/m;tp53 m/m* cohort (f), and the *tp53 m/m* cohort (g). (h) Distribution of ages at tumor diagnosis segregated by *brca2* genotype and tumor ploidy. Median ages at tumor diagnosis are indicated by a red bar and are shown in red text. (i) Distribution of ages at tumor diagnosis segregated by *brca2* genotype, sex, and tumor ploidy. Median ages at tumor diagnosis are indicated by a red bar and shown in red text.

Table 2: Impact of *brca2* genotype and sex[a] on the relative proportions of zebrafish cancers in diploid and aneuploid categories.

Ploidy category	*brca2 m/m;tp53 m/m*	*tp53 m;m*
Diploid	25 (48%)	18 (35%)
Aneuploid	27 (52%)	33 (65%)
Hypodiploid aneuploid	*4*	*3*
Hyperdiploid aneuploid	*19*	*23*
Tetraploid aneuploid	*1*	*0*
Complex	*3*	*7*
Ploidy category[b]	Females	Males
Diploid	17 (33%)	26 (52%)
Aneuploid	35 (67%)	24 (48%)
Hypodiploid aneuploid	*4*	*3*
Hyperdiploid aneuploid	*25*	*16*
Tetraploid aneuploid	*1*	*0*
Complex	*5*	*5*

[a]The sex for one zebrafish was not determined and is not included in the comparison of ploidy in females versus males.
[b]Categorization of ploidy outcomes by sex includes all cancer-bearing zebrafish without segregation by *brca2* genotype. Ploidy outcomes segregated by both sex and genotype are presented in Figure 3(d).

and tumor location (coelom or ocular region) was statistically significant (p = 0.0241, Chi-square test).

To determine if the site of tumor origin influenced ploidy outcome, we assessed the numbers of cancers in each ploidy category arising in coelomic versus ocular locations (Figure 3(c)). Because *brca2* genotype significantly influenced tumor location, ploidy outcomes were assessed only within genotypic groups. For cancers arising in the coelomic region, *brca2*-associated cancers were classified as diploid or aneuploid in equal proportions (n = 15, 50%, for both categories). Non-*brca2*-associated coelomic cancers were predominantly classified as aneuploid (n = 27, 68%). These outcomes were similar to the ploidy outcomes for each genotypic group (Figure 3(b)). For cancers arising in the ocular region, both *brca2*-associated and non-*brca2*-associated cancers were classified as diploid or aneuploid in relatively similar proportions. There was no statistically significant association between location and ploidy outcome (diploid versus aneuploid) for either genotypic group (*brca2 m/m;tp53 m/m*, p = 0.5890; *tp53 m/m*, p = 0. 0.1545; Chi-square test).

To determine the effect of sex on ploidy outcome in zebrafish cancers, we assessed the numbers of cancers in each ploidy category for male and female zebrafish (Figure 3(d) and Table 2). The numbers of males and females were similar in each genotypic group (Table 1) and there was no statistically significant association between *brca2* genotype and sex (p = 0.6920, Chi-square test). Therefore, ploidy outcomes were assessed within genotypic groups and within the entire study population. In both *brca2 m/m;tp53 m/m* and *tp53 m/m* cohorts, the proportions of aneuploid cancers were higher in females than in males of the same genotype (Figure 3(d)). In the *brca2 m/m;tp53 m/m* cohort, 59% of cancers in females were aneuploid (n = 16) versus 42% in males (n = 10). In the *tp53 m/m* cohort, 76% of cancers in females were aneuploid (n = 19) versus 54% in males (n = 14). Despite these differences, there was no statistically significant association between sex and ploidy outcome (diploid versus aneuploid) within genotypic groups (*brca2 m/m;tp53 m/m*, p = 0.2085; *tp53 m/m*, p = 0. 0955; Chi-square test). However, assessment of the entire study population without segregation by *brca2* genotype revealed that the association between sex and ploidy outcome was statistically significant (p = 0.0477), with aneuploid cancers occurring more frequently in female zebrafish (Table 2).

3.5. brca2 Genotype, Sex, Tumor Ploidy, and Survival Outcome Are Interrelated in Cancer-Bearing Zebrafish. We have previously shown that age at tumor diagnosis is statistically significantly lower in *brca2 m/m;tp53 m/m* zebrafish compared to *tp53 m/m* zebrafish [23]. This finding is consistent with survival outcomes in the current study population, which indicated that *brca2* mutation significantly decreases survival time (Figure 3(e), Figures S5A and B, and Table S3). The median age at tumor diagnosis was 8.2 months for *brca2 m/m;tp53 m/m* zebrafish and 10.8 months for *tp53 m/m* zebrafish (Table 1).

Given the difference in ploidy outcomes between male and female zebrafish (Figure 3(d)), we evaluated survival outcomes in male and female cohorts within each genotypic group (Figures 3(f) and 3(g)). Because *brca2* genotype significantly impacted age at tumor diagnosis, survival outcomes were assessed only within genotypic groups. In both *brca2 m/m;tp53 m/m* and *tp53 m/m* zebrafish cohorts, females had a lower median age at tumor diagnosis than males (Table 1), and survival times for females were significantly lower (Figures 3(f) and 3(g), and Table S3).

In human cancers, aneuploidy is often a negative prognostic factor associated with decreased survival time [17–22]. Therefore, we looked for an association between survival time and ploidy outcome for both *brca2 m/m;tp53 m/m* and *tp53 m/m* zebrafish cohorts. In *brca2 m/m;tp53 m/m* zebrafish, the median age at tumor diagnosis was similar for zebrafish with diploid versus aneuploid cancers (Figure 3(h)). In *tp53 m/m* zebrafish, the median age at tumor diagnosis was lower for

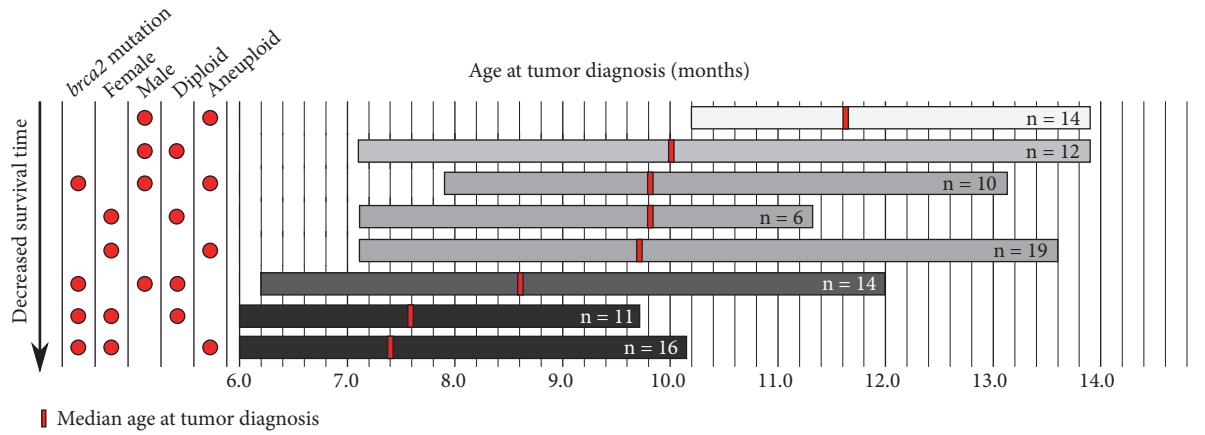

Figure 4: Factors contributing to decreased survival time in cancer-bearing zebrafish. Cohorts are represented by horizontal bars and the numbers of individual zebrafish per cohort are indicated. The horizontal width of each bar shows the range of ages at tumor diagnosis within each cohort, and the vertical red line indicates the median age at tumor diagnosis for each cohort. The combination of filled red circles shown to the left of each horizontal bar indicates the defining characteristics of the cohort with regard to *brca2* mutation status, sex, and tumor ploidy. Cohorts are distributed vertically by decreasing survival time, and color range of horizontal bars from light grey to black reflects longest to shortest survival time, respectively.

zebrafish with diploid versus aneuploid cancers (Figure 3(h)). There was no statistically significant difference in survival time for zebrafish with diploid versus aneuploid cancers in either genotypic group (Figures S5C and D and Table S3).

Next, we evaluated for an association between survival time, sex, and ploidy outcome for both *brca2 m/m;tp53 m/m* and *tp53 m/m* zebrafish cohorts. In both *brca2 m/m;tp53 m/m* and *tp53 m/m* zebrafish female cohorts, the median age at tumor diagnosis was similar regardless of ploidy status (Figure 3(i)). In contrast, in both *brca2 m/m;tp53 m/m* and *tp53 m/m* zebrafish male cohorts, the median age at tumor diagnosis was lower for male zebrafish with diploid cancers (Figure 3(i)). We evaluated survival time among individuals of the same sex and genotype that developed diploid versus aneuploid cancers. Within each subgroup of the same genotype and sex, there was no statistically significant difference in survival time based on tumor ploidy (Figures S5E-H and Table S3).

We identified two independent variables, *brca2* genotype and sex, that significantly impacted outcomes in this study. Both *brca2* mutation and female sex were associated with significantly decreased survival time, and female sex was associated with a significantly increased proportion of aneuploid cancers. Combined evaluation of *brca2* genotype, sex, and tumor ploidy did not identify a significant interaction among these three variables (Table S4). However, the three groups with the lowest median ages at tumor diagnosis were defined by a combination of (1) *brca2* mutation and female sex (either diploid or aneuploid status) or (2) *brca2* mutation and diploid status (either male or female sex) (Figure 4). These data suggest that zebrafish with these combined variables experience a decrease in survival time.

4. Discussion

Genomic instability is a hallmark of cancer cells and a critical contributor to the ongoing genetic evolution that accompanies malignant progression. Chromosomal instability (CIN) is one of the most common forms of genomic instability identified in cancer cells and contributes to the development of both structural aberrations (e.g., rearrangements, amplifications, and deletions) and numerical aberrations (aneuploidy) [37, 38]. Aneuploidy can be an indication of ongoing CIN in cancer cells [39, 40] and is often a negative prognostic indicator in humans with cancer [17–22]. However, this may not be a universal paradigm [16]. Aneuploidy may represent a stable state in cancer cells and does not necessarily indicate ongoing CIN [22, 40–43]. It has also been proposed that aneuploidy may itself induce CIN and thus contribute to a progressively greater level of aneuploidy in cancers [44, 45]. Thus, the development of aneuploidy in cancer cells may be both a cause and consequence of genomic instability in cancer.

The tumor suppressor BRCA2 participates in multiple pathways during both meiosis and mitosis that are critical for maintaining genomic integrity, and loss of BRCA2 function can lead to both structural aberrations and aneuploidy [2]. In this study, we used a *brca2*-mutant/*tp53*-mutant zebrafish line to investigate the impact of *brca2* mutation on cell cycle progression and ploidy outcome in normal tissue (testicular germ cells and somatic cells) and cancers. These heritable *brca2* and *tp53* mutations in zebrafish are similar in location and type to pathologic *BRCA2* and *TP53* mutations in humans [23, 29]. We have previously demonstrated genetic similarities between *BRCA2*-associated human and zebrafish cancers, such as the collaborative effect of *TP53* mutation on carcinogenesis and the loss of heterozygosity in cancer cells [23, 30].

Given *BRCA2*'s role in the resolution of DNA breaks generated during prophase I of meiosis I [3, 4], we first assessed nonneoplastic germ cells from adult zebrafish. As the large size of zebrafish oocytes precludes analysis by flow cytometry, we focused these studies on zebrafish testes. We and others have shown that *Brca2* is expressed in

spermatogonia and spermatocytes in vertebrate testes [3, 23, 46] and that testes from *Brca2*-mutant animals exhibit arrested spermatogenesis [3, 4, 23]. In the current study, testes from *brca2 m/m* zebrafish showed an accumulation of cells with 4C DNA content, indicating arrest in meiosis I before completion of the first meiotic cell division. These findings are consistent with previous studies of meiotic progression in *Brca2*-deficient mouse testes [3, 4]. We identified a significantly increased proportion of cells in S-phase from *brca2*-mutant testes. This finding could reflect cell cycle delay; alternatively, it is possible that some cells categorized as S-phase were aneuploid, with DNA content between 2C and 4C. Additional studies will be required to distinguish between these possibilities.

Studies in *Tp53*-deficient mouse models and *Drosophila* have identified a physiologic function for p53 during mitosis and meiosis in gonads [47–50]. In mammalian and zebrafish testes, the mitotic phase of spermatogenesis encompasses development of type A and type B spermatogonia, with type A representing a less differentiated population than type B [33, 36]. These mitotic germ cells undergo both proliferation and differentiation before entering meiosis I as preleptotene spermatocytes [51]. In *Tp53*-deficient mice, type A spermatogonia are significantly increased [47]; spermatogonia are also increased in *tp53*-deficient *Drosophila* [48]. Similarly, we observed that *tp53 m/m* zebrafish testes exhibited significant expansion of the type A spermatogonial population, which corresponded to a significant increase in the proportion of cells with 2C DNA content. Spermatogonial expansion in *Tp53*-deficient mice and Drosophila was attributed to the loss of p53-dependent programmed cell death in mitotic germ cells [47, 48]. p53 was also expressed during meiotic recombination in mouse and *Drosophila* germ cells following the induction of double-strand DNA breaks by the topoisomerase Spo11 [47, 50]. However, loss of p53 does not appear to alter meiotic progression in germ cells in the absence of additional stimuli (e.g., ionizing radiation) [47, 50], although meiotic recombination frequency is reduced [50]. Similarly, our data suggests that loss of p53 does not alter meiotic progression in zebrafish testes: the proportions of cells in 1C, 4C, and S-phase compartments were equivalent in *tp53 m/m* testes compared to wild type testes, and *tp53 m/m* testes were histologically normal.

Strikingly, combined mutations in *brca2* and *tp53* resulted in meiotic arrest and a dramatic accumulation of cells with 2C DNA content, correlating to significantly increased numbers of both type A and type B spermatogonia. These data indicate the significant expansion of mitotic germ cells in *brca2 m/m;tp53 m/m* zebrafish testes. The predominance of type A spermatogonia, which are less differentiated than type B spermatogonia, suggests that spermatogonial differentiation is suppressed in *brca2 m/m;tp53 m/m* zebrafish testes. These outcomes are distinct from the effects of *brca2* or *tp53* mutations alone in zebrafish testes, which caused meiotic arrest or selective type A spermatogonial expansion, respectively. We have not identified a similar effect in published studies of *Brca2*-mutant;*Tp53*-mutant mouse models; a synergistic suppressive effect on germ cell expansion during the initiation of meiosis has been described in testes from juvenile mice with combined mutations in *Brca2* and *Palb2* [4]. However, combined mutations in *tp53* and *rad54* have been shown to alter germ cell numbers in *Drosophila* ovary [50]. Rad54 functions downstream of Brca2 and is essential for homology-directed recombination and DNA repair [52]. *Drosophila* ovaries with combined *tp53* and *rad54* mutations showed a variable, frequently increased number of mitotic germ cells (known as nurse cells) [50], which is comparable to the outcome we observed in *brca2 m/m;tp53 m/m* zebrafish testes.

The above-described effects of combined *brca2* and *tp53* mutations on mitotic germ cells (spermatogonia) in zebrafish suggest the interesting possibility that concurrent mutations in *BRCA2* and *TP53* could synergistically promote proliferation and suppress differentiation, which has important implications in the context of cancer initiation. Spermatogenesis is considered to be a classical stem cell-driven process, providing a model for analyzing stem cell physiology and behavior that may be applicable to stem cell populations in other tissues [53, 54]. It is possible that tissue stem and progenitor cells in other sites, which are potential sources for the emergence of cancer stem cells, may be similarly affected by combined *BRCA2* and *TP53* mutations. In support of this concept, *BRCA1* mutation or knockdown has been linked to increased stem/progenitor cell populations and dedifferentiation of stem cells in human breast and mouse mammary tissues [55, 56]. Also, women with *BRCA1*- or *BRCA2*-associated cancer had an increased frequency of breast stem cells in noncancerous breast tissue, which were identified by expression of the stem and progenitor cell marker ALDH [57]. P53 has a known role in the maintenance and regulation of both embryonic and adult stem cells, and wild type p53 suppresses self-renewal and induces differentiation of stem cells after DNA damage (reviewed by Aloni-Grinstein R et al.) [58]. Additionally, proliferation is increased in p53-deficient stem and progenitor cells [59–61]. Together these studies suggest that further investigation of a potentially synergistic role for *BRCA2* and *TP53* mutations in disrupting stem and progenitor cell homeostasis may provide new insight into how mutations in these genes modulate carcinogenesis.

Next, we assessed nonneoplastic somatic tissues and cancers from adult zebrafish. DNA content analysis of nonneoplastic somatic tissues from zebrafish indicated that *brca2* mutation does not alter ploidy in these cells. This outcome is similar to what has been observed in mammalian cells, namely, that normal, nonneoplastic cells generally do not tolerate aneuploidy [37, 43, 44, 62]. We identified a small percentage of aneuploid cells in four somatic tissue samples but cannot rule out the possibility that these tissues contained early-stage cancers not detectable by stereomicroscopic examination. In zebrafish cancers, we observed that diploidy was more common in *brca2*-associated cancers than non-*brca2*-associated cancers, although this difference was not statistically significant. In comparison, diploid and aneuploid cancers reportedly occur in roughly similar proportions in human *BRCA2*-associated and non-*BRCA2*-associated cancers [14–16]. Contrastingly, aneuploidy and polyploidy were increased in *Brca2*-inactivated tumor cell lines derived from a mouse model of pancreatic ductular adenocarcinoma

[63]. Overall, our data from *brca2*-associated zebrafish cancers parallels previous reports that *BRCA2* mutation does not significantly increase the rate of aneuploidy in human cancers.

We additionally considered sex as a variable that might influence tumor ploidy in zebrafish. Aneuploidy was significantly more common in female zebrafish in the full study population, although significance was not maintained when study cohorts were segregated by *brca2* genotype. To our knowledge, the impact of sex on tumor ploidy has not been previously reported in zebrafish cancer models. In humans, gender is not linked to the development of global numerical aberrations in cancers, although numerical aberrations specifically affecting the sex chromosomes (gonosomes) occur more frequently in cancers from males [64]. However, gender-specific structural aberrations affecting both gonosomes and autosomes are reported in some cancer types that may be biologically and prognostically significant [64–67]. The factors that drive accumulation of these gender-associated genomic changes are not yet defined. Our zebrafish model will be an informative tool for investigating how sex impacts the accumulation of genetic and genomic changes during carcinogenesis.

Finally, we evaluated survival outcome in cancer-bearing zebrafish in the context of the three major variables analyzed in this study (*brca2* genotype, sex, and tumor ploidy). We have previously reported that *brca2*-mutant zebrafish develop tumors at a significantly younger age than non-*brca2*-mutant zebrafish [23], which was also observed in this study. We additionally identified a significant impact of sex on survival outcome: females in both genotypic groups developed tumors at a statistically significant younger age than males. We are unaware of any previous report of a zebrafish cancer model that experiences a significant disparity in survival outcome based on sex. In humans, survival outcomes in females are generally better than in males [68]. However, there are some cancer types for which survival outcomes are reversed; i.e. survival outcomes in women are worse than in men [69, 70]; such differences have also been linked to response to targeted therapies [71]. Gender-associated differences in survival outcome have yet to be explained in humans, although multiple possible contributors, including hormonal signaling, environmental exposures, DNA repair defects, and other factors, have been postulated [65, 70]. The potential contributions of such factors to carcinogenesis in our zebrafish model are not yet known.

Ploidy is an independent prognostic factor for survival across a variety of human cancer types, with aneuploidy associated with worse prognosis [17–22]. Within both genotypic groups of cancer-bearing zebrafish in this study, we found that median survival times in females with diploid versus aneuploid cancers were similar, while median survival times for males with diploid cancers were lower than for males with aneuploid cancers. This finding is surprising, given that aneuploidy is generally linked to worse prognosis in human cancer patients. However, diploidy has been correlated to worse prognosis in *BRCA2*-associated human breast cancers [16]. In our study, ploidy did not emerge as a variable that significantly contributed to survival outcome in cancer-bearing zebrafish. Since we identified both *brca2* genotype and sex as variables that significantly influenced survival outcome, we could not assess the impact of ploidy on survival outcome independently from these variables. As a result, we cannot rule out the possibility that ploidy would have been found to significantly affect survival outcome in a larger study population. In comparison, the aforementioned study of ploidy status and survival outcome in human breast cancer patients with and without *BRCA2* mutation presented data from almost 3,000 patients that was acquired over a 50-year period [16].

We observed the lowest median survival times in zebrafish with (1) *brca2* mutation and female sex and (2) *brca2* mutation and diploid cancer (Figure 4). Although diploidy is typically linked to relative genomic stability, diploid cancers may actually be "pseudodiploid," exhibiting complex genomic alterations that do not impact total chromosomal content. This condition has been described in diploid *BRCA2*-associated human cancers [15] and was proposed as a contributor to poor prognosis in patients with diploid *BRCA2*-associated cancers [16]. Similarly, near-diploid colorectal cancers have been shown to possess extensive genomic changes that may be essential in carcinogenesis [72]. On the other hand, not all aneuploid cancers experience ongoing CIN but rather exhibit relative genomic stability [22, 40–43]. It is therefore possible that, in our model system, diploid or aneuploid categorizations do not reflect the level of genomic stability in these zebrafish cancers. Further studies are underway to investigate more deeply the genetic and genomic alterations that characterize cancers in our zebrafish model and determine the impact of *brca2* mutation and sex on these alterations.

5. Conclusions

Our findings confirm that the individual effects of *brca2* and *tp53* mutations on testicular germ cell development are conserved in zebrafish and reveal that combined *brca2* and *tp53* mutations collaborate to promote accumulation of spermatogonia while suppressing spermatogonial differentiation. Our findings additionally identify both *brca2* genotype and sex as independent variables that significantly affect survival outcome in cancer-bearing zebrafish. While ploidy outcome in zebrafish cancers did not significantly affect survival outcome, ploidy was significantly influenced by sex. Finally, we determined that diploidy is not linked to better survival outcome in cancer-bearing zebrafish: the worst survival outcomes were observed with (1) *brca2* mutation and female sex and (2) *brca2* mutation and diploid cancer. These studies provide new insight into the impact of combined *BRCA2* and *TP53* mutations on germ cell development and identify key influences of *BRCA2* mutation, sex, and ploidy on survival outcome in vertebrate cancer.

Data Availability

All data generated or analyzed during this study are included in this published article (and its Supplementary Information files). The zebrafish lines described in this work (wild type

(AB), *brca2*^{hg5} mutant, and *tp53*^{zdf1} mutant) are maintained at the Shive laboratory and may be accessed by contacting the corresponding author.

Conflicts of Interest

The authors declare no conflicts of interest.

Authors' Contributions

H. R. Shive conceived and designed the experiments. L. Mensah, J. L. Ferguson, and H. R. Shive performed the experiments. H. R. Shive analyzed and interpreted the data and prepared figures. L. Mensah, J. L. Ferguson, and H. R. Shive wrote the paper.

Acknowledgments

This work was supported by NIH K01OD021419 and by NC State University, College of Veterinary Medicine.

Supplementary Materials

The supplementary materials include Supplementary Figure Legends, Supplementary Figures S1–S5, and Supplementary Tables S1–S4. Presented in the Supplementary Figures are the following data: Figure S1, gating strategies for analysis of flow cytometry data from testes, nonneoplastic somatic cells, and cancer cells; Figure S2, representative histologic images of testes from *brca2 m/m;tp53 m/m* and *tp53 m/m* zebrafish; Figure S3, distributions of cells (mean percent of gated cells) according to DNA content in nonneoplastic somatic tissues and cancers; Figure S4, example of disparate ploidy outcomes from two anatomically distinct cancers derived from the same zebrafish; and, Figure S5, analysis of survival outcome with respect to various population characteristics (*brca2* mutation status, sex, and tumor ploidy). Presented in the Supplementary Tables are the following data: Table S1, comparison of DNA content and spermatogonia counts in testes from wild type, *tp53 m/m*; *brca2 m/m*, and *brca2* m/m;tp53 m/m zebrafish; Table S2, definition of DNA ploidy categories determined by the calculated DNA index; Table S3, summary of statistical analyses of survival outcomes in cancer-bearing zebrafish; and, Table S4, summary of statistical analyses assessing the impact of multiple variables on survival outcomes in cancer-bearing zebrafish. *(Supplementary Materials)*

References

[1] E. Duro and A. L. Marston, "From equator to pole: splitting chromosomes in mitosis and meiosis," *Genes & Development*, vol. 29, pp. 109–122, 2015.

[2] A. R. Venkitaraman, "Tumour suppressor mechanisms in the control of chromosome stability: Insights from BRCA2," *Molecules and Cells*, vol. 37, no. 2, pp. 95–99, 2014.

[3] S. K. Sharan, A. Pyle, V. Coppola et al., "BRCA2 deficiency in mice leads to meiotic impairment and infertility," *Development*, vol. 131, no. 1, pp. 131–142, 2004.

[4] S. A. Hartford, R. Chittela, X. Ding et al., "Interaction with PALB2 is essential for maintenance of genomic integrity by BRCA2," *PLoS Genetics*, vol. 12, no. 8, p. e1006236, 2016.

[5] K. Seeliger, S. Dukowic-Schulze, R. Wurz-Wildersinn et al., "BRCA2 is a mediator of RAD51- and DMC1-facilitated homologous recombination in Arabidopsis thaliana," *New Phytologist*, vol. 193, no. 2, pp. 364–375, 2012.

[6] K. J. Patel, V. P. Yu, H. Lee et al., "Involvement of Brca2 in DNA repair," *Molecular Cell*, vol. 1, no. 3, pp. 347–357, 1998.

[7] H. Lee, A. H. Trainer, L. S. Friedman et al., "Mitotic checkpoint inactivation fosters transformation in cells lacking the breast cancer susceptibility gene, Brca2," *Molecular Cell*, vol. 4, no. 1, pp. 1–10, 1999.

[8] E. Choi, P.-G. Park, H.-O. Lee et al., "BRCA2 fine-tunes the spindle assembly checkpoint through reinforcement of BubR1 acetylation," *Developmental Cell*, vol. 22, no. 2, pp. 295–308, 2012.

[9] M. J. Daniels, Y. Wang, M. Lee, and A. R. Venkitaraman, "Abnormal cytokinesis in cells deficient in the breast cancer susceptibility protein BRCA2," *Science*, vol. 306, no. 5697, pp. 876–879, 2004.

[10] M. Lee, M. J. Daniels, M. J. Garnett, and A. R. Venkitaraman, "A mitotic function for the high-mobility group protein HMG20b regulated by its interaction with the BRC repeats of the BRCA2 tumor suppressor," *Oncogene*, vol. 30, no. 30, pp. 3360–3369, 2011.

[11] N. Ayoub, E. Rajendra, X. Su, A. D. Jeyasekharan, R. Mahen, and A. R. Venkitaraman, "The carboxyl terminus of Brca2 links the disassembly of Rad51 complexes to mitotic entry," *Current Biology*, vol. 19, no. 13, pp. 1075–1085, 2009.

[12] T. Menzel, V. Nähse-Kumpf, A. N. Kousholt et al., "A genetic screen identifies BRCA2 and PALB2 as key regulators of G2 checkpoint maintenance," *EMBO Reports*, vol. 12, no. 7, pp. 705–712, 2011.

[13] K. Schlacher, N. Christ, N. Siaud, A. Egashira, H. Wu, and M. Jasin, "Double-strand break repair-independent role for BRCA2 in blocking stalled replication fork degradation by MRE11," *Cell*, vol. 145, no. 4, pp. 529–542, 2011.

[14] A. B. Jonsdottir, O. A. Stefansson, J. Bjornsson, J. G. Jonasson, H. M. Ogmundsdottir, and J. E. Eyfjord, "Tetraploidy in BRCA2 breast tumours," *European Journal of Cancer*, vol. 48, no. 3, pp. 305–310, 2012.

[15] O. A. Stefansson, J. G. Jonasson, K. Olafsdottir et al., "Genomic and phenotypic analysis of BRCA2 mutated breast cancers reveals co-occurring changes linked to progression," *Breast Cancer Research*, vol. 13, p. R95, 2011.

[16] L. Tryggvadottir, E. J. Olafsdottir, G. H. Olafsdottir et al., "Tumour diploidy and survival in breast cancer patients with BRCA2 mutations," *Breast Cancer Research and Treatment*, vol. 140, no. 2, pp. 375–384, 2013.

[17] O. P. Kallioniemi, G. Blanco, M. Alavaikko et al., "Tumour DNA ploidy as an independent prognostic factor in breast cancer," *British Journal of Cancer*, vol. 56, no. 5, pp. 637–642, 1987.

[18] K. Herman, A. Gruchala, A. Niezabitowski et al., "Prognostic factors in retroperitoneal sarcomas: ploidy of DNA as a predictor of clinical outcome," *Journal of Surgical Oncology*, vol. 71, pp. 32–35, 1999.

[19] A. E. Pinto, S. Andre, and J. Soares, "Short-term significance of DNA ploidy and cell proliferation in breast carcinoma: a multivariate analysis of prognostic markers in a series of 308 patients," *Journal of Clinical Pathology*, vol. 52, pp. 604–611, 1999.

[20] P. San Miguel-Fraile, R. Carrillo-Gijon, J. L. Rodriguez-Peralto, and I. A. Badiola, "Prognostic significance of DNA ploidy and proliferative index (MIB-1 index) in childhood rhabdomyosarcoma," *American Journal of Clinical Pathology*, vol. 121, pp. 358–365, 2004.

[21] D. Choma, J. P. Daures, X. Quantin, and J. L. Pujol, "Aneuploidy and prognosis of non-small-cell lung cancer: a meta-analysis of published data," *British Journal of Cancer*, vol. 85, pp. 14–22, 2001.

[22] L. M. Zasadil, E. M. Britigan, and B. A. Weaver, "2n or not 2n: Aneuploidy, polyploidy and chromosomal instability in primary and tumor cells," *Seminars in Cell and Developmental Biology*, vol. 24, pp. 370–379, 2013.

[23] H. R. Shive, R. R. West, L. J. Embree et al., "brca2 in zebrafish ovarian development, spermatogenesis, and tumorigenesis," *Proceedings of the National Acadamy of Sciences of the United States of America*, vol. 107, no. 45, pp. 19350–19355, 2010.

[24] B. Evers and J. Jonkers, "Mouse models of BRCA1 and BRCA2 deficiency: past lessons, current understanding and future prospects," *Oncogene*, vol. 25, pp. 5885–5897, 2006.

[25] T. Crook, L. A. Brooks, S. Crossland et al., "p53 mutation with frequent novel condons but not a mutator phenotype in BRCA1- and BRCA2-associated breast tumours," *Oncogene*, vol. 17, pp. 1681–1689, 1998.

[26] S. J. Ramus, L. G. Bobrow, P. D. Pharoah et al., "Increased frequency of TP53 mutations in BRCA1 and BRCA2 ovarian tumours," *Genes, Chromosomes and Cancer*, vol. 25, no. 2, pp. 91–96, 1999.

[27] R. Roy, J. Chun, and S. N. Powell, "BRCA1 and BRCA2: different roles in a common pathway of genome protection," *Nature Reviews Cancer*, vol. 12, pp. 68–78, 2011.

[28] S. Gretarsdottir, S. Thorlacius, R. Valgardsdottir et al., "BRCA2 and p53 mutations in primary breast cancer in relation to genetic instability," *Cancer Research*, vol. 58, no. 5, pp. 859–862, 1998.

[29] S. Berghmans, R. D. Murphey, E. Wienholds et al., "tp53 mutant zebrafish develop malignant peripheral nerve sheath tumors," *Proceedings of the National Acadamy of Sciences of the United States of America*, vol. 102, no. 2, pp. 407–412, 2005.

[30] H. R. Shive, R. R. West, L. J. Embree et al., "BRCA2 and TP53 collaborate in tumorigenesis in zebrafish," *PLoS One*, vol. 9, article e87177, 2014.

[31] L. A. White, J. M. Sexton, and H. R. Shive, "Histologic and immunohistochemical analyses of soft tissue sarcomas From brca2-mutant/tp53-mutant zebrafish are consistent with neural crest (schwann cell) origin," *Veterinary Pathology*, vol. 54, no. 2, pp. 320–327, 2017.

[32] J. Schindelin, I. Arganda-Carreras, and E. Frise, "Fiji: an open-source platform for biological-image analysis," *Nature Methods*, vol. 9, no. 7, pp. 676–682, 2012.

[33] M. C. Leal, E. R. Cardoso, R. H. Nóbrega et al., "Histological and stereological evaluation of zebrafish (Danio rerio) spermatogenesis with an emphasis on spermatogonial generations," *Biology of Reproduction*, vol. 81, no. 1, pp. 177–187, 2009.

[34] E. Rotgers, S. Cisneros-Montalvo, K. Jahnukainen, J. Sandholm, J. Toppari, and M. Nurmio, "A detailed protocol for a rapid analysis of testicular cell populations using flow cytometry," *Andrology*, vol. 3, no. 5, pp. 947–955, 2015.

[35] J. S. Ross, G. P. Linette, J. Stec, M. S. Ross, S. Anwar, and A. Boguniewicz, "DNA ploidy and cell cycle analysis in breast cancer," *American Journal of Clinical Pathology*, vol. 120, no. suppl_1, pp. S72–S84, 2003.

[36] E. C. Roosen-Runge and L. O. Giesel Jr., "Quantitative studies on spermatogenesis in the albino rat," *American Journal of Anatomy*, vol. 87, Article ID 1000870102, pp. 1–30, 1950.

[37] L. C. Funk, L. M. Zasadil, and B. A. Weaver, "Living in CIN: mitotic infidelity and its consequences for tumor promotion and suppression," *Developmental Cell*, vol. 39, pp. 638–652, 2016.

[38] S. Negrini, V. G. Gorgoulis, and T. D. Halazonetis, "Genomic instability–an evolving hallmark of cancer," *Nature Reviews Molecular Cell Biology*, vol. 11, pp. 220–228, 2010.

[39] S. L. Thompson, S. F. Bakhoum, and D. A. Compton, "Mechanisms of chromosomal instability," *Current Biology*, vol. 20, pp. R285–R295, 2010.

[40] T. A. Potapova, J. Zhu, and R. Li, "Aneuploidy and chromosomal instability: a vicious cycle driving cellular evolution and cancer genome chaos," *Cancer and Metastasis Reviews*, vol. 32, pp. 377–389, 2013.

[41] D. J. Gordon, B. Resio, and D. Pellman, "Causes and consequences of aneuploidy in cancer," *Nature Reviews Genetics*, vol. 13, pp. 189–203, 2012.

[42] Z. Storchova and C. Kuffer, "The consequences of tetraploidy and aneuploidy," *Journal of Cell Science*, vol. 121, pp. 3859–3866, 2008.

[43] R. H. van Jaarsveld and G. Kops, "Difference makers: chromosomal instability versus aneuploidy in cancer," *Trends in Cancer*, vol. 2, pp. 561–571, 2016.

[44] S. Santaguida and A. Amon, "Short- and long-term effects of chromosome mis-segregation and aneuploidy," *Nature Reviews Molecular Cell Biology*, vol. 16, pp. 473–485, 2015.

[45] M. Giam and G. Rancati, "Aneuploidy and chromosomal instability in cancer: a jackpot to chaos," *Cell Division*, vol. 10, article 3, 2015.

[46] P. E. Blackshear, S. M. Goldsworthy, J. F. Foley et al., "Brca1 and Brca2 expression patterns in mitotic and meiotic cells of mice," *Oncogene*, vol. 16, no. 1, pp. 61–68, 1998.

[47] T. L. Beumer, H. L. Roepers-Gajadien, I. S. Gademan et al., "The role of the tumor suppressor p53 in spermatogenesis," *Cell Death & Differentiation*, vol. 5, no. 8, pp. 669–677, 1998.

[48] F. Napoletano, B. Gibert, K. Yacobi-Sharon et al., "p53-dependent programmed necrosis controls germ cell homeostasis during spermatogenesis," *PLoS Genetics*, vol. 13, article e1007024, 2017.

[49] M. Xiong, I. C. Ferder, Y. Ohguchi, and N. Wang, "Quantitative analysis of male germline stem cell differentiation reveals a role for the p53-mTORC1 pathway in spermatogonial maintenance," *Cell Cycle*, vol. 14, no. 18, pp. 2905–2913, 2015.

[50] W. J. Lu, J. Chapo, I. Roig, and J. M. Abrams, "Meiotic recombination provokes functional activation of the p53 regulatory network," *Science*, vol. 328, no. 5983, pp. 1278–1281, 2010.

[51] P. P. Lie, C. Y. Cheng, and D. D. Mruk, "Coordinating cellular events during spermatogenesis: a biochemical model," *Trends in Biochemical Sciences*, vol. 34, pp. 366–373, 2009.

[52] A. V. Mazin, O. M. Mazina, D. V. Bugreev, and M. J. Rossi, "Rad54, the motor of homologous recombination," *DNA Repair*, vol. 9, pp. 286–302, 2009.

[53] J. M. Oatley and R. L. Brinster, "Regulation of spermatogonial stem cell self-renewal in mammals," *Annual Review of Cell and Developmental Biology*, vol. 24, pp. 263–286, 2008.

[54] S. Yoshida, "Elucidating the identity and behavior of spermatogenic stem cells in the mouse testis," *Reproduction*, vol. 144, no. 3, pp. 293–302, 2012.

[55] F. Bai, H. L. Chan, A. Scott et al., "BRCA1 suppresses epithelial-to-mesenchymal transition and stem cell dedifferentiation during mammary and tumor development," *Cancer Research*, vol. 74, no. 21, pp. 6161–6172, 2014.

[56] S. Liu, C. Ginestier, E. Charafe-Jauffret et al., "BRCA1 regulates human mammary stem/progenitor cell fate," *Proceedings of the National Academy of Sciences of the United States of America*, vol. 105, pp. 1680–1685, 2008.

[57] B. L. Isfoss, B. Holmqvist, H. Jernstrom, P. Alm, and H. Olsson, "Women with familial risk for breast cancer have an increased frequency of aldehyde dehydrogenase expressing cells in breast ductules," *BMC Clinical Pathology*, vol. 13, pp. 13–28, 2013.

[58] R. Aloni-Grinstein, Y. Shetzer, T. Kaufman, and V. Rotter, "p53: the barrier to cancer stem cell formation," *FEBS Lett588*, pp. 2580–2589, 2014.

[59] A. Armesilla-Diaz, G. Elvira, and A. Silva, "p53 regulates the proliferation, differentiation and spontaneous transformation of mesenchymal stem cells," *Experimental Cell Research*, vol. 315, pp. 3598–3610, 2009.

[60] H. Liu, D. Jia, A. Li et al., "P53 regulates neural stem cell proliferation and differentiation via bmp-smad1 signaling and ID1," *Stem Cells and Development*, vol. 22, no. 6, pp. 913–927, 2013.

[61] A. M. McConnell, C. Yao, A. R. Yeckes et al., "p53 regulates progenitor cell quiescence and differentiation in the airway," *Cell Reports*, vol. 17, no. 9, pp. 2173–2182, 2016.

[62] K. Tanaka and T. Hirota, "Chromosomal instability: A common feature and a therapeutic target of cancer," *Biochim Biophys Acta*, vol. 1866, pp. 64–75, 2016.

[63] M. Rowley, A. Ohashi, G. Mondal et al., "Inactivation of Brca2 promotes Trp53-associated but inhibits KrasG12D-dependent pancreatic cancer development in mice," *Gastroenterology*, vol. 140, no. 4, pp. 1303–1313, 2011.

[64] S. Schulze and I. Petersen, "Gender and ploidy in cancer survival," *Cellular oncology (Dordrecht)*, vol. 34, pp. 199–208, 2011.

[65] J. Zhang, S. Yan, X. Liu et al., "Gender-related prognostic value and genomic pattern of intra-tumor heterogeneity in colorectal cancer," *Carcinogenesis*, vol. 38, no. 8, pp. 837–846, 2017.

[66] R. H. Ali, M. J. Marafie, M. S. Bitar et al., "Gender-associated genomic differences in colorectal cancer: Clinical insight from feminization of male cancer cells," *International Journal of Molecular Sciences*, vol. 15, no. 10, pp. 17344–17365, 2014.

[67] L. Bottarelli, C. Azzoni, F. Necchi et al., "Sex chromosome alterations associate with tumor progression in sporadic colorectal carcinomas," *Clinical Cancer Research*, vol. 13, no. 15, pp. 4365–4370, 2007.

[68] M. B. Cook, K. A. McGlynn, S. S. Devesa et al., "Sex disparities in cancer mortality and survival," *Cancer Epidemiology, Biomarkers & Prevention*, vol. 20, pp. 1629–1637, 2011.

[69] H. A. Risch, G. R. Howe, M. Jain et al., "Are female smokers at higher risk for lung cancer than male smokers? A case-control analysis by histologic type," *American Journal of Epidemiology*, vol. 138, no. 1-2, pp. 281–293, 1993.

[70] J. Dobruch, S. Daneshmand, M. Fisch et al., "Gender and bladder cancer: a collaborative review of etiology, biology, and outcomes," *European Urology*, vol. 69, no. 2, pp. 300–310, 2016.

[71] J. A. Pinto, C. S. Vallejos, L. E. Raez et al., "Gender and outcomes in non-small cell lung cancer: an old prognostic variable comes back for targeted therapy and immunotherapy?" *ESMO Open*, vol. 3, article e000344, 2018.

[72] M. Muleris, A. Chalastanis, N. Meyer et al., "Chromosomal instability in near-diploid colorectal cancer: a link between numbers and structure," *PLoS ONE*, vol. 3, article e1632, 2008.